CHLORIDE CONCENTRATION AND BLOW-THROUGH ANALYSES FOR CONCRETE BRIDGE DECK REHABILITATION USING HYDRODEMOLITION

Prepared For:

Utah Department of Transportation
Research & Innovation Division

Final Report
November 2020

DISCLAIMER

ACKNOWLEDGEMENTS

i

TECHNICAL REPORT ABSTRACT

1. Report No. UT-20.27	2. Government Accession No. N/A	3. Recipient's Catalog No. N/A
4. Title and Subtitle CHLORIDE CONCENTRATION AND BLOW-THROUGH ANALYSES FOR CONCRETE BRIDGE DECK REHABILITATION USING HYDRODEMOLITION	5. Report Date November 2020	
	6. Performing Organization Code N/A	
7. Author(s) W. Spencer Guthrie, Ph.D., Elizabeth A. Roper	8. Performing Organization Report No. N/A	
9. Performing Organization Name and Address Brigham Young University Department of Civil and Environmental Engineering 430 Engineering Building Provo, UT 84602	10. Work Unit No. 5H08419H	
	11. Contract or Grant No. 15-8775	
12. Sponsoring Agency Name and Address Utah Department of Transportation 4501 South 2700 West P.O. Box 148410 Salt Lake City, UT 84114-8410	13. Type of Report & Period Covered Final, March 2016 to May 2018	
	14. Sponsoring Agency Code PIC No. UT14.403	
15. Supplementary Notes Prepared in cooperation with the Utah Department of Transportation and the U.S. Department of Transportation, Federal Highway Administration		

16. Abstract

The objectives of this research were 1) to investigate the effects of hydrodemolition treatment timing on chloride concentration profiles in concrete bridge decks for depths of concrete removal below the top mat of reinforcing steel and 2) to investigate factors that influence the occurrence of blow-throughs in concrete bridge decks when hydrodemolition is used. The scope of this research included a questionnaire survey of hydrodemolition companies to summarize common practices in the field, numerical modeling of chloride concentration to investigate hydrodemolition treatment timing on typical Utah bridge decks, and structural analysis to investigate factors that influence the occurrence of blow-throughs during hydrodemolition.

The survey responses are valuable for understanding typical practices and were used to design the numerical experiments. The results of numerical modeling indicate that, when a surface treatment is used, the chloride concentration at either the top or bottom mat of reinforcing steel does not reach or exceed 2.0 lb of chloride per cubic yard of concrete after rehabilitation during the 75 years of simulated bridge deck service life. The results also indicate that, when a surface treatment is not used, the chloride concentration at the top mat of reinforcement exceeds 2.0 lb of chloride per cubic yard of concrete within 10, 15, and 20 years after rehabilitation for original cover depth values of 2.0, 2.5, and 3.0 in., respectively. The results of structural analysis indicate that the factor of safety against blow-throughs significantly increases with increasing values of transverse rebar spacing and concrete compressive strength and decreasing values of depth of removal below the bottom of the top reinforcing mat, orifice size, and water pressure within the investigated ranges of these parameters.

17. Key Words Blow-through, chloride concentration, concrete bridge deck, diffusion, hydrodemolition, surface treatment	18. Distribution Statement Not restricted. Available through: UDOT Research & Innovation Div. 4501 South 2700 West P.O. Box 148410 Salt Lake City, UT 84114-8410 www.udot.utah.gov/go/research		23. Registrant's Seal N/A
19. Security Classification (of this report) Unclassified	20. Security Classification (of this page) Unclassified	21. No. of Pages 107	22. Price N/A

TABLE OF CONTENTS

LIST OF TABLES

LIST OF FIGURES

LIST OF ACRONYMS

BYU	Brigham Young University
FHWA	Federal Highway Administration
NIST	National Institute of Standards and Technology
OCD	original cover depth

<u>**EXECUTIVE SUMMARY**</u>

The objectives of this research were 1) to investigate the effects of hydrodemolition treatment timing on chloride concentration profiles in concrete bridge decks for depths of concrete removal below the top mat of reinforcing steel and 2) to investigate factors that influence the occurrence of blow-throughs in concrete bridge decks when hydrodemolition is used. The research results are intended to provide engineers with guidance about the latest timing of hydrodemolition that can maintain a chloride concentration level below 2.0 lb of chloride per cubic yard of concrete at the levels of both the top and bottom mats of reinforcing steel, as well as about conditions that may indicate a higher probability of blow-through during hydrodemolition. The scope of this research included a questionnaire survey of hydrodemolition companies to summarize common practices in the field, numerical modeling of chloride concentration to investigate hydrodemolition treatment timing on typical Utah bridge decks, and structural analysis to investigate factors that influence the occurrence of blow-throughs during hydrodemolition.

While some survey respondents indicated that certain parameters vary, depending on the project, the responses are valuable for understanding typical practices and were used to design the numerical experiments. The numerical modeling generated chloride concentration profiles through a 75-year service life given a specific original cover depth (OCD), treatment time, and surface treatment usage. The results indicate that, when a surface treatment is used, the concentration at either the top or bottom mat of reinforcing steel does not reach or exceed 2.0 lb of chloride per cubic yard of concrete after rehabilitation during the 75 years of simulated bridge deck service life. The results also indicate that, when a surface treatment is not used, the chloride concentration at the top mat of reinforcement exceeds 2.0 lb of chloride per cubic yard of concrete within 10, 15, and 20 years after rehabilitation for OCD values of 2.0, 2.5, and 3.0 in., respectively. The numerical experiments generated results in terms of the main effect of each input variable on the occurrence of blow-throughs and interactions among selected input variables. For each analysis, blow-through can be expected when the calculated factor of safety is less than 1.0. The factor of safety significantly increases with increasing values of transverse rebar spacing and concrete compressive strength and decreasing values of depth of removal

1

below the bottom of the top reinforcing mat, orifice size, and water pressure within the ranges of these parameters investigated in this experimentation. The factor of safety is relatively insensitive to jet angle. For both case studies evaluated in this research, the blow-through analysis correctly predicted a high or low potential for blow-through on the given deck.

1.0 INTRODUCTION

1.1 Problem Statement

Chloride-induced corrosion of reinforcing steel is one of the leading causes of concrete bridge deck deterioration (Grace et al. 2004, Lees 1992, Mays 1992, Mindess et al. 2003, Suryavanshi et al. 1998, Zhang et al. 1998). Chloride ions, generally resulting from the application of deicing salts as part of winter road maintenance, can diffuse into the surface of a concrete bridge deck and interact with the embedded reinforcing steel. Steel reinforcement typically begins to corrode at a chloride concentration of 2.0 lb of chloride per cubic yard of concrete, forming expansive corrosion products (Hema et al. 2004). As concrete is relatively weak in tension, the tensile forces exerted by the corrosion products cause the surrounding concrete to crack (Patnaik and Baah 2015). Eventually, such cracking can lead to delaminations and potholes on the bridge deck surface, which decrease the structural integrity, ride quality, and service life of the bridge deck (Patnaik and Baah 2015).

Repair of these distresses requires removal and replacement of the damaged concrete. One technique that is especially useful for partial-depth concrete removal is hydrodemolition (Hopwood et al. 2015, Momber 2005, Wenzlick 2002). This technique, which is becoming an increasingly common practice in Utah, involves removal of deteriorated concrete from the top surface of a concrete bridge deck using a high-pressure water jet as illustrated in Figure 1-1 (Wenzlick 2002). Following removal of the old concrete, new concrete is placed to restore or increase, as needed, the original deck thickness and specified design strength (Wenzlick 2002). A surface treatment is commonly applied to the new deck surface to prevent future ingress of chloride ions and/or water (Birdsall et al. 2007, Hopwood et al. 2015, Swamy and Tanikawa 1993).

Unlike traditional concrete removal techniques such as milling, which is limited to depths shallower than the top mat of reinforcing steel (Guthrie et al. 2008), hydrodemolition can be used to remove concrete from around and even below the top mat of reinforcing steel as shown in Figure 1-2 (Wenzlick 2002). Thus, bridge decks that may no longer be suitable for repair using
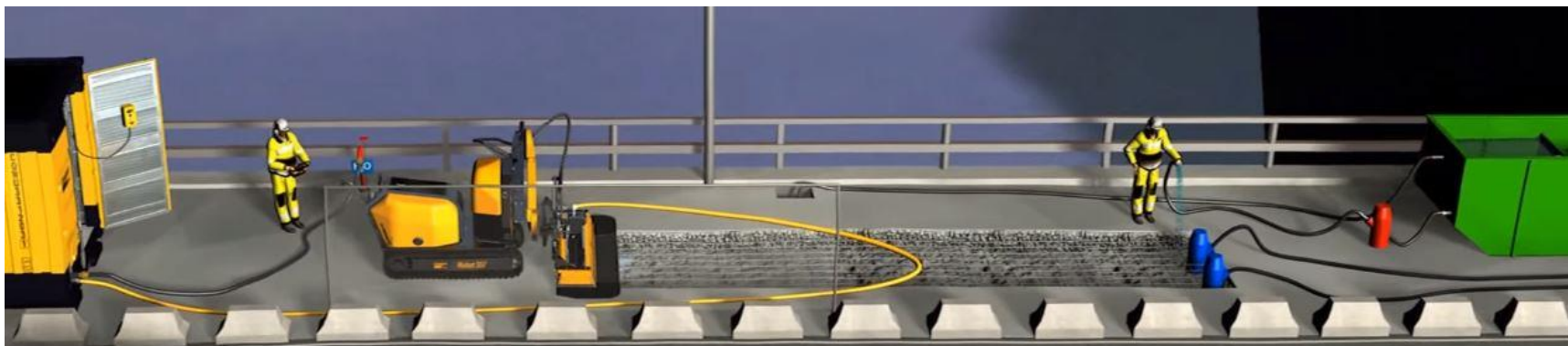
Figure 1-1: Schematic of hydrodemolition equipment.
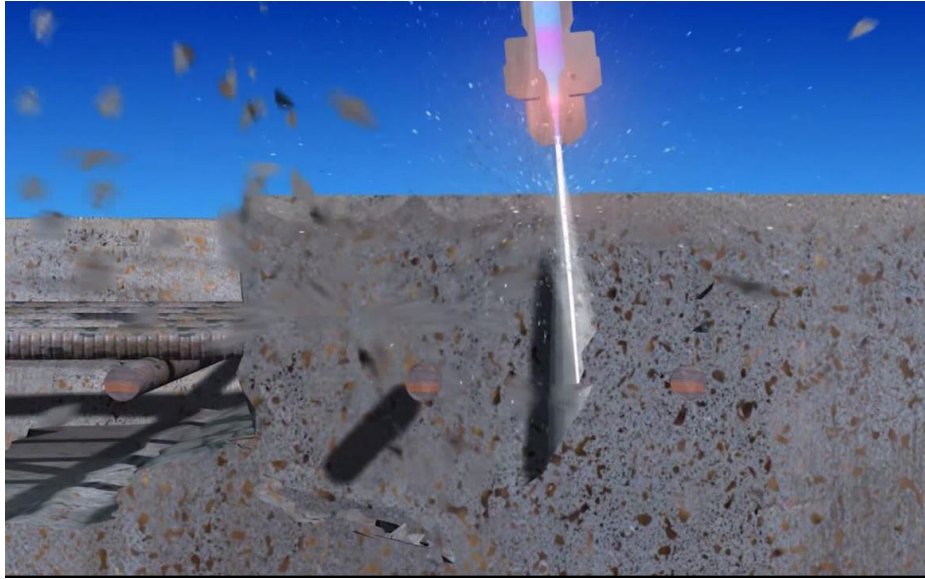
Figure 1-2: Schematic of concrete removal below the top mat of reinforcing steel using hydrodemolition equipment.

traditional concrete removal techniques, due to the development of critical chloride concentrations at depths deeper than the top mat of reinforcing steel, may still be good candidates for repair using hydrodemolition. In these cases, depending on the chloride concentrations at the time of hydrodemolition and the depth of concrete removal below the top mat of reinforcing steel, the service life of the deck may be significantly extended. Specifically, a sufficient quantity of chloride ions must be removed from the deck so that, after application of a surface treatment preventing further chloride ingress, equilibration of the remaining chloride ions in the repaired deck does not result in a chloride concentration greater than or equal to 2.0 lb of chloride per cubic yard of concrete at the top or bottom mat of reinforcing steel. While the effects of treatment timing on deck service life have been analyzed for traditional repair techniques involving removal of concrete to depths shallower than the top mat of reinforcing steel (Guthrie et al. 2008), the effects of treatment timing on deck service life have not been analyzed for repair involving hydrodemolition of concrete to depths deeper than the top mat of reinforcing steel.

When hydrodemolition is used to remove concrete to depths deeper than the top mat of reinforcing steel, the high-pressure water jet can sometimes blow through the entire depth of a concrete bridge deck, which is a very undesirable outcome (Hopwood et al. 2015). Such "blow-

throughs" result in several major problems. One is that falling concrete debris can cause personal injury to people and/or damage to property under the bridge. Another is that the holes in the deck are not only hazardous to construction workers but they prevent containment of the hydrodemolition water, which can be harmful to the environment if not properly treated prior to being released. Finally, the occurrence of blow-throughs can significantly increase the cost of bridge deck repair because of the requirement for additional formwork and concrete material. While blow-throughs have been observed to occur in deck sections characterized by extensive cracking and efflorescence, they can also occur without warning in a seemingly sound bridge deck. While some limited anecdotal information exists about potentially influential factors (ICRI 2014), structural analyses are needed to quantify the effects of water pressure, jet orifice size, angle of impact, reinforcement dimensions, and concrete compressive strength on the occurrence of blow-throughs during hydrodemolition.

1.2 Research Objectives and Scope

The objectives of this research were 1) to investigate the effects of hydrodemolition treatment timing on chloride concentration profiles in concrete bridge decks for depths of concrete removal below the top mat of reinforcing steel and 2) to investigate factors that influence the occurrence of blow-throughs in concrete bridge decks when hydrodemolition is used. The research results are intended to provide engineers with guidance about the latest timing of hydrodemolition that can maintain a chloride concentration level below 2.0 lb of chloride per cubic yard of concrete at the levels of both the top and bottom mats of reinforcing steel, as well as about conditions that may indicate a higher probability of blow-through during hydrodemolition. The scope of this research included a questionnaire survey of hydrodemolition companies to summarize common practices in the field, numerical modeling of chloride concentration to investigate hydrodemolition treatment timing on typical Utah bridge decks, and structural analysis to investigate factors that influence the occurrence of blow-throughs during hydrodemolition. In particular, the results of the questionnaire survey were used to identify appropriate inputs for the blow-through analysis.

1.3 Outline of Report

This report contains five chapters. This chapter defines the problem statement, introduces the research, and states the research objectives and scope. Chapter 2 provides background information obtained from a literature review about chloride-induced corrosion of reinforcing steel, removal of deteriorated concrete using hydrodemolition, and application of surface treatments to concrete bridge decks. Chapter 3 details the procedures for the questionnaire survey, chloride concentration analysis, and blow-through analysis, and Chapter 4 presents the results of the survey and analyses. Chapter 5 provides a summary together with conclusions and recommendations resulting from this research.

2.0 BACKGROUND

2.1 Overview

Developed from a literature review performed for this research, the following sections discuss chloride-induced corrosion of reinforcing steel, removal of deteriorated concrete using hydrodemolition, and application of surface treatments to concrete bridge decks.

2.2 Chloride-Induced Corrosion of Reinforcing Steel

With time, the diffusion and accumulation of chloride ions in reinforced concrete causes a breakdown of the protective environment that concrete naturally provides for reinforcing steel. Typically, the threshold value at which chloride ions initiate corrosion of reinforcing steel is 2.0 lb of chloride per cubic yard of concrete (Hema et al. 2004). Diffusion occurs as chloride ions move in response to spatial differences in chloride concentration (Mays 1992), traveling from areas of higher concentration to areas of lower concentration (Freeze and Cheery 1979). In cold regions, such as Utah, chloride ions are introduced to the surface of concrete bridge decks in the form of deicing salts. After dissolution in water, chloride ions can diffuse into the concrete matrix and disperse to areas of lower concentration over time (Arora et al. 1997). The depth of chloride penetration into concrete over a given time period is governed by the chloride diffusion coefficient and the chloride concentration gradient (Grace et al. 2004). The diffusion coefficient is a measure of the rate at which chloride ions can diffuse through the concrete over time, while the concentration gradient is a measure of the degree to which the ions are dispersed throughout the concrete matrix. Larger diffusion coefficients and higher concentration gradients allow the chloride ions to diffuse more rapidly through the concrete.

According to Fick's first law of diffusion, chloride ions diffuse in the direction of decreasing chloride concentration (Poulsen and Mejlbro 2006). Therefore, chloride ions can diffuse in any direction, including upward and downward, depending on the chloride concentration gradient. Thus, when new chloride-free concrete is placed on top of an existing chloride-laden concrete bridge deck, for example, chloride ions present in the existing concrete

can diffuse upwards through the new concrete and downwards through the existing concrete over time.

Especially in cold regions, winter road maintenance practices affect chloride concentrations at the surface of bridge decks through the application of deicing salts. With all other factors held constant, the surface chloride concentration for bridges that receive more deicing salt applications is higher than that of bridges that receive fewer deicing salt applications. Furthermore, precipitation leads to higher moisture contents within the concrete matrix, which causes higher diffusion coefficients and greater ionic conduction (Guthrie et al. 2006). However, lower temperatures reduce ionic mobility, which results in lower diffusion rates during periods of cold weather (Clark and Hawley 1966, Lewis 2001).

To a large degree, the water-cement ratio and degree of hydration of the concrete determine the properties of the concrete matrix. Specifically, diffusion is limited by the degree of saturation and the continuity of pore water within the concrete matrix (Survananshi et al. 1998). As the degree of saturation and the continuity of pore water increase, the rate of diffusion increases (Zhang et al. 1998). For a given concrete mixture, the external chloride loading and cover depth govern the time required for chloride ions to accumulate in critical concentrations near the reinforcing steel. Cover depths for concrete bridge decks are typically in the range of 2.0 to 3.0 in. (Hema et al. 2004) and are usually measured with reference to the transverse steel, which is frequently located above and below the longitudinal steel in the top and bottom mats of reinforcement, respectively.

Diffusion of chloride ions through the concrete matrix can lead to corrosion of the embedded reinforcing steel, deterioration of the surrounding concrete, and failure of the structure if left untreated. Various treatments and rehabilitation methods may be employed to maintain the safety and serviceability of concrete bridge decks.

2.3 Removal of Deteriorated Concrete Using Hydrodemolition

Over time, chloride-induced corrosion necessitates rehabilitation of concrete bridge decks. The cost and extent of such work are dependent on the amount of deterioration that has occurred within the concrete. If the deterioration is limited to the concrete in the upper half of the deck, partial-depth repairs are appropriate. However, if the deterioration has extended into the lower half of the deck, full-depth repair is often necessary (Wenzlick 2002). Methods for removing deteriorated concrete from a bridge deck include jackhammering, milling, and hydrodemolition (Wenzlick 2002). While the first two methods generate harmful vibrations that can induce micro-cracking in the surrounding concrete and lead to further deterioration of the deck, hydrodemolition has proven to be less damaging to the existing concrete structure when used appropriately.

Hydrodemolition is the use of high-pressure water jets to remove deteriorated concrete from the surface of a structure (ICRI 2014). In the process of rehabilitating concrete bridge decks, new concrete is placed following hydrodemolition to restore or increase, as needed, the original deck thickness and specified design strength. Hydrodemolition is typically used for partial-depth repair rather than full-depth repair. The process involves use of fully-automated, high-pressure water jets with constant pressure, frequently exceeding 20 ksi, to remove concrete from the top surface of the deck (Momber 2005). In some cases, concrete is uniformly removed to a predetermined depth, regardless of the degree of localized deterioration (Momber 2005). In other cases, a depth specification is not given, and the depth of concrete removal is governed mainly by the degree of deterioration (ICRI 2014); the high-pressure water jets are calibrated to remove low-strength and damaged concrete while leaving sound concrete in place on the concrete bridge deck (Wenzlick 2002). Therefore, in areas where concrete is in poor condition, concrete is removed to a greater depth. When the top mat of reinforcing steel is exposed, the hydrodemolition process also removes corrosion products from the steel. One to four passes of a hydrodemolition jet is typically required to achieve the desired outcomes (Momber 2005).

Specific advantages and disadvantages apply to the use of hydrodemolition as part of the rehabilitation process for a concrete bridge deck. The main advantages of hydrodemolition include increased cost effectiveness, decreased time consumption, increased adhesion between

the concrete substrate and the new concrete, and decreased damage to the existing structure (Momber 2005, Wenzlick 2002). Removing deteriorated concrete from only the upper portion of the bridge deck decreases rehabilitation costs when compared to full-depth removal, and the high-pressure water jets can remove unsound concrete at a quicker rate than other methods, such as jackhammering, which decreases the time necessary to complete rehabilitation (ICRI 2014, Wenzlick 2002). Adhesion between concrete layers increases as the greater exposed surface area of the substrate leads to improved mechanical interlock with the new concrete (Harries et al. 2013, ICRI 2014, Momber 2005); in particular, the increased pull-off strength of layers applied to hydrodemolished surfaces is a notable advantage of hydrodemolition compared to other concrete removal methods. Decreased damage to the existing structure is possible because the process does not generate harmful vibrations like jackhammering or milling (ICRI 2014, Wenzlick 2002).

The main disadvantages associated with hydrodemolition include environmental and safety concerns. Environmental concerns arise when even small quantities of the waste water, which has high levels of alkalinity and harmful solutes, bypass the collection system and enter the surrounding landscape (Momber 2005). The intensity of this problem is exacerbated when hydrodemolition is applied to bridges spanning water bodies or other environmentally sensitive areas. In these situations, extra care must be taken to also guard against the occurrence of blow-throughs, which can result from application of the high-pressure water jets to unsound concrete with extensive cracking, low-strength layers, or other defects (Hopwood 2015, ICRI 2014). Blow-throughs are also a safety concern; while people may be injured and/or property may be damaged by falling debris, the resulting holes in the bridge deck are also a significant hazard for construction personnel performing the rehabilitation work. Therefore, minimizing the occurrence of blow-throughs is critical.

2.4 Application of Surface Treatments to Concrete Bridge Decks

One method of effectively and economically disrupting the ingress of chloride ions and/or moisture is adding a surface treatment (Birdsall et al. 2007, Swamy and Tanikawa 1993). Following a rehabilitation method involving removal of deteriorated material and placement of

11

new concrete, for example, a surface treatment can be applied to seal the rehabilitated concrete deck against further chloride ingress. In some cases, application of a surface treatment can be delayed after deck rehabilitation, but the maximum extension in service life of concrete bridge decks is obtained if surface treatments are placed before chloride concentrations have reached critical levels at the top mat of reinforcing steel (Birdsall et al. 2007, Guthrie et al. 2008, Zhang et al. 1998). To achieve the desired outcome, appropriate materials, deck preparation techniques, and placement methods must be utilized (Basheer et al. 1998).

The materials generally used in surface treatments applied to concrete bridge decks include binders and aggregates. The binders are typically urethane, silicon-based, or epoxy products, which function both as adhesives and as sealants (Guthrie et al. 2005). In many instances, aggregates are mixed with or broadcast into the binders to provide skid resistance and to protect the binders from ultraviolet radiation (Guthrie et al. 2005).

Appropriate deck preparation is necessary to ensure adequate adhesion between the concrete substrate and the applied surface treatment (Pan et al. 2016). A concrete bridge deck surface should be cleaned and roughened, using shot blasting, for example, to facilitate increased bond strength between the concrete substrate and the surface treatment (Guthrie et al. 2005). Following this roughening process, all debris should be removed from the deck surface, and, depending on the moisture content of the concrete, the deck may also need to be dried (Guthrie et al. 2005); the presence of moisture on the deck surface or in the substrate can significantly reduce the bond strength (Guthrie et al. 2005, Pan et al. 2016).

Proper placement methods should be utilized to ensure that the surface treatment performs according to its design. While the materials comprising the surface treatment may be adequate, improper construction can cause premature failure of the surface treatment (Pan et al. 2016). The condition of the concrete substrate, treatment application method, amount of treatment material, curing time, and exposure to early trafficking can govern the performance of the surface treatment (Pan et al. 2016, Weyers et al. 1993).

2.5 Summary

Developed from a literature review performed for this research, this chapter discusses chloride-induced corrosion of reinforcing steel, removal of deteriorated concrete using hydrodemolition, and application of surface treatments to concrete bridge decks. With time, the diffusion and accumulation of chloride ions in reinforced concrete causes a breakdown of the protective environment that concrete naturally provides for reinforcing steel. Typically, the threshold value at which chloride ions initiate corrosion of reinforcing steel is 2.0 lb of chloride per cubic yard of concrete. Diffusion of chloride ions through the concrete matrix can lead to corrosion of the embedded reinforcing steel, deterioration of the surrounding concrete, and failure of the structure if left untreated. Various treatments and rehabilitation methods may be employed to maintain the safety and serviceability of concrete bridge decks.

Methods for removing deteriorated concrete from a bridge deck include jackhammering, milling, and hydrodemolition. Hydrodemolition is the use of high-pressure water jets to remove deteriorated concrete from the surface of a structure. Specific advantages and disadvantages apply to the use of hydrodemolition as part of the rehabilitation process for a concrete bridge deck. The main advantages of hydrodemolition include increased cost effectiveness, decreased time consumption, increased adhesion between the substrate and new concrete, and decreased damage to the existing structure. The main disadvantages associated with hydrodemolition include environmental and safety concerns.

One method of effectively and economically disrupting the ingress of chloride ions and/or moisture is adding a surface treatment. Following a rehabilitation method involving removal of deteriorated material and placement of new concrete, for example, a surface treatment can be applied to seal the rehabilitated concrete deck against further chloride ingress. To achieve the desired outcome, appropriate materials, deck preparation techniques, and placement methods must be utilized.

3.0 EXPERIMENTAL METHODOLOGY

3.1 Overview

The objectives of this research were met by conducting a questionnaire survey of hydrodemolition companies, performing numerical modeling of chloride concentration to investigate hydrodemolition treatment timing on typical Utah bridge decks, and using structural analysis to investigate factors that influence the occurrence of blow-throughs during hydrodemolition. This chapter describes the methodology employed in the survey, explains the procedures utilized for numerical modeling of chloride concentration, and details the blow-through analyses.

3.2 Questionnaire Survey

A questionnaire survey was conducted by telephone and email to assess current practices of selected hydrodemolition companies that rehabilitate concrete bridge decks throughout the country, and the survey findings were used to design the numerical experiments subsequently performed in this research. In particular, the survey results informed the numerical experiments performed to investigate factors that influence the occurrence of blow-throughs in concrete bridge decks when hydrodemolition is used. Various hydrodemolition companies were selected based on their experience with hydrodemolition of bridge decks in climates and conditions similar to those in Utah, where deicing salts are routinely applied to bridges as part of winter maintenance.

A total of five persons, who were typically the managers of the hydrodemolition companies, participated in the survey. Each survey respondent was asked the following nine questions regarding hydrodemolition procedures for concrete bridge deck rehabilitation:

- Which states are serviced by the hydrodemolition company?
- What nozzle type is used for hydrodemolition of concrete bridge decks?
- What nozzle (orifice) size is typically used for hydrodemolition of concrete bridge decks?
- What water pressure is typically used for hydrodemolition of concrete bridge decks?

- What is the flow rate of the water through the nozzle jet?

- What is the standoff distance, or height that the hydrodemolition nozzle operates above the bridge deck?

- At what angle relative to the bridge deck surface does the hydrodemolition jet typically operate?

- What is the typical transverse speed of hydrodemolition jets on concrete bridge decks?

- How often do blow-throughs of the concrete bridge deck occur during hydrodemolition?

The answers to these questions were compiled to assess the current bridge deck rehabilitation practices of these hydrodemolition companies.

3.3 Chloride Concentration Analysis

Numerical modeling was performed to investigate the effects of hydrodemolition treatment timing on chloride concentration profiles in concrete bridge decks for depths of concrete removal below the top mat of reinforcing steel. Based on communications with UDOT engineers to determine current practice, appropriate ranges of removal and overlay depths were selected for use in the modeling process. In addition, typical ranges in bridge deck thickness, original cover depth (OCD), and depth and size of steel reinforcement were selected.

Numerical modeling of chloride concentration was performed using a software program developed by the National Institute of Standards and Technology (NIST) (Bentz 2016). The program uses the one-dimensional approximation for diffusion based on Fick's second law, shown as Equation 3-1, to simulate the diffusion of chlorides through concrete (Poulsen and Mejlbro 2006):

$$\frac{\partial c}{\partial t} = D \frac{\partial^2 c}{\partial x^2} \tag{3-1}$$

where:

$\quad\quad C$ = chloride concentration, mol/m^3

$\quad\quad t$ = time, s

$\quad\quad D$ = diffusion coefficient, m^2/s

15

$x=$ position, m

The program considers several user-specified internal and external variables that affect chloride diffusion through concrete. Among the internal variables are concrete properties such as water-cement ratio, degree of hydration, volume fraction of aggregate, air content, diffusion coefficients, and initial chloride concentration. The values of these parameters were specified in this research to be the same for both the original concrete in the bridge deck and the concrete placed to restore the deck following hydrodemolition.

The external variables include average monthly temperature, surface chloride concentration, and unexposed boundary condition. Average monthly temperatures used in the numerical modeling program to represent Utah are shown in Table 3-1. The initial chloride concentration of the new concrete was assumed to be 0.0 g chloride/g cement. At the exposed boundary condition, a cyclic loading of chlorides on the top surface of the bridge deck was specified to simulate the seasonal exposure of bridges in Utah to deicing salt in the absence of a surface treatment; after a simulated surface treatment application, the chloride concentration at the top surface of the bridge deck was specified to be zero, as the treatment, if maintained over time, should prevent future ingress of chloride ions and/or water. The chloride concentration at the unexposed boundary condition was specified as "constant at zero" to reflect the absence of

Table 3-1: Monthly Temperature and Chloride Concentration Inputs for Chloride Concentration Analysis

Month	Temperature (ºC)	Chloride, C_s (mol/liter)
January	-2.3	4.273
February	1.2	3.865
March	5.4	3.326
April	9.8	2.800
May	14.9	2.429
June	20.6	2.311
July	25.5	2.479
August	24.2	2.887
September	18.4	3.427
October	11.8	3.952
November	4.9	4.324
December	-1.3	4.441

stay-in-place metal forms, which are no longer commonly used in Utah, on the bottom of the bridge deck (Guthrie et al. 2006).

The function used to approximate the surface chloride concentration through a typical year is given in Equation 3-2:

$$C = 3.38 + 1.07 \cdot cos\left(\frac{\pi \cdot t}{6}\right) \qquad\qquad (3\text{-}2)$$

where:

C = chloride concentration of pore water for month t, mol/L

t = month of year from 1 to 12 to represent January to December, respectively.

This function was developed by previous researchers at Brigham Young University (BYU) (Birdsall et al. 2007). The development process involved measurement of average chloride concentration profiles for several concrete bridge decks in Utah and use of numerical modeling to iteratively determine a single surface chloride concentration model that provided the best possible matches between simulated and measured chloride data (Birdsall et al. 2007).

As shown in Table 3-2, specific inputs for the numerical modeling program were determined from local climatic conditions and with assistance from personnel at NIST. The beginning month of exposure shown in Table 3-2 refers to the first month of the winter season when snow and icy conditions generally necessitate application of deicing salts to roads and bridges to increase driver safety. The member thickness is the deck thickness, and the water-cementitious material ratio, volume fraction of aggregate, air content, and diffusion coefficient were specified to match typical concrete mixture designs used for bridge deck construction in Utah (Birdsall et al. 2007). (To achieve a constant diffusion coefficient with time in the simulations, the constant diffusion coefficient was set to the desired value, and the initial diffusion coefficient was set to 0, as required in the numerical modeling program.) The time before exposure begins was set to reflect the expectation that a deck would not be exposed to deicing salts until at least 28 days following construction. The degree of hydration, empirical coefficient, activation energy, Langmuir isotherm constants, rate constants for binding, and cement compound contents were specified according to recommendations from NIST personnel. The external chloride concentration values were computed from Equation 3-2, which generates

Table 3-2: Concrete Exposure and Property Inputs for Chloride Concentration Analysis

Property	Value
Beginning Month of Exposure	October
Member Thickness (m)	0.203, 0.229, or 0.254
Water-Cementitious Material Ratio, w/cm	0.44
Degree of Hydration	0.8
Volume Fraction of Aggregate (%)	65
Air Content (%)	6
Initial Chloride Concentration of Concrete (g Chloride/ g Cement)	0
Initial Diffusion Coefficient, D_i (m^2/s)	0
Constant Diffusion Coefficient, D_{inf} (m^2/s)	1.30E-11
Empirical Coefficient, m	0.6
Time before Exposure Begins (days)	28
Ratio of Surface-to-Bulk Diffusion Coefficients	1
Thickness of Surface Layer (mm)	0
Activation Energy for Diffusion (kJ/mol)	40
Langmuir Isotherm Alpha Constant	1.67
Langmuir Isotherm Beta Constant	4.08
Rate Constant of Binding (s^{-1})	1.00E-07
C_3A Content of Cement (%)	5
C_4AF Content of Cement (%)	5
Rate Constant for Aluminate Reactions with Chloride (s^{-1})	1.00E-08

higher chloride concentrations for the months of October through February because these are the months that typically require deicing salt applications. Selection of the indicated values ensured as much consistency as possible with previous research performed at BYU (Birdsall et al. 2007, Guthrie et al. 2008).

For the specified bridge deck thicknesses of 8.0, 9.0, and 10.0 in., corresponding OCDs of 2.0, 2.5, and 3.0 in. (relative to the transverse reinforcing steel) were used in the simulations. Specific removal depths chosen for numerical modeling were computed as the sum of a given OCD, the diameter of a No. 5 reinforcing bar (0.625 in.) typically comprising the top mat, and an additional depth of 0.75 in. below the top mat that is assumed to occur as hydrodemolition contractors meet the required removal depth of 0.50 in. specified by UDOT (because precise control of the depth of removal is not possible, an additional 0.25 in. of concrete is assumed to be removed, on average, during the hydrodemolition process). The resulting total removal depths, which were 3.375, 3.875, and 4.375 in., effectively represent the "worst-case" scenario for the numerical modeling; with the transverse bar being used as the datum in the top mat of

reinforcing steel, the removal depths are shallower than if the longitudinal bar had been used, and the reduced removal depth corresponds to a greater amount of chloride-contaminated concrete being left in the bridge deck.

Besides removing potentially chloride-contaminated concrete from immediately around the reinforcing steel, extending the depth of concrete removal below the top mat of reinforcing steel also allows mechanical interlock with the new concrete placed after hydrodemolition. The concrete, which usually has a nominal maximum aggregate size of 0.75 in., can flow under the reinforcing steel and thereby largely eliminate the possibility of debonding from the surface of the original concrete.

Using these parameters, each simulation differed based on total duration of chloride exposure, time at which hydrodemolition is performed, OCD, depth of removal by the high-pressure water jet, and application of a surface treatment on the rehabilitated concrete deck. With these variables accounted for, extensive numerical modeling of chloride concentration profiles was performed. Specifically, crossing the various levels of the experimental factors in a full-factorial structure generated a total of 36 unique combinations, or scenarios. Specifically, the experimentation included OCDs of 2.0, 2.5, and 3.0 in. (with corresponding removal depths of 3.375, 3.875, and 4.375 in.), treatment times of 25, 30, 35, 40, 45, and 50 years following deck construction; and the presence or absence of an applied surface treatment. In the modeling, all aspects of rehabilitation, including hydrodemolition, placement of new concrete, and application of a surface treatment, as applicable, were assumed to occur at the same time. The numerical modeling for each scenario was performed at 5-year intervals for a simulated 75-year service life as recommended by the Federal Highway Administration (FHWA 2011).

Modeling of the decks without treatment was performed first to develop a baseline chloride concentration profile to which the chloride concentration profiles for various treatment times were compared. To develop the baseline profile, treatment timing was set at 1,000,000 days to ensure that the treatment would not affect the numerical modeling results during the simulation period. Modeling was then performed for each unique combination of OCD, treatment time, and surface treatment application to produce chloride concentration profiles that would be expected after rehabilitation was performed. The latest timing of rehabilitation that

maintained a chloride concentration level below 2.0 lb of chloride per cubic yard of concrete at the levels of both the top and bottom mats of reinforcing steel was identified for each unique combination of OCD and surface treatment application. Appendix A includes images of the numerical modeling program with sample inputs for rehabilitation with a surface treatment application performed at a bridge deck age of 25 years.

3.4 Blow-Through Analysis

For this research, a spreadsheet was developed to investigate six modes of failure, or blow-through, that can potentially be experienced by a concrete bridge deck during hydrodemolition. These modes of failure include bending, one-way shear, and two-way shear, each of which is analyzed in both the orientation where the length is greater than the width and in the orientation where the length is less than the width. For any of these failure modes, if the capacity of the concrete deck section is less than the relevant force or moment applied by the high-pressure water jet, blow-through can be expected. The factor of safety against blow-through is calculated as the shear or moment capacity of the simulated concrete deck section divided by the shear force or moment imparted by the high-pressure water jet.

In the spreadsheet, the concrete between two longitudinal bars and two transverse bars within the bottom mat of reinforcing steel is analyzed using the Euler-Bernoulli simplified beam theory (Gere and Goodno 2013). Figure 3-1 shows the area of analysis in the plane of the bottom mat of reinforcing steel, with the length l of the beam being equal to the spacing between
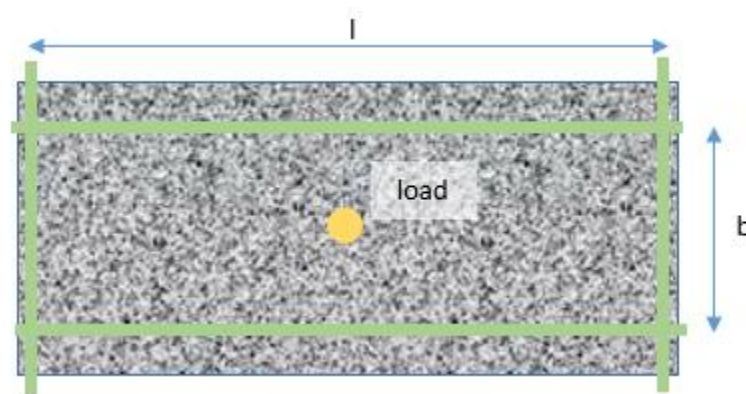
Figure 3-1: Area of blow-through analysis between two longitudinal bars and two transverse bars in the bottom mat of reinforcing steel.

longitudinal reinforcing bars and the width *b* of the beam being equal to the spacing between transverse reinforcing bars. The height of the beam is defined as the vertical distance from the middle of the longitudinal bar in the bottom mat of reinforcing steel to the hydrodemolished concrete surface between the top and bottom mats of reinforcing steel; any concrete below the bottom mat of reinforcing steel is disregarded in the analysis. Defining the beam height with reference to the longitudinal bar instead of the transverse bar in the bottom mat effectively represents the "worst-case" scenario for the analysis; because the longitudinal bar is positioned just above the transverse bar within the bottom mat of reinforcing steel, the beam height is lower for a given removal depth than if the transverse bar had been used, and the lower beam height corresponds to a higher probability of blow-through during hydrodemolition. (Because the top mat of reinforcing steel is above the hydrodemolished concrete surface, it is not included in the analysis; although the physical presence of the top mat of reinforcing steel may prevent point loading of the beam in certain locations, it is not otherwise expected to affect the occurrence of blow-throughs.)

As a simplification in this research, the concrete within the beam is assumed to be intact, without cracking or other distresses, and is also assumed to have homogenous mechanical properties, such as compressive strength. However, the perimeter of the beam is assumed to be cracked on all four sides and is assumed to be simply supported along two parallel sides coinciding with the two longitudinal bars or the two transverse bars, depending on the analysis; because this "worst-case" approach disregards the structural benefits of possible concrete continuity across the reinforcing steel, the analysis yields deliberately conservative results in this respect.

Several calculations are required in the analysis of the simulated concrete beam, including those for modulus of rupture, moment of inertia, maximum moment, cracking moment, maximum shear force, one-way shear strength, and two-way shear strength. The modulus of rupture is calculated using Equation 3-3 (McCormac and Brown 2015):

$$f_r = 7.5\lambda\sqrt{f_c'} \tag{3-3}$$

where:

f_r = modulus of rupture of the concrete beam, psi

λ = correction for unit weight of the concrete based on the type of concrete ($\lambda = 1$ for normal concrete, $\lambda = 0.85$ for sand-lightweight concrete, and $\lambda = 0.75$ for all-lightweight concrete)

f_c' = compressive strength of the concrete, psi

The moment of inertia for analysis in the cases where the length is greater than the width and where the length is less than the width is computed using Equation 3-4 (McCormac and Brown 2015):

$$I = \frac{bh^3}{12}$$ (3-4)

where:

I = moment of inertia of the concrete beam, in.$^{-4}$

b = horizontal width of the concrete beam, in.

h = vertical distance from the middle of the longitudinal bar in the bottom mat of reinforcing steel to the hydrodemolished concrete surface, in.

The maximum moment experienced by the beam is calculated using Equation 3-5 (McCormac and Brown 2015):

$$M_{max} = \frac{P \sin \theta L}{4}$$ (3-5)

where:

M_{max} = maximum moment experienced by the concrete beam, ft-lb

P = point load exerted on the deck from the high-pressure water jet, lb

θ = angle between the jet and the deck surface with respect to vertical (0 degrees is perpendicular to the horizontal plane of the deck surface), degrees

L = horizontal length of the concrete beam, in.

The cracking moment of the concrete beam is calculated using Equation 3-6 (McCormac and Brown 2015):

$$M_{cr} = \frac{f_r I}{y}$$ (3-6)

where:

M_{cr} = cracking moment of the concrete beam, ft-lb

f_r = modulus of rupture of the concrete beam, psi

I = moment of inertia, in.$^{-4}$

y = vertical distance to the neutral axis of the beam from the middle of the
longitudinal bar on the bottom mat of reinforcing steel, in.

The maximum shear force experienced by the beam is calculated using Equation 3-7 (McCormac and Brown 2015):

$$V_{max} = \frac{P \sin \theta}{2} \qquad (3\text{-}7)$$

where:

V_{max} = maximum shear force experienced by the concrete beam, lb

P = point load exerted on the deck surface from the high-pressure water jet, lb

θ = angle between the jet and the deck surface with respect to vertical (0 degrees
is perpendicular to the horizontal plane of the deck surface), degrees

The one-way shear strength of the beam is computed using Equation 3-8 (McCormac and Brown 2015):

$$V_{c1} = 2\lambda\sqrt{f_c'}bh \qquad (3\text{-}8)$$

where:

V_{c1} = one-way shear strength of the concrete beam, lb

λ = correction for unit weight of the concrete based on the type of concrete ($\lambda = 1$
for normal concrete, $\lambda = 0.85$ for sand-lightweight concrete, and $\lambda = 0.75$ for
all-lightweight concrete)

f_c' = compressive strength of the concrete, psi

b = horizontal width of the concrete beam, in.

h = vertical distance from the middle of the longitudinal bar in the bottom mat of
reinforcing steel to the hydrodemolished concrete surface, in.

The two-way shear strength, or punching shear strength, of the concrete beam is calculated using Equation 3-9 (McCormac and Brown 2015):

$$V_{c2} = 4\lambda\sqrt{f_c'}bh \qquad\qquad (3\text{-}9)$$

where:

V_{c2} = two-way shear strength, or punching shear, of the concrete beam, lb

λ = correction for unit weight of the concrete based on the type of concrete ($\lambda = 1$ for normal concrete, $\lambda = 0.85$ for sand-lightweight concrete, and $\lambda = 0.75$ for all-lightweight concrete)

f_c' = compressive strength of the concrete, psi

b = horizontal width of the concrete beam, in.

h = vertical distance from the middle of the longitudinal bar in the bottom mat of reinforcing steel to the hydrodemolished concrete surface, in.

The bridge deck parameters that were used as inputs in the blow-through analysis are bridge deck thickness, OCD, reinforcing bar size, longitudinal rebar spacing, transverse rebar spacing, type of concrete, concrete compressive strength, and removal depth. The bridge deck thickness typically varies from 7.0 to 10.0 in., with OCD values ranging from 2.0 to 3.0 in. The reinforcing bar size for bridge decks usually ranges from No. 4 to No. 10, and the transverse and longitudinal bars are assumed to be the same size in the analysis. Typically, the longitudinal bar spacing is 12 in., while the transverse bar spacing ranges from 6 to 12 in. The types of concrete that can be evaluated in the analysis include normal-weight, sand-lightweight, and all-lightweight concrete. The concrete compressive strength should be in the range of 1,000 to 9,000 psi, and it should be measured prior to hydrodemolition; if cores cannot be tested, estimates of the compressive strength may be obtained using a nondestructive device such as the Schmidt rebound hammer, for example. The removal depth is assumed to range from 0.25 to 1.50 in. below the bottom of the transverse bar in the top mat of reinforcing steel.

The hydrodemolition equipment parameters that were used as inputs in the blow-through analysis are orifice size, water pressure, and angle of jet with respect to vertical. The ranges of these parameters were selected using the results of the questionnaire survey. The orifice diameter

typically ranges from 0.10 to 0.25 in.; while smaller diameters can be used, diameters larger than 0.25 in. are not recommended for hydrodemolition of concrete bridge decks. Water pressure varies from 10 to 40 ksi. The angle of the jet ranges from 0 to 90 degrees, where 0 degrees is perpendicular to the horizontal plane of the deck surface. In the blow-through analysis, the high-pressure water jet is assumed to have a cross-sectional diameter equal to the orifice diameter as it contacts the deck surface, and the force of the jet on the deck surface is therefore calculated as the product of the orifice area and the water pressure.

Following development of the spreadsheet, numerical experiments were performed to investigate factors that influence the occurrence of blow-throughs in concrete bridge decks when hydrodemolition is used. In one experiment, the main effect of each input variable on the occurrence of blow-throughs was evaluated by sequentially changing the value of the given variable across a typical range while holding the values of all other variables constant. In another experiment, the interactions among selected input variables were evaluated through a full-factorial experimental design set up to specifically simulate conditions representative of current UDOT practice. For the full-factorial experiment, the remaining concrete thickness above the bottom mat of reinforcing steel was held constant at 2.0 in., representing a removal depth of 0.75 in. below the bottom of the top mat of reinforcing steel; this is the average removal depth that is assumed to occur as hydrodemolition contractors meet the required removal depth of 0.50 in. typically specified by UDOT for hydrodemolition of concrete bridge decks.

Finally, the blow-through analysis was applied to two case studies on bridge decks in northern Utah that were rehabilitated using hydrodemolition. One bridge deck, which was constructed in 1972 and rehabilitated in 2015 at an age of 43 years, experienced significant blow-throughs; the other bridge deck, which was constructed in 1988 and rehabilitated in 2016 at an age of 28 years, experienced insignificant blow-throughs. In each case study, possible values of input variables were selected from bridge plans provided by UDOT, photographs and measurements taken during and after hydrodemolition, and information obtained from the hydrodemolition contractors. Specifically, supporting information from the bridge plans is given in Appendices B and C for case studies #1 and #2, respectively. Compilation of this information

allowed development of expected "worst-case" scenarios that were then investigated for each deck using the blow-through analysis.

3.5 Summary

The objectives of this research were met by conducting a questionnaire survey of hydrodemolition companies, performing numerical modeling of chloride concentration to investigate hydrodemolition treatment timing on typical Utah bridge decks, and using structural analysis to investigate factors that influence the occurrence of blow-throughs during hydrodemolition. This chapter describes the methodology employed in the survey, explains the procedures utilized for numerical modeling of chloride concentration, and details the blow-through analyses.

A questionnaire survey was conducted by telephone and email to assess current practices of selected hydrodemolition companies that rehabilitate concrete bridge decks throughout the country. The survey findings were used to design the numerical experiments performed to investigate factors that influence the occurrence of blow-throughs in concrete bridge decks when hydrodemolition is used. A total of five survey participants, who were typically the managers of the hydrodemolition companies, responded to the survey, and their answers were compiled to assess the current bridge deck rehabilitation practices of these hydrodemolition companies.

Numerical modeling was performed to investigate the effects of hydrodemolition treatment timing on chloride concentration profiles in concrete bridge decks for depths of concrete removal below the top mat of reinforcing steel. Based on communications with UDOT engineers to determine current practice, appropriate ranges of removal and overlay depths were selected for use in the modeling process. Crossing the various levels of the experimental factors in a full-factorial structure generated a total of 36 unique combinations, or scenarios. Modeling of the decks without treatment was performed first to develop a baseline chloride concentration profile to which the chloride concentration profiles for various treatment times were compared. Modeling was then performed for each unique combination of OCD, treatment time, and surface treatment application to produce chloride concentration profiles that would be expected after

rehabilitation was performed. The latest timing of rehabilitation that maintained a chloride concentration level below 2.0 lb of chloride per cubic yard of concrete at the levels of both the top and bottom mats of reinforcing steel was identified for each unique combination of OCD and surface treatment application.

For this research, a spreadsheet was developed to investigate six modes of failure, or blow-through, that can potentially be experienced by a concrete bridge deck during hydrodemolition. These modes of failure include bending, one-way shear, and two-way shear, each of which is analyzed in both the orientation where the length is greater than the width and in the orientation where the length is less than the width. For any of these failure modes, if the capacity of the concrete deck section is less than the relevant force or moment applied by the high-pressure water jet, blow-through can be expected. The factor of safety against blow-through is calculated as the shear or moment capacity of the concrete section divided by the shear force or moment imparted by the high-pressure water jet. Several calculations are required in the analysis of the simulated concrete beam, including those for modulus of rupture, moment of inertia, maximum moment, cracking moment, maximum shear force, one-way shear strength, and two-way shear strength. The bridge deck parameters that were used as inputs in the blow-through analysis are bridge deck thickness, OCD, reinforcing bar size, longitudinal rebar spacing, transverse rebar spacing, type of concrete, concrete compressive strength, and removal depth. The hydrodemolition equipment parameters that were used as inputs in the blow-through analysis are orifice size, water pressure, and angle of jet. Following development of the spreadsheet, numerical experiments were performed to investigate factors that influence the occurrence of blow-throughs in concrete bridge decks when hydrodemolition is used. Finally, the blow-through analysis was applied to two case studies on bridge decks in northern Utah that were rehabilitated using hydrodemolition.

4.0 RESULTS AND ANALYSIS

4.1 Overview

This chapter presents the results of the questionnaire survey, chloride concentration analysis, and blow-through analysis performed in this research.

4.2 Questionnaire Survey

The responses received in the questionnaire survey conducted to assess current practices of selected hydrodemolition companies are shown in Table 4-1. All of the survey participants provide hydrodemolition services in states with harsh winter climates, similar to Utah, which necessitate the use of deicing salts on bridge decks and other roadways to ensure a higher level of driver safety when temperatures are below freezing. While some respondents indicated that certain parameters vary, depending on the project, the information in Table 4-1 is valuable for understanding typical practices and was used to design the numerical experiments performed to investigate factors that influence the occurrence of blow-throughs in concrete bridge decks when hydrodemolition is used.

The survey responses indicate that both oscillating and rotating nozzle types are used in hydrodemolition of concrete bridge decks. An oscillating nozzle oscillates in the longitudinal direction as it moves transversely across the deck along a track while inclined at a fixed angle that sprays the water jet in the direction of transverse movement (ICRI 2014). A rotating nozzle rotates about its center while maintaining a slight fixed angle with respect to its vertical axis as it moves transversely across the deck along a track. In the past, hydrodemolition projects involving concrete bridge decks typically used an oscillating nozzle; however, current practice is moving towards use of the more efficient rotating nozzle. A typical orifice size is either 0.10 in. or 0.25 in, with most of the respondents using 0.10 in. Some respondents indicated that an orifice size of 0.25 in. is inappropriate for hydrodemolition of concrete bridge decks because the greater force exerted by the high-pressure water jet with a larger orifice size increases the likelihood of blow-throughs. The water pressure ranges from 10 to 40 ksi, and flow rates generally range from 40 to

Table 4-1: Questionnaire Survey Results

Company	States Serviced	Nozzle Type	Orifice Size (in.)	Water Pressure (ksi)	Flow Rate (gpm)	Standoff Distance (in.)	Jet Angle (degrees)	Transverse Speed (fps)	Blow-through
A	HI, MA, NJ, UT	Oscillating	Varies	10-40	Unknown	Varies	Unknown	Varies	Occurs Regularly
B	Midwest, TX	Oscillating	0.25	12-20	50-70	2.0	20	Varies	Occurs Regularly
C	Midwest, AK, CA, WA	Rotating	0.10	15-30	40	< 1.0	Unknown	Varies	Occurs Regularly
D	GA, LA, MI, NY, OH, UT	Rotating	0.10	34	48	0.5	Unknown	0.5	Occurs Regularly
E	FL, NV, UT	Oscillating	0.10	20	43	1.0	0-15	Varies	Occurs Regularly

70 gallons per minute. The standoff distance, or the height that the hydrodemolition nozzle operates above the bridge deck, varies between 0.5 and 2.0 in., and the maximum jet angle relative to vertical is reported to be 15 or 20 degrees. While one respondent indicated that the transverse speed of the water jet is about 0.5 fps, all other respondents indicated that it varies by project.

All survey participants reported that blow-throughs are a common occurrence when using hydrodemolition on concrete bridge decks. A few mentioned that blow-throughs are most common on bridge decks with efflorescence on the underside of the deck, which is usually an indication that the deck has experienced extensive cracking and may have high chloride concentrations. As previously discussed in Chapters 1 and 2, chloride ions from deicing salts can lead to corrosion of the reinforcing steel and deterioration of the surrounding concrete. Blow-throughs can then occur as the high-pressure water jet breaks through the unsound concrete.

4.3 Chloride Concentration Analysis

The numerical modeling performed to investigate the effects of hydrodemolition treatment timing on chloride concentration profiles in concrete bridge decks for depths of concrete removal below the top mat of reinforcing steel generated chloride concentration profiles through a 75-year service life given a specific OCD, treatment time, and surface treatment usage. From these profiles, graphs of chloride concentration through time at the levels of both the top and bottom mats of reinforcing steel were prepared for each OCD value and surface treatment usage included in the modeling. Examples of graphs prepared for the top and bottom mats of reinforcing steel are given in Figures 4-1 and 4-2, respectively, for a bridge deck with a 2.0-in. OCD, a 3.375-in. removal depth, and an applied surface treatment, while similar graphs for the same conditions but without an applied surface treatment are given in Figures 4-3 and 4-4. Simulated treatment times are shown at 5-year intervals from 25 to 50 years of deck age, which is typical of current practice in Utah.

The full sets of figures are provided in Appendices D through G. For each treatment year, these figures were used to determine the maximum chloride concentration that would occur at
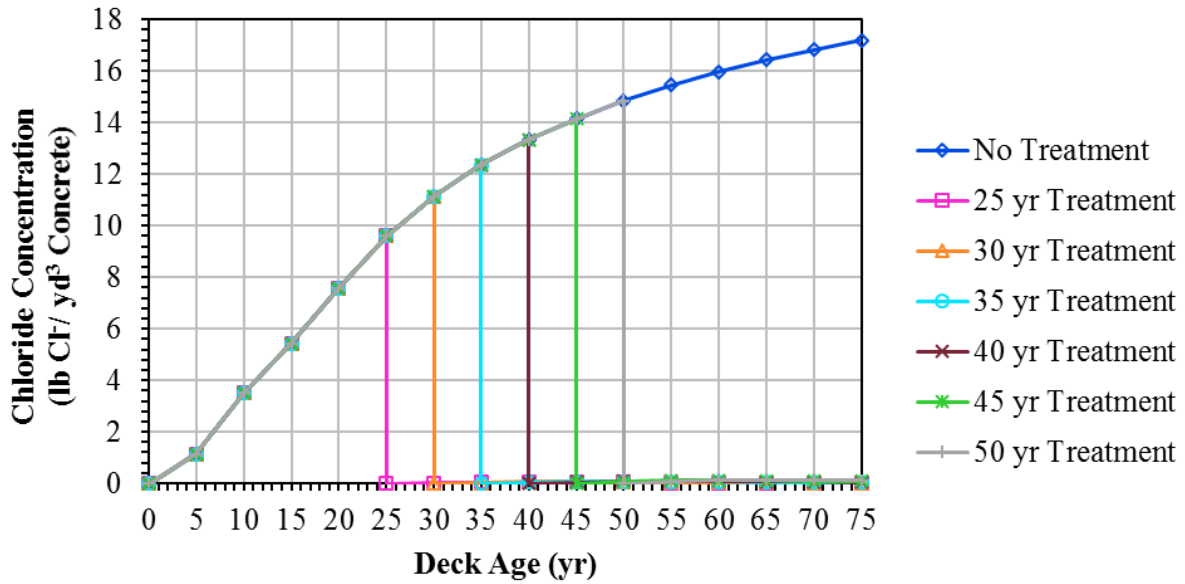
Figure 4-1: Simulated chloride concentrations at the top mat of reinforcement for a deck with a 2.0-in. OCD and a 3.375-in. removal depth with an applied surface treatment.
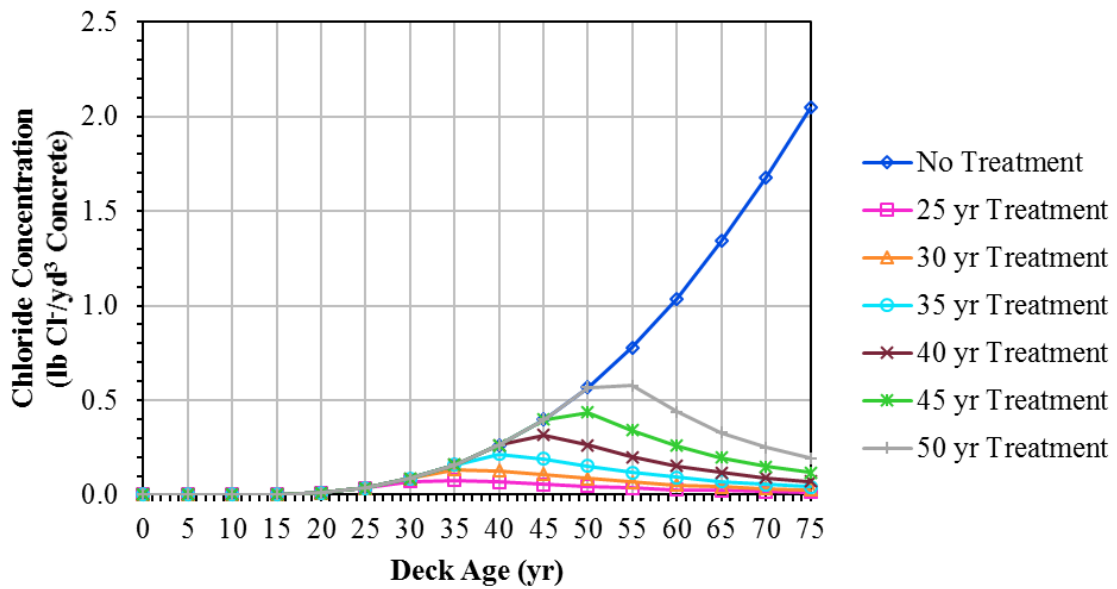
Figure 4-2: Simulated chloride concentrations at the bottom mat of reinforcement for a deck with a 2.0-in. OCD and a 3.375-in. removal depth with an applied surface treatment.
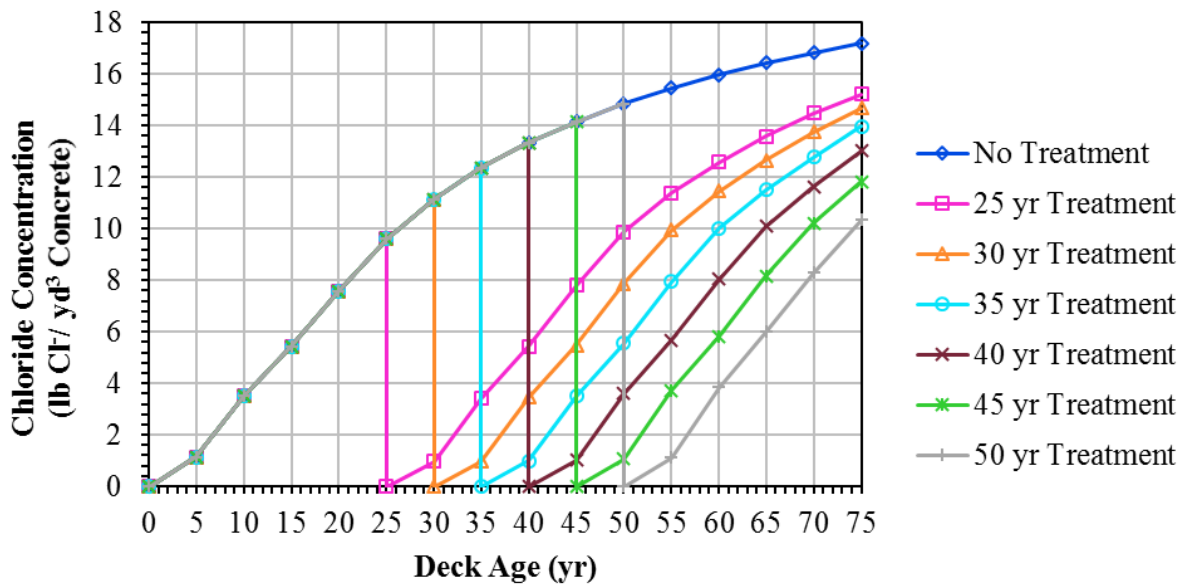
Figure 4-3: Simulated chloride concentrations at the top mat of reinforcement for a deck with a 2.0-in. OCD and a 3.375-in. removal depth without an applied surface treatment.
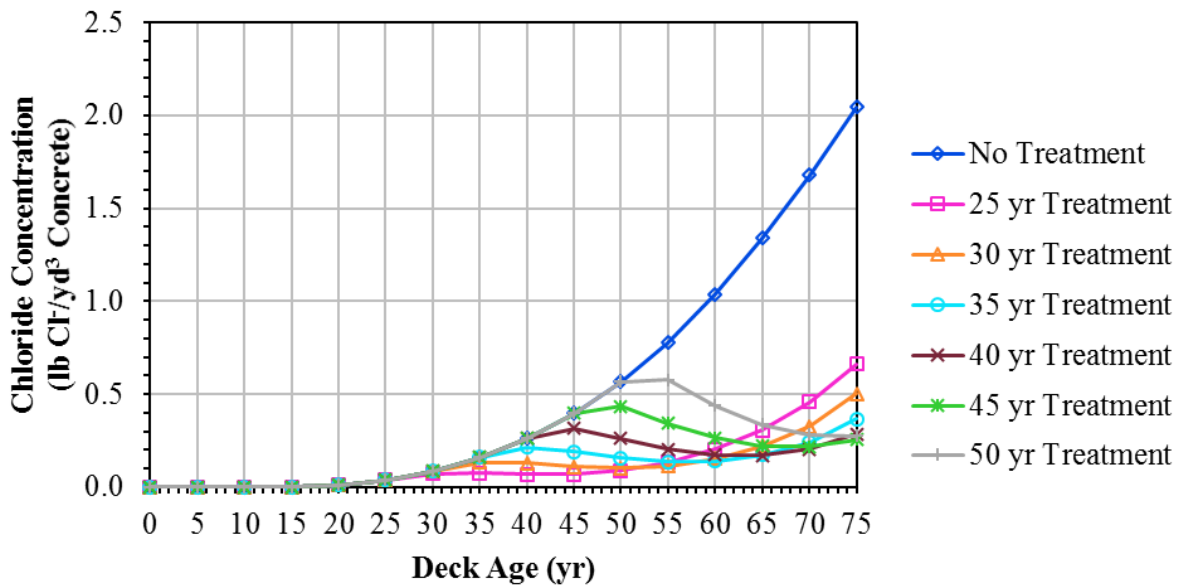
Figure 4-4: Simulated chloride concentrations at the bottom mat of reinforcement for a deck with a 2.0-in. OCD and a 3.375-in. removal depth without an applied surface treatment.

both mats of reinforcing steel after hydrodemolition and the deck age at which these maximum values occurred. In addition, when the maximum chloride concentration was greater than the threshold of 2.0 lb of chloride per cubic yard of concrete, the deck age at which the threshold was reached was also determined.

Tables 4-2 to 4-7 summarize the results obtained for the 36 unique scenarios that were produced from crossing the various levels of the experimental factors. Consistent with the numerical modeling, the treatment years and deck ages shown in the tables are rounded to the nearest 5 years, as the exact deck ages at which either the maximum chloride concentrations were reached or the chloride concentrations exceeded the threshold value were not calculated.

Table 4-2: Maximum Chloride Concentrations for a 2.0-in. OCD with a Surface Treatment

Treatment Year	Maximum Chloride Concentration after Treatment at Top Mat (lb Cl^-/yd^3 Concrete)	Year of Maximum Value at Top Mat	Maximum Chloride Concentration after Treatment at Bottom Mat (lb Cl^-/yd^3 Concrete)	Year of Maximum Value at Bottom Mat
25	0.04	40	0.08	35
30	0.06	45	0.13	35
35	0.07	50	0.21	40
40	0.09	55	0.32	45
45	0.12	60	0.44	50
50	0.15	65	0.58	55

Table 4-3: Maximum Chloride Concentrations for a 2.5-in. OCD with a Surface Treatment

Treatment Year	Maximum Chloride Concentration after Treatment at Top Mat (lb Cl^-/yd^3 Concrete)	Year of Maximum Value at Top Mat	Maximum Chloride Concentration after Treatment at Bottom Mat (lb Cl^-/yd^3 Concrete)	Year of Maximum Value at Bottom Mat
25	0.02	40	0.03	35
30	0.03	45	0.06	40
35	0.04	50	0.09	40
40	0.06	55	0.15	45
45	0.07	60	0.22	50
50	0.09	65	0.31	55

Table 4-4: Maximum Chloride Concentrations for a 3.0-in. OCD with a Surface Treatment

Treatment Year	Maximum Chloride Concentration after Treatment at Top Mat (lb Cl⁻/yd³ Concrete)	Year of Maximum Value at Top Mat	Maximum Chloride Concentration after Treatment at Bottom Mat (lb Cl⁻/yd³ Concrete)	Year of Maximum Value at Bottom Mat
25	0.01	40	0.01	35
30	0.02	45	0.03	40
35	0.03	50	0.05	45
40	0.04	55	0.07	50
45	0.05	60	0.11	50
50	0.06	65	0.16	55

Table 4-5: Maximum Chloride Concentrations for a 2.0-in. OCD without a Surface Treatment

Treatment Year	Maximum Chloride Concentration after Treatment at Top Mat (lb Cl⁻/yd³ Concrete)	Year of Maximum Value at Top Mat	Maximum Chloride Concentration after Treatment at Bottom Mat (lb Cl⁻/yd³ Concrete)	Year of Maximum Value at Bottom Mat	Year Chloride Concentration at Top Mat ≥ 2.0 lb Cl⁻/yd³ Concrete
25	15.21	75	0.66	75	35
30	14.68	75	0.50	75	40
35	13.97	75	0.37	75	45
40	13.01	75	0.32	45	50
45	11.84	75	0.44	50	55
50	10.34	75	0.58	55	60

Tables 4-2, 4-3, and 4-4 show the results for a bridge deck with an applied surface treatment for OCD values of 2.0, 2.5, and 3.0 in., respectively. The results indicate that, when a surface treatment is used, the concentration at either the top or bottom mat of reinforcing steel does not reach or exceed 2.0 lb of chloride per cubic yard of concrete after rehabilitation during the 75 years of simulated bridge deck service life. With a majority of the original chloride ions being removed during the hydrodemolition process and with a surface treatment preventing further chloride ion ingress after hydrodemolition, changes in the chloride concentration over time are caused by upward and downward diffusion of the chloride ions that remain in the

Table 4-6: Maximum Chloride Concentrations for a 2.5-in. OCD without a Surface Treatment

Treatment Year	Maximum Chloride Concentration after Treatment at Top Mat (lb Cl⁻/yd³ Concrete)	Year of Maximum Value at Top Mat	Maximum Chloride Concentration after Treatment at Bottom Mat (lb Cl⁻/yd³ Concrete)	Year of Maximum Value at Bottom Mat	Year Chloride Concentration at Top Mat ≥ 2.0 lb Cl⁻/ yd³ Concrete
25	11.83	75	0.29	75	40
30	11.03	75	0.21	75	45
35	10.09	75	0.15	75	50
40	8.95	75	0.15	45	55
45	7.53	75	0.22	50	60
50	5.77	75	0.31	55	65

Table 4-7: Maximum Chloride Concentrations for a 3.0-in. OCD without a Surface Treatment

Treatment Year	Maximum Chloride Concentration after Treatment at Top Mat (lb Cl⁻/yd³ Concrete)	Year of Maximum Value at Top Mat	Maximum Chloride Concentration after Treatment at Bottom Mat (lb Cl⁻/yd³ Concrete)	Year of Maximum Value at Bottom Mat	Year Chloride Concentration at Top Mat ≥ 2.0 lb Cl⁻/ yd³ Concrete
25	9.28	75	0.13	75	45
30	8.37	75	0.09	75	50
35	7.32	75	0.06	75	55
40	6.13	75	0.07	50	60
45	4.82	75	0.11	50	65
50	3.62	75	0.16	55	70

original concrete substrate. Due to their closer proximity to the bottom mat of reinforcing steel, the chloride ions reach maximum values at the bottom mat 5 to 10 years before they reach maximum values at the top mat, and the maximum values at the bottom mat are generally at least twice as high as the maximum values at the top mat.

Tables 4-5, 4-6, and 4-7 show the results for a bridge deck without an applied surface treatment for OCD values of 2.0, 2.5, and 3.0 in., respectively. The results indicate that, when a

surface treatment is not used, the chloride concentration at the top mat of reinforcing steel exceeds 2.0 lb of chloride per cubic yard of concrete within 10, 15, and 20 years after rehabilitation for OCD values of 2.0, 2.5, and 3.0 in., respectively. Although a majority of the original chloride ions are removed during the hydrodemolition process, the absence of a surface treatment allows further chloride ion ingress after hydrodemolition. Therefore, changes in chloride concentration over time are caused not only by upward and downward diffusion of the chloride ions that remain in the original concrete substrate, but also by chloride ingress that results from the application of deicing salts. The results of the numerical modeling clearly suggest that a surface treatment should be applied as part of the rehabilitation process to seal the deck against further chloride ingress; although the results indicate that the chloride concentration at the bottom mat of reinforcing steel does not reach or exceed 2.0 lb of chloride per cubic yard of concrete during the 75 years of simulated bridge deck service life, the top mat of reinforcing steel will experience chloride-induced corrosion beginning 10 to 20 years after rehabilitation without an applied surface treatment.

4.4 Blow-Through Analysis

The numerical experiments performed to investigate factors that influence the occurrence of blow-throughs in concrete bridge decks when hydrodemolition is used generated results in terms of the main effect of each input variable on the occurrence of blow-throughs and interactions among selected input variables. In addition, the blow-through analysis was applied to two bridge decks in northern Utah that were rehabilitated using hydrodemolition. For each analysis, blow-through can be expected when the calculated factor of safety is less than 1.0, but a minimum factor of safety of 3.0, as commonly specified in engineering practice, is desired to guard against blow-through.

Regarding the main effects of each input variable on the occurrence of blow-throughs, Table 4-8 lists the range, interval, and average for each input parameter that was varied in the experimentation. The parameters include transverse rebar spacing, concrete compressive strength, depth of removal below the bottom of the top reinforcing mat, orifice size, water pressure, and jet angle. The parameters that were held constant include reinforcing bar size,

Table 4-8: Ranges of Parameters for Evaluation of Main Effects in Blow-Through Analysis

Statistic	Transverse Rebar Spacing (in.)	Concrete Compressive Strength (psi)	Depth of Removal below Bottom of Top Reinforcing Mat (in.)	Orifice Size (in.)	Water Pressure (ksi)	Jet Angle (degrees)
Range	6-12	2,000-8,000	0.25-1.25	0.10, 0.25	10-40	0-20
Interval	1	1,000	0.25	NA	5	5
Average	9	5,000	0.75	0.10	25	10

longitudinal rebar spacing, and concrete type. Specifically, based on typical UDOT practice, a No. 5 reinforcing bar size was assumed, the longitudinal rebar spacing was set at 12 in., and normal concrete, as opposed to lightweight concrete, was specified.

The main effects are presented in Figures 4-5 to 4-10, in which a dashed horizontal line marks a factor of safety of 3.0. The factor of safety significantly increases with increasing values of transverse rebar spacing and concrete compressive strength and decreasing values of depth of removal below the bottom of the top reinforcing mat, orifice size, and water pressure within the ranges of these parameters investigated in this experimentation. The factor of safety is relatively insensitive to jet angle. While a factor of safety less than 1.0 did not occur in these analyses of main effects, a factor of safety less than 3.0 occurred for an orifice size of 0.25 in., which supports the observation by some questionnaire survey respondents who indicated that an orifice size of 0.25 in. is inappropriate for hydrodemolition of concrete bridge decks because the greater force exerted by the high-pressure water jet with a larger orifice size increases the likelihood of blow-throughs. In all cases, the governing mode of failure for each parameter investigated in the experiment was the bending moment in the orientation where the length of the concrete beam is greater than the width of the concrete beam.

Regarding the interactions among selected input variables, Table 4-9 lists the range and interval for each input parameter that was varied in the experimentation. The parameters include transverse rebar spacing, concrete compressive strength, and water pressure. The parameters that were held constant include reinforcing bar size, longitudinal rebar spacing, concrete type, depth
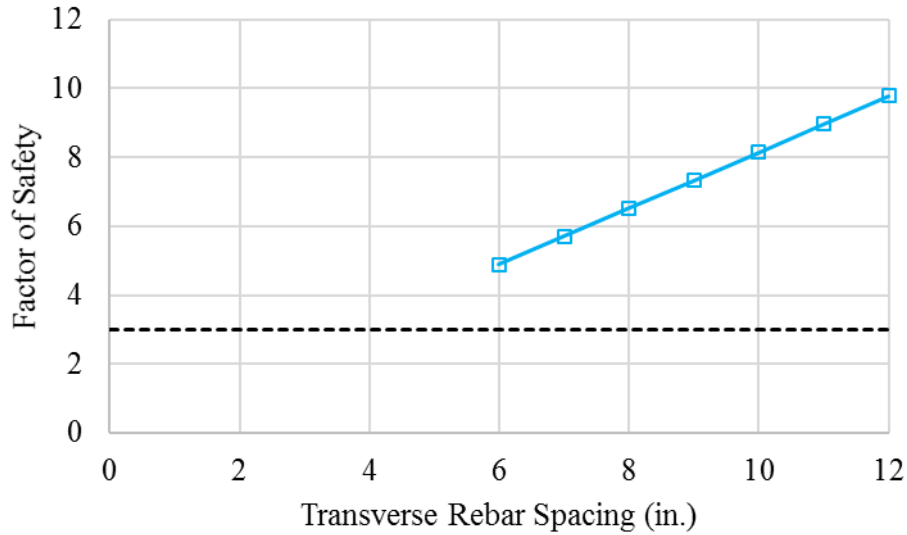
Figure 4-5: Main effect of transverse rebar spacing.
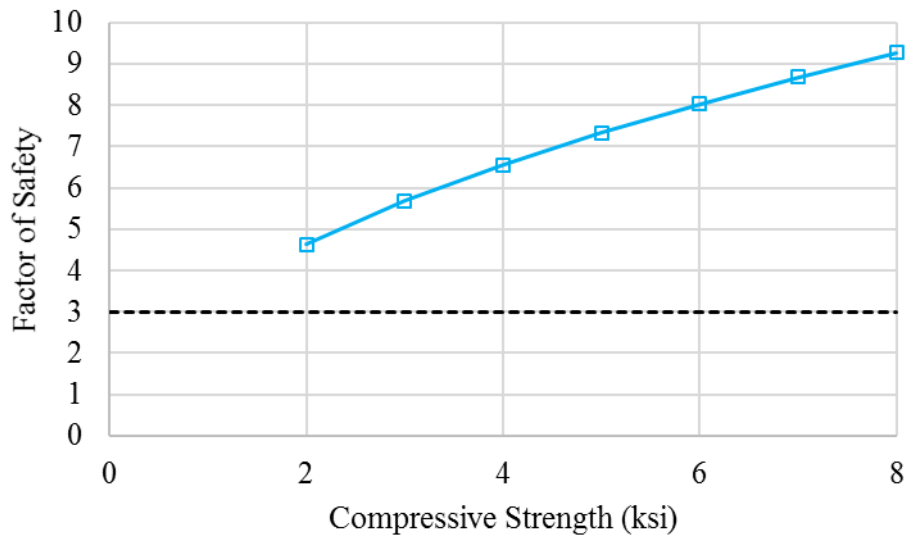
Figure 4-6: Main effect of concrete compressive strength.

of removal below the bottom of the top reinforcing mat, orifice size, and jet angle. Specifically, based on typical UDOT practice, a No. 5 reinforcing bar size was assumed, the longitudinal rebar spacing was set at 12 in., normal concrete was specified, the depth of removal below the bottom of the top reinforcing mat was set at 0.75 in., the orifice size was set at 0.10 in., and the jet angle was set at 10 degrees. As previously stated, a depth of removal of 0.75 in. below the top
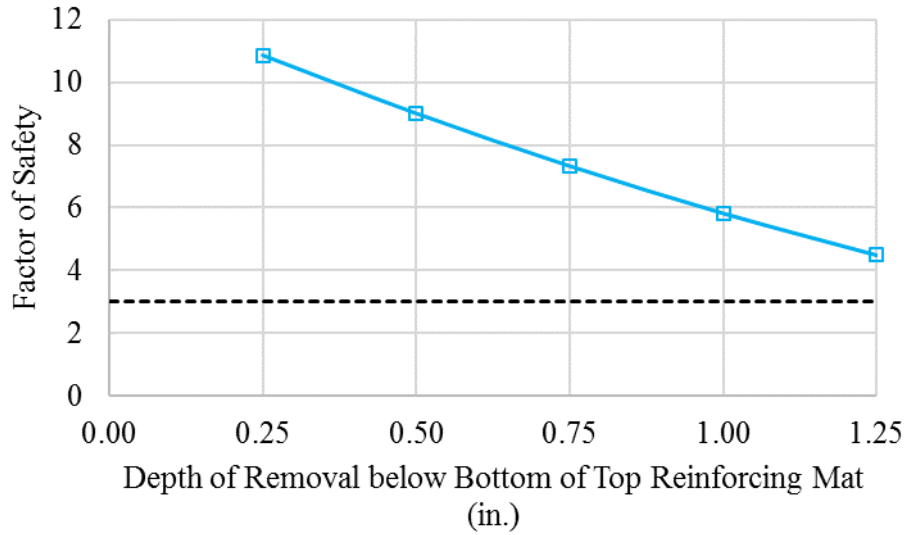
Figure 4-7: Main effect of depth of removal below bottom of top reinforcing mat.
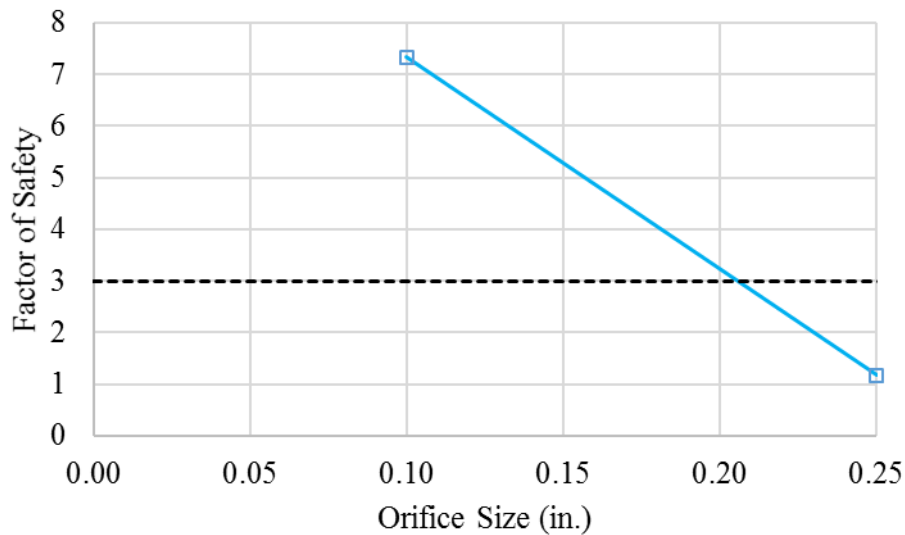
Figure 4-8: Main effect of orifice size.

reinforcing mat corresponds to a remaining concrete thickness above the bottom reinforcing mat of 2.0 in. The orifice size was held constant at 0.10 in. because that was the orifice size used by the majority of the survey respondents, and the results of the earlier experimentation (in terms of the main effect of each input variable) support selection of this value for minimizing the occurrence of blow-through. A jet angle of 10 degrees with respect to the vertical axis of the nozzle was selected as an average value for most hydrodemolition projects.

39
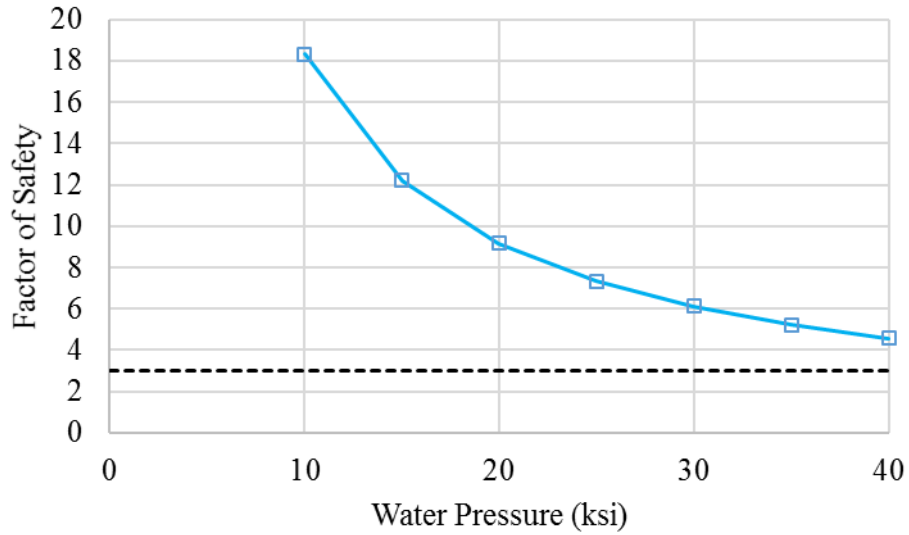
Figure 4-9: Main effect of water pressure.
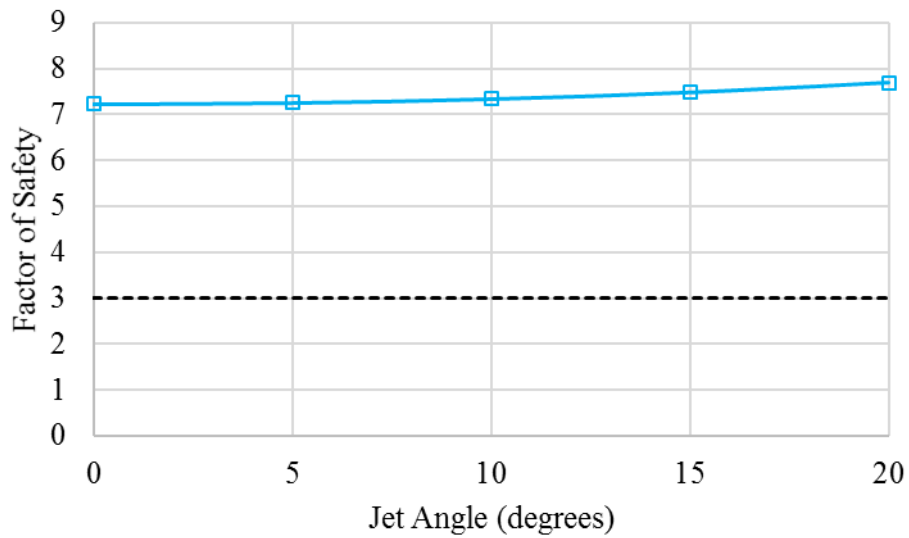
Figure 4-10: Main effect of jet angle.

Table 4-9: Ranges of Parameters for Evaluation of Interactions in Blow-Through Analysis

Statistic	Transverse Rebar Spacing (in.)	Concrete Compressive Strength (psi)	Water Pressure (ksi)
Range	6-12	2,000-8,000	10-40
Interval	2	2,000	10

The interactions are presented in Figures 4-11 to 4-14, in which a dashed horizontal line again marks a factor of safety of 3.0. While a factor of safety less than 1.0 did not occur in these analyses of interactions, a factor of safety less than 3.0 occurred for four combinations of the input parameters. The specific values of transverse rebar spacing, concrete compressive strength, and water pressure in those combinations are presented in Table 4-10. The values typically represent low transverse rebar spacing, low concrete compressive strength, and high water pressure. These combinations, and equivalent combinations not explicitly analyzed, should be avoided in practice to minimize the occurrence of blow-through during hydrodemolition. Furthermore, because the analysis performed in this research does not directly account for the possibility of cracking within the simulated concrete beam, the actual factors of safety may be considerably lower than those calculated and reported in Figures 4-5 to 4-14. In all cases, the governing mode of failure for each parameter investigated in the experiment was the bending moment in the orientation where the length of the concrete beam is greater than the width of the concrete beam.
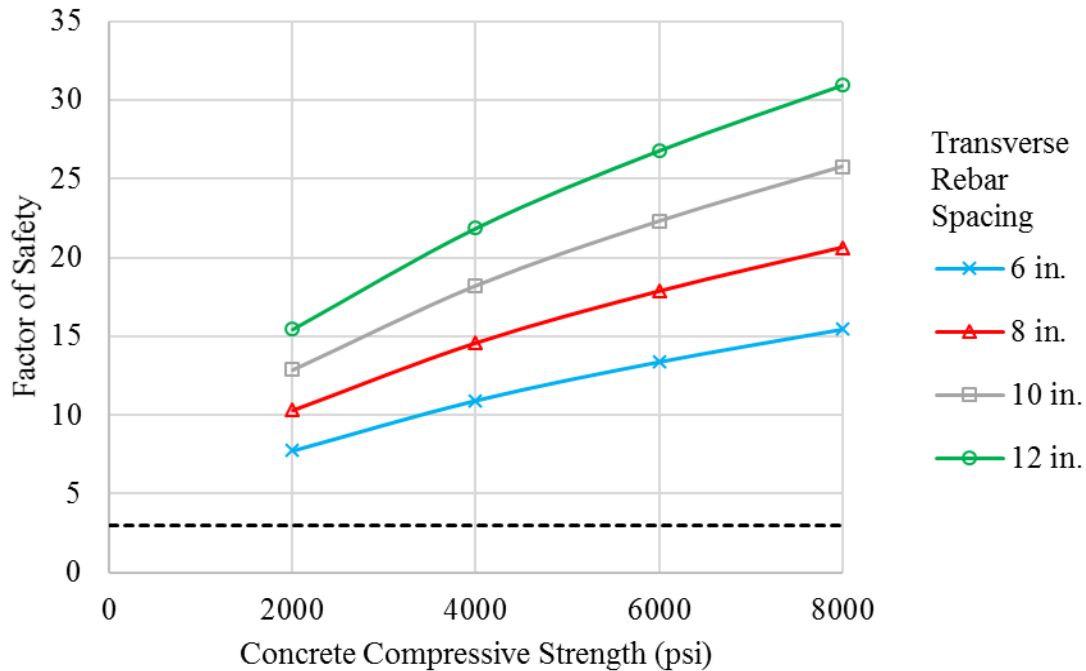
Figure 4-11: Interaction between concrete compressive strength and transverse rebar spacing for water pressure of 10 ksi.
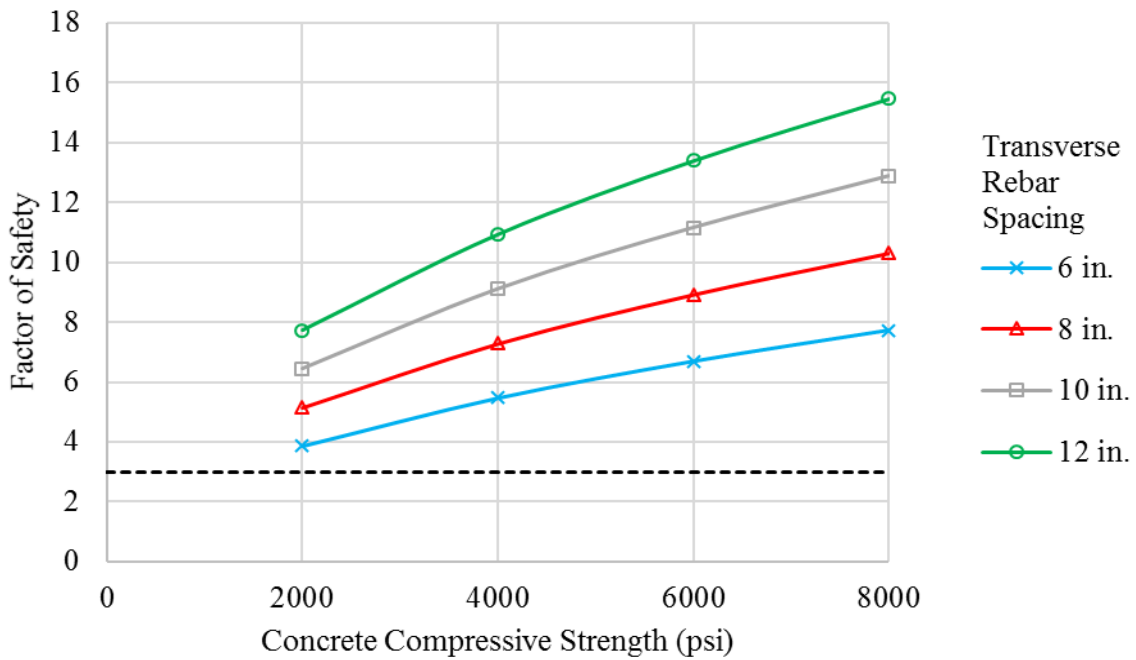
Figure 4-12: Interaction between concrete compressive strength and transverse rebar spacing for water pressure of 20 ksi.
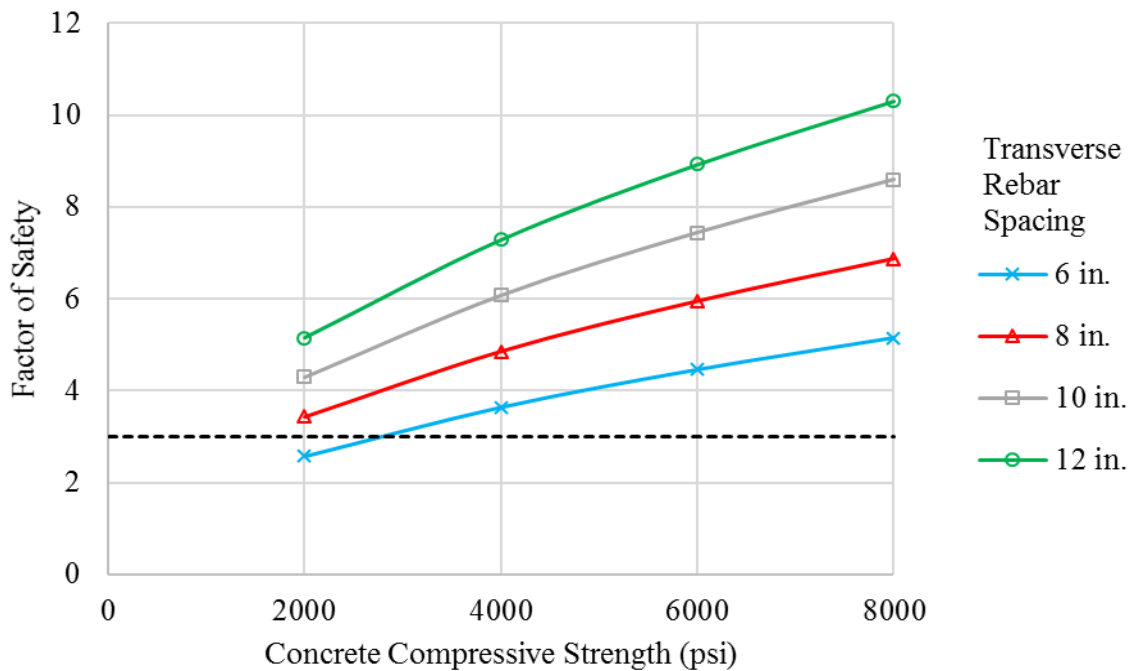
Figure 4-13: Interaction between concrete compressive strength and transverse rebar spacing for water pressure of 30 ksi.
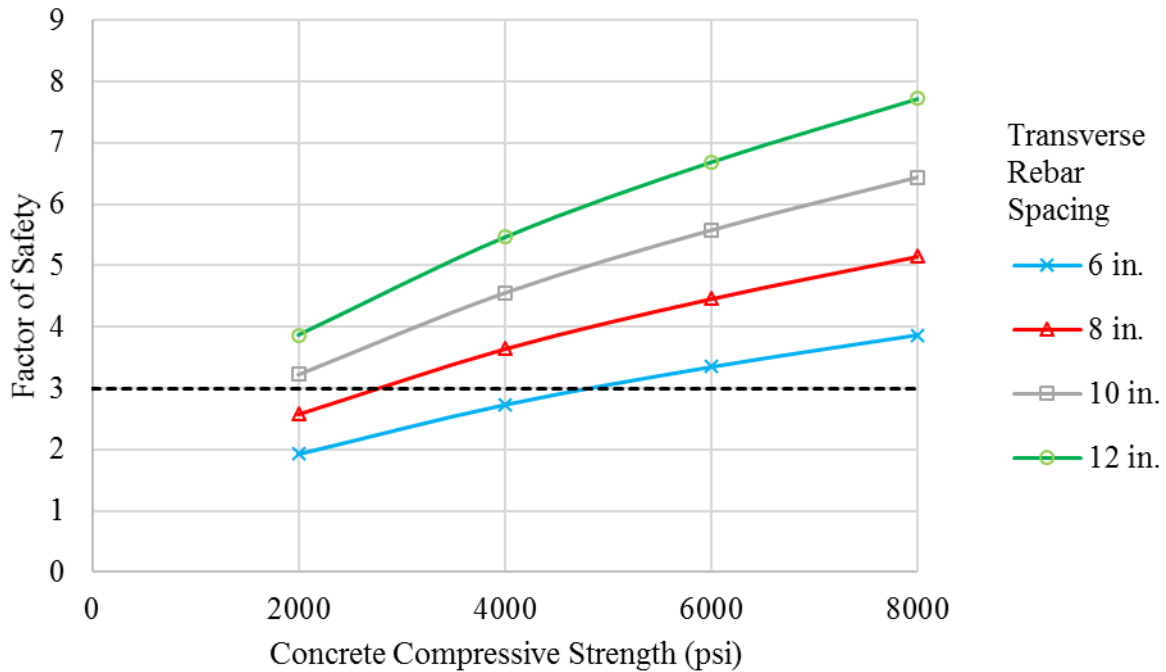
Figure 4-14: Interaction between concrete compressive strength and transverse rebar spacing for water pressure of 40 ksi.

Table 4-10: Parameter Combinations with Factor of Safety Less Than 3.0

Combination	Transverse Rebar Spacing (in.)	Concrete Compressive Strength (psi)	Water Pressure (ksi)	Factor of Safety
1	6	2,000	30	2.58
2	6	2,000	40	1.96
3	8	2,000	40	2.58
4	6	4,000	40	2.73

Application of the blow-through analysis to two case studies on bridge decks in northern Utah that were rehabilitated using hydrodemolition generated results for several actual "worst-case" scenarios for both bridge decks. In the analyses, the total removal depth was calculated as the sum of the OCD for the top mat, the diameter of the transverse bar in the top mat, the diameter of the longitudinal bar in the top mat, and the specified depth of removal below the top

mat. In addition, the height of the concrete beam was calculated as the difference between the deck thickness and the sum of the total removal depth, the 1.0-in. OCD for the bottom mat specified for both decks, the diameter of the transverse bar in the bottom mat, and half the diameter of the longitudinal bar in the bottom mat.

The extent of blow-through that occurred during hydrodemolition of the bridge deck investigated for case study #1 is shown in Figure 4-15, in which the areas that experienced blow-through are outlined. The blow-throughs were concentrated in areas between girders where the bottom of the deck was unsupported. Analysis showed that approximately 10.8 percent of the total bridge deck area experienced blow-through during hydrodemolition, which is a significant
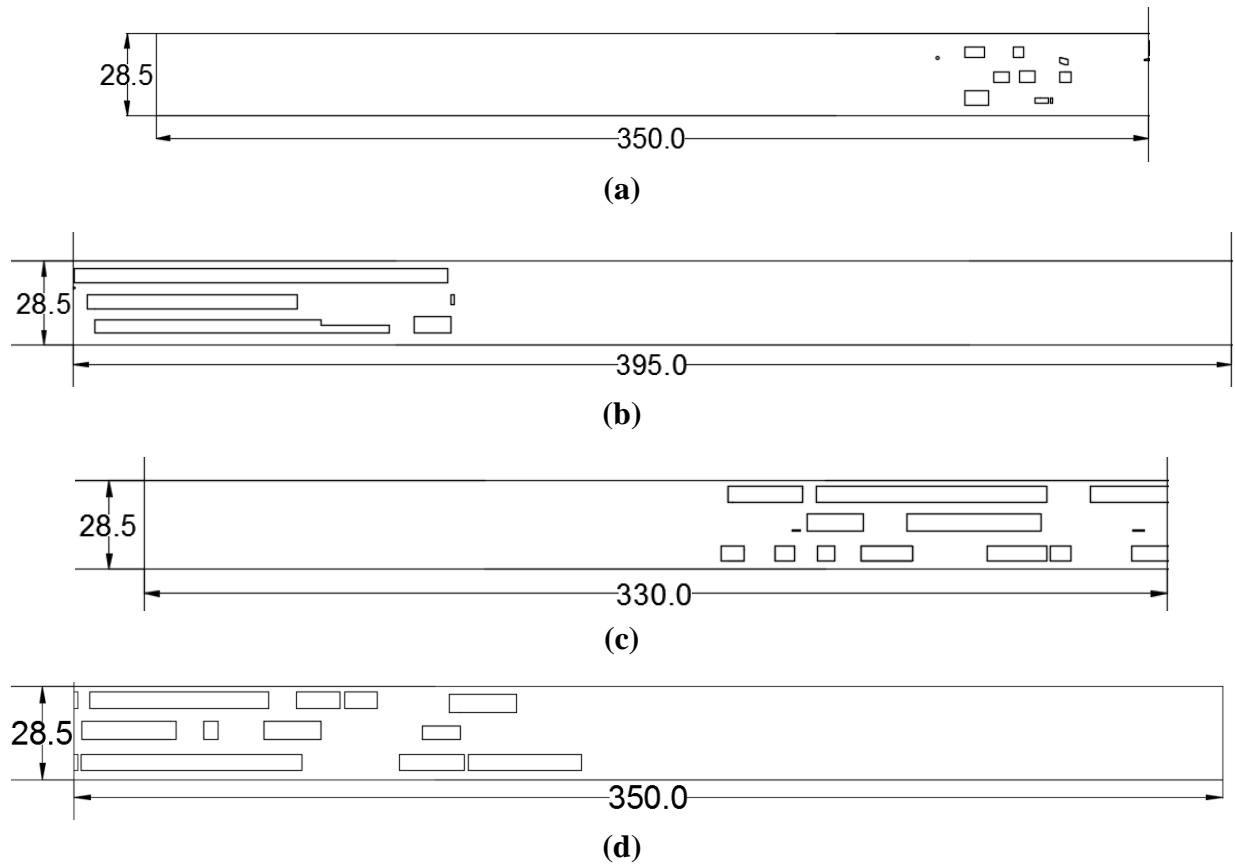
Figure 4-15: Blow-through map for case study #1: (a) 0-350 ft, (b) 350-745 ft, (c) 745-1,075 ft, and (d) 1,075-1,425 ft.

amount considering that the total bridge deck area is high at 40,613 ft^2. An example of the extensive blow-through damage on the bridge deck in case study #1, photographed after hydrodemolition, is shown in Figure 4-16.

For case study #1, the values of several input parameters needed to perform a blow-through analysis of this bridge deck were determined. The original bridge deck had a thickness of 7.5 in. (Guthrie et al. 2014). The OCD for the top mat of reinforcing steel was 2.0 in., while the OCD for the bottom mat of reinforcing steel was 1.0 in. For the transverse reinforcement, No. 4 and No. 5 bars were used in both the top and bottom mats. For the longitudinal reinforcement, No. 9 and No. 10 bars were used in the top mat, and No. 5 bar was used in the bottom mat. The longitudinal reinforcement spacing generally varied from 10 to 12 in., while the transverse reinforcement spacing generally varied from 4 to 7 in. The deck was constructed using normal concrete. The actual concrete compressive strength at the time of hydrodemolition was estimated to vary from 2,000 to 4,000 psi. The depth of concrete removal below the top mat of reinforcing steel was estimated to vary from 0.50 to 1.00 in. An oscillating nozzle was used, and the orifice size was 0.10 in. The water pressure for this project was 20 ksi, and the jet angle was held constant at 10 degrees with respect to the vertical axis of the nozzle.

Figure 4-16: Significant blow-through of the deck in case study #1.

As shown in Table 4-11, nine scenarios were analyzed for case study #1 to evaluate the potential for blow-through on this deck. These scenarios are based on variations in the longitudinal and transverse reinforcing bar sizes in the top and bottom mats, transverse rebar

Table 4-11: Blow-through Analysis Results for Various Scenarios for Case Study #1

Input Parameter	Scenario								
	1	2	3	4	5	6	7	8	9
Top Longitudinal Reinforcing Bar Size	No. 10	No. 10	No. 10	No. 10	No. 10	No. 10	No. 9	No. 9	No. 9
Top Transverse Reinforcing Bar Size	No. 4	No. 4	No. 4	No. 4	No. 4	No. 4	No. 4	No. 4	No. 4
Bottom Longitudinal Reinforcing Bar Size	No. 5	No. 5	No. 5	No. 5	No. 5	No. 5	No. 5	No. 5	No. 5
Bottom Transverse Reinforcing Bar Size	No. 4	No. 4	No. 4	No. 4	No. 4	No. 4	No. 4	No. 4	No. 4
Assumed Transverse Rebar Spacing (in.)	6	4	5	4	6	7	6	5	6
Concrete Compressive Strength (psi)	4000	4000	3000	2000	4000	4000	4000	3000	3000
Removal Depth below Top Longitudinal Bar (in.)	0.75	0.75	0.75	0.50	1.00	1.00	1.00	1.00	1.00
Minimum Factor of Safety	1.40	0.93	1.01	0.97	0.86	1.00	1.15	0.93	0.99
Predicted Blow-through	No	Yes	No	Yes	Yes	No	No	Yes	Yes

spacing (the longitudinal rebar spacing was held constant at 12 in. in the analyses), concrete compressive strength, and depth of concrete removal. For all nine scenarios, the governing mode of failure is the bending moment in the orientation where the length of the concrete beam is greater than the width of the concrete beam. Five of the nine scenarios resulted in a factor of safety less than 1.0, and all of the scenarios resulted in a factor of safety less than 3.0. Therefore, although the factors of safety may have actually been lower, due to extensive cracking and efflorescence on the bottom of the deck as shown in Figure 4-17, the blow-through analysis developed in this research correctly predicted a high potential for blow-through on this deck.

The extent of blow-through that occurred during hydrodemolition of the bridge deck investigated for case study #2 is shown in Figure 4-18, in which the areas that experienced blow-through are outlined. Analysis showed that less than 1.0 percent of the total bridge deck area experienced blow-through during hydrodemolition, which is an insignificant amount considering that the total bridge deck area is low at 5,210 ft^2. An example of the minimal blow-through damage on the bridge deck in case study #2, photographed after hydrodemolition, is shown in Figure 4-19.

Figure 4-17: Significant efflorescence and cracking on the underside of the deck in case study #1.

47
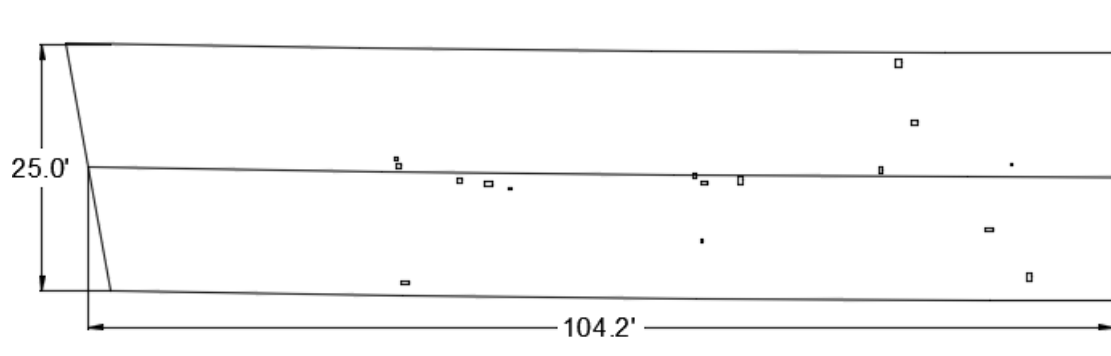
(a)
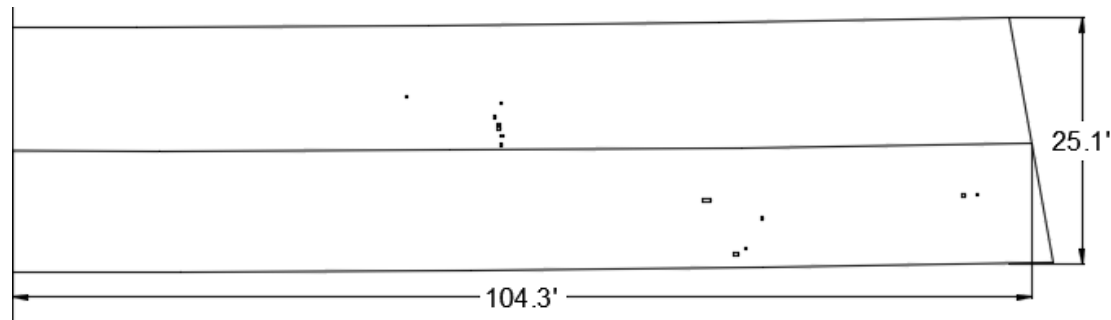
(b)

Figure 4-18: Blow-through map for case study #2: (a) 0-104.2 ft and (b) 104.2-208.5 ft.

Figure 4-19: Insignificant blow-through of the deck in case study #2.

For case study #2, the values of several input parameters needed to perform a blow-through analysis of this bridge deck were determined. The original bridge deck had a thickness of 8.5 in. The OCD for the top mat of reinforcing steel was 2.0 in., while the OCD for the bottom mat of reinforcing steel was 1.0 in. For the transverse reinforcement, No. 5 bars were used in both the top and bottom mats. For the longitudinal reinforcement, No. 7 bars were used in the top mat, and No. 5 and No. 7 bars were used in the bottom mat. The longitudinal reinforcement spacing generally varied from 10 to 12 in., while the transverse reinforcement spacing generally varied from 4 to 6 in. The deck was constructed using normal concrete. The actual concrete compressive strength at the time of hydrodemolition was estimated to vary from 2,000 to 4,000 psi. The depth of concrete removal below the top mat of reinforcing steel was estimated to vary from 0.50 to 1.00 in. A rotating nozzle was used, and the orifice size was 0.10 in. The water pressure for this project was 34 ksi, and the jet angle was held constant at 10 degrees with respect to the vertical axis of the nozzle.

As shown in Table 4-12, nine scenarios were analyzed for case study #2 to evaluate the potential for blow-through on this deck. As in case study #1, these scenarios are based on variations in the longitudinal and transverse reinforcing bar sizes in the top and bottom mats, transverse rebar spacing (the longitudinal rebar spacing was held constant at 12 in. in the analyses), concrete compressive strength, and depth of concrete removal. For all nine scenarios, the governing mode of failure is the bending moment in the orientation where the length of the concrete beam is greater than the width of the concrete beam. Although eight of the nine scenarios resulted in a factor of safety less than 3.0, none of the scenarios resulted in a factor of safety less than 1.0. Therefore, although the factors of safety may have actually been lower, due to minor cracking on the bottom of the deck as shown in Figure 4-20, the blow-through analysis developed in this research correctly predicted a low potential for blow-through on this deck.

Table 4-12: Blow-through Analysis Results for Various Scenarios for Case Study #2

Input Parameter	Scenario								
	1	2	3	4	5	6	7	8	9
Top Longitudinal Reinforcing Bar Size	No. 5	No. 7	No. 7	No. 7	No. 7	No. 7	No. 7	No. 7	No. 7
Top Transverse Reinforcing Bar Size	No. 5	No. 5	No. 5	No. 5	No. 5	No. 5	No. 5	No. 5	No. 5
Bottom Longitudinal Reinforcing Bar Size	No. 5	No. 7	No. 7	No. 7	No. 7	No. 7	No. 7	No. 7	No. 7
Bottom Transverse Reinforcing Bar Size	No. 5	No. 5	No. 5	No. 5	No. 5	No. 5	No. 5	No. 5	No. 5
Assumed Transverse Rebar Spacing (in.)	6	6	4	4	5	5	5	4	6
Concrete Compressive Strength (psi)	4000	4000	2000	2000	2000	2000	3000	3000	3000
Removal Depth below Top Longitudinal Bar (in.)	0.75	0.75	0.75	1.00	0.75	1.00	0.75	1.00	1.00
Minimum Factor of Safety	3.95	2.88	1.36	1.07	1.70	1.33	2.08	1.31	1.96
Predicted Blow-through	No	No	No	No	No	No	No	No	No

Figure 4-20: Insignificant efflorescence and cracking on the underside of the deck in case study #2.

4.5 Summary

This chapter presents the results of the questionnaire survey, chloride concentration analysis, and blow-through analysis performed in this research. Regarding the questionnaire survey conducted to assess current practices of selected hydrodemolition companies, while some respondents indicated that certain parameters vary, depending on the project, the survey responses are valuable for understanding typical practices and were used to design the numerical experiments performed to investigate factors that influence the occurrence of blow-throughs in concrete bridge decks when hydrodemolition is used. All survey participants reported that blow-throughs are a common occurrence when using hydrodemolition on concrete bridge decks. A few mentioned that blow-throughs are most common on bridge decks with efflorescence on the underside of the deck, which is usually an indication that the deck has experienced extensive cracking and may have high chloride concentrations.

The numerical modeling performed to investigate the effects of hydrodemolition treatment timing on chloride concentration profiles in concrete bridge decks for depths of concrete removal below the top mat of reinforcing steel generated chloride concentration profiles through a 75-year service life given a specific OCD, treatment time, and surface treatment usage.

The results indicate that, when a surface treatment is used, the concentration at either the top or bottom mat of reinforcing steel does not reach or exceed 2.0 lb of chloride per cubic yard of concrete after rehabilitation during the 75 years of simulated bridge deck service life. The results also indicate that, when a surface treatment is not used, the chloride concentration at the top mat of reinforcement exceeds 2.0 lb of chloride per cubic yard of concrete within 10, 15, and 20 years after rehabilitation for OCD values of 2.0 2.5, and 3.0 in., respectively.

The numerical experiments performed to investigate factors that influence the occurrence of blow-throughs in concrete bridge decks when hydrodemolition is used generated results in terms of the main effect of each input variable on the occurrence of blow-throughs and interactions among selected input variables. In addition, the blow-through analysis was applied to two bridge decks in northern Utah that were rehabilitated using hydrodemolition. For each analysis, blow-through can be expected when the calculated factor of safety is less than 1.0, but a minimum factor of safety of 3.0, as commonly specified in engineering practice, is desired to guard against blow-through. The factor of safety significantly increases with increasing values of transverse rebar spacing and concrete compressive strength and decreasing values of depth of removal below the bottom of the top reinforcing mat, orifice size, and water pressure within the ranges of these parameters investigated in this experimentation. The factor of safety is relatively insensitive to jet angle. While a factor of safety less than 1.0 did not occur in the analyses of interactions, a factor of safety less than 3.0 occurred for four combinations of the input parameters. These combinations, and equivalent combinations not explicitly analyzed, should be avoided in practice to minimize the occurrence of blow-through during hydrodemolition.

Application of the blow-through analysis to two case studies on bridge decks in northern Utah that were rehabilitated using hydrodemolition generated results for several actual "worst-case" scenarios for both bridge decks. Nine scenarios were analyzed for each case study to evaluate the potential for blow-through. For case study #1, five of the nine scenarios resulted in a factor of safety less than 1.0, and all of the scenarios resulted in a factor of safety less than 3.0. Given that approximately 10.8 percent of the total bridge deck area experienced blow-through during hydrodemolition, the blow-through analysis developed in this research correctly predicted a high potential for blow-through on this deck. For case study #2, eight of the nine scenarios

resulted in a factor of safety less than 3.0, but none of the scenarios resulted in a factor of safety less than 1.0. Given that less than 1.0 percent of the total bridge deck area experienced blow-through during hydrodemolition, the blow-through analysis developed in this research correctly predicted a low potential for blow-through on this deck.

5.0 CONCLUSION

5.1 Summary

The objectives of this research were 1) to investigate the effects of hydrodemolition treatment timing on chloride concentration profiles in concrete bridge decks for depths of concrete removal below the top mat of reinforcing steel and 2) to investigate factors that influence the occurrence of blow-throughs in concrete bridge decks when hydrodemolition is used. The objectives of this research were met by conducting a questionnaire survey of hydrodemolition companies, performing numerical modeling of chloride concentration to investigate hydrodemolition treatment timing on typical Utah bridge decks, and using structural analysis to investigate factors that influence the occurrence of blow-throughs during hydrodemolition.

A questionnaire survey was conducted by telephone and email to assess current practices of selected hydrodemolition companies that rehabilitate concrete bridge decks throughout the country. The survey findings were used to design the numerical experiments performed to investigate factors that influence the occurrence of blow-throughs in concrete bridge decks when hydrodemolition is used. A total of five survey participants, who were typically the managers of the hydrodemolition companies, responded to the survey, and their answers were compiled to assess the current bridge deck rehabilitation practices of these hydrodemolition companies.

Numerical modeling was performed to investigate the effects of hydrodemolition treatment timing on chloride concentration profiles in concrete bridge decks for depths of concrete removal below the top mat of reinforcing steel. Based on communications with UDOT engineers to determine current practice, appropriate ranges of removal and overlay depths were selected for use in the modeling process. Crossing the various levels of the experimental factors in a full-factorial structure generated a total of 36 unique combinations, or scenarios. Modeling of the decks without treatment was performed first to develop a baseline chloride concentration profile to which the chloride concentration profiles for various treatment times were compared. Modeling was then performed for each unique combination of OCD, treatment time, and surface

treatment application to produce chloride concentration profiles that would be expected after rehabilitation was performed. The latest timing of rehabilitation that maintained a chloride concentration level below 2.0 lb of chloride per cubic yard of concrete at the levels of both the top and bottom mats of reinforcing steel was identified for each unique combination of OCD and surface treatment application.

For this research, a spreadsheet was developed to investigate six modes of failure, or blow-through, that can potentially be experienced by a concrete bridge deck during hydrodemolition. These modes of failure include bending, one-way shear, and two-way shear, each of which is analyzed in both the orientation where the length is greater than the width and in the orientation where the length is less than the width. For any of these failure modes, if the capacity of the concrete deck section is less than the relevant force or moment applied by the high-pressure water jet, blow-through can be expected. The factor of safety against blow-through is calculated as the shear or moment capacity of the concrete section divided by the shear force or moment imparted by the high-pressure water jet. Several calculations are required in the analysis of the simulated concrete beam, including those for modulus of rupture, moment of inertia, maximum moment, cracking moment, maximum shear force, one-way shear strength, and two-way shear strength. The bridge deck parameters that were used as inputs in the blow-through analysis are bridge deck thickness, OCD, reinforcing bar size, longitudinal rebar spacing, transverse rebar spacing, type of concrete, concrete compressive strength, and removal depth. The hydrodemolition equipment parameters that were used as inputs in the blow-through analysis are orifice size, water pressure, and angle of jet. Following development of the spreadsheet, numerical experiments were performed to investigate factors that influence the occurrence of blow-throughs in concrete bridge decks when hydrodemolition is used. Finally, the blow-through analysis was applied to two case studies on bridge decks in northern Utah that were rehabilitated using hydrodemolition.

5.2 Findings

While some survey respondents indicated that certain parameters vary, depending on the project, the responses are valuable for understanding typical practices and were used to design

the numerical experiments performed to investigate factors that influence the occurrence of blow-throughs in concrete bridge decks when hydrodemolition is used. All survey participants reported that blow-throughs are a common occurrence when using hydrodemolition on concrete bridge decks. A few mentioned that blow-throughs are most common on bridge decks with efflorescence on the underside of the deck, which is usually an indication that the deck has experienced extensive cracking and may have high chloride concentrations.

The numerical modeling performed to investigate the effects of hydrodemolition treatment timing on chloride concentration profiles in concrete bridge decks for depths of concrete removal below the top mat of reinforcing steel generated chloride concentration profiles through a 75-year service life given a specific OCD, treatment time, and surface treatment usage. The results indicate that, when a surface treatment is used, the concentration at either the top or bottom mat of reinforcing steel does not reach or exceed 2.0 lb of chloride per cubic yard of concrete after rehabilitation during the 75 years of simulated bridge deck service life. The results also indicate that, when a surface treatment is not used, the chloride concentration at the top mat of reinforcement exceeds 2.0 lb of chloride per cubic yard of concrete within 10, 15, and 20 years after rehabilitation for OCD values of 2.0 2.5, and 3.0 in., respectively.

The numerical experiments performed to investigate factors that influence the occurrence of blow-throughs in concrete bridge decks when hydrodemolition is used generated results in terms of the main effect of each input variable on the occurrence of blow-throughs and interactions among selected input variables. In addition, the blow-through analysis was applied to two bridge decks in northern Utah that were rehabilitated using hydrodemolition. For each analysis, blow-through can be expected when the calculated factor of safety is less than 1.0, but a minimum factor of safety of 3.0, as commonly specified in engineering practice, is desired to guard against blow-through. The factor of safety significantly increases with increasing values of transverse rebar spacing and concrete compressive strength and decreasing values of depth of removal below the bottom of the top reinforcing mat, orifice size, and water pressure within the ranges of these parameters investigated in this experimentation. The factor of safety is relatively insensitive to jet angle. While a factor of safety less than 1.0 did not occur in the analyses of interactions, a factor of safety less than 3.0 occurred for four combinations of the input

parameters. These combinations, and equivalent combinations not explicitly analyzed, should be avoided in practice to minimize the occurrence of blow-through during hydrodemolition.

Application of the blow-through analysis to two case studies on bridge decks in northern Utah that were rehabilitated using hydrodemolition generated results for several actual "worst-case" scenarios for both bridge decks. Nine scenarios were analyzed for each case study to evaluate the potential for blow-through. For case study #1, five of the nine scenarios resulted in a factor of safety less than 1.0, and all of the scenarios resulted in a factor of safety less than 3.0. Given that approximately 10.8 percent of the total bridge deck area experienced blow-through during hydrodemolition, the blow-through analysis developed in this research correctly predicted a high potential for blow-through on this deck. For case study #2, eight of the nine scenarios resulted in a factor of safety less than 3.0, but none of the scenarios resulted in a factor of safety less than 1.0. Given that less than 1.0 percent of the total bridge deck area experienced blow-through during hydrodemolition, the blow-through analysis developed in this research correctly predicted a low potential for blow-through on this deck.

5.3 Recommendations

Hydrodemolition should be considered as an effective means of removing chloride-contaminated concrete from immediately around and even below the top mat of reinforcing steel and allowing mechanical interlock with the new concrete placed after hydrodemolition. For bridge decks typical of those in Utah, treatment times corresponding to deck ages ranging from 25 to at least 50 years can be specified to achieve significant extensions in deck service life. To maximize deck service life, a surface treatment should be applied to seal the rehabilitated concrete deck against further chloride ingress.

The blow-through analysis developed in this research has potential for use as a tool for determining if bridge decks that are no longer suitable for repair using traditional concrete removal techniques may still be good candidates for repair using hydrodemolition. As the blow-through analysis assumes that the concrete within the simulated beam is intact, without cracking or other distresses, the resulting calculations should be supplemented with visual inspection of

the deck; extensive cracking and efflorescence on the bottom of the deck may indicate a higher probability of blow-through during hydrodemolition.

REFERENCES

Arora, P., Popov, B. N., Haran, B., Ramasubramanian, M., Popva, S., and White, R. E. (1997). "Corrosion initiation time of steel reinforcement in a chloride environment: A one dimensional solution." *Elsevier J. Corros Sci*, 39(4), 739-759.

Basheer, L., Cleland, D. J., and Long, A. E. (1998). "Protection provided by surface treatments against chloride induced corrosion." *Springer J. Mat. and Struct.*, 31(211), 459-464.

Bentz, D. P. (2007). "Prediction of a chloride ion penetration profile for a concrete." <http://ciks.cbt.nist.gov/~bentz/clpen2.html> (June 1, 2016).

Birdsall, A. W., Guthrie, W. S., and Bentz, D. P. (2007). "Effects of initial surface treatment timing on chloride concentrations in concrete bridge decks." *Transportation Research Record*, 2028, 103-110.

Clark, G. L., and Hawley, G. G. (1966). *The encyclopedia of chemistry*, Reinhold Publishing Corporation, New York, NY.

Federal Highway Administration (FHWA). (2011). *Bridge preservation guide*, Publication Number FHWA-HIF-11042, Washington, DC.

Freeze, R., and Cheery, J. (1979). *Groundwater*, Prentice Hall, NJ.

Gere, J. M., and Goodno, B. J. (2013). *Mechanics of materials*, Eighth Edition, Cengage Learning, Stamford, CT.

Grace, N., Hanson, J., and AbdelMessih, H. (2004). *Inspection and deterioration of bridge decks constructed using stay-in-place metal forms and epoxy-coated reinforcement*, Research Report R, Michigan Department of Transportation, Lansing, MI.

Guthrie, W. S., Nelsen, T., and Ross, L. A. (2005). *Performance of concrete bridge deck surface treatments*, Report No. UT-05.05, Utah Department of Transportation, Salt Lake City, UT.

Guthrie, W. S., Frost, S. L., Birdsall, A. W., Linford, E. T., Ross, L. A., Crane, R. A., and Eggett, D. L. (2006). "Effect of stay-in-place metal forms on performance of concrete bridge decks." *Transportation Research Record*, 1958, 33-41.

Guthrie, W. S., Nolan, C. D., and Bentz, D. P. (2008). "Effect of initial scarification and overlay treatment timing on chloride concentrations in concrete bridge decks." *Transportation Research Record*, 2220, 66-74.

Guthrie, W. S., Flannery, D. L., Baxter, J. S., and Mazzeo, B. A. (2014). *Demonstration of vertical impedance and acoustic impact-echo testing for condition assessment of a concrete bridge deck with a concrete overlay and polymer surface treatment*, Research Report, Utah Department of Transportation, Salt Lake City, UT.

Harries, K., McCabe, M., and Sweriduk, M. (2013). *Structural evaluation of slab rehabilitation by method of hydrodemolition and latex modified overlay*, Report No. FHWA-PA-2013-006-PIT WO 01, Pennsylvania Department of Transportation, Harrisburg, PA.

Hema, J., Guthrie, W. S., and Fonseca, F. (2004). *Concrete bridge deck condition assessment and improvement strategies*, Report No. UT-04.16, Utah Department of Transportation, Salt Lake City, UT.

Hopwood, T., Goff, C., Wells, D., and Palle, S. (2015). *Hydrodemolition and use of a rapid early strength latex modified concrete overlay*, Report No. KTC-TA-15-01/KHIT6-15-1F, Kentucky Transportation Cabinet, Flemingsbury, KY.

International Concrete Repair Institute (ICRI). (2014). *Guide for the preparation of concrete surfaces for repair using hydrodemolition methods*, Guideline No. 310.3R-2014, Rosemont, IL.

Lees, T. P. (1992). "Deterioration mechanisms." *Durability of concrete structures*, G. Mays, ed., E & FN SPON, London, UK.

Lewis, R. J. (2001). *Hawley's condensed chemical dictionary*, Fourteenth Edition, John Wiley and Sons, Inc., New York, NY.

Mays, G. (1992). *Durability of concrete structures*, E & FN SPON, London, UK.

McCormac, J. C., and Brown, R. H. (2015). *Design of reinforced concrete*, Tenth Edition, Wiley, New York, NY.

Mindess, S., Young, J. F., and Darwin, D. (2003). *Concrete*, Second Edition, Prentice Hall, NJ.

Momber, A. W. (2005). *Hydrodemolition of concrete surfaces and reinforced concrete structures*, Aachen University, Aachen, Germany.

Pan, X., Shi, Z., Shi, C., Ling, T., and Li, N. (2016). "A review of concrete surface treatment Part 1: types and mechanisms." *Elsevier J. Constr. Bldg. Mat.*, 132(1), 578-590.

Patnaik, A., and Baah, P. (2015). *Cracking behavior of structural slab bridge decks*, Report No. FHWA/OH-2015/4, Ohio Department of Transportation, Columbus, OH.

Poulsen, E., and Mejlbro, E. (2006). *Diffusion of chloride in concrete: Theory and application*, Taylor and Francis, Inc., New York, NY.

Suryavanshi, A. K., Swamy, R. N., and McHugh, S. (1998). "Chloride penetration into reinforced concrete slabs." *Canadian J. of Civ. Eng.*, 25(1), 87-95.

Swamy, R. N., and Tanikawa, S. (1993). "An external surface coating to protect concrete and steel from aggressive environments." *Springer J. Mat. and Struct.*, 26(162), 465-478.

Wenzlick, J. D. (2002). *Hydrodemolition and repair of bridge decks*, Report No. RDTO2-002, Missouri Department of Transportation, Jefferson City, MO.

Weyers, R. E., Prowell, B. D., Sprinkel, M. M., and Vorster, M. (1993). *Concrete bridge protection, repair, and rehabilitation relative to reinforcement corrosion: A methods application manual*, Report No. SHRP-S-360, Strategic Highway Research Program, Washington, DC.

Zhang, J. Z., McLoughlin, I. M., and Buenfeld, N. R. (1998). "Modeling of chloride diffusion into surface-treated concrete." *Elsevier J. Cem. Concr. Comp.*, 20(4), 253-261.

APPENDIX A: SAMPLE INPUTS FOR CHLORIDE CONCENTRATION ANALYSIS

Figure A-1 contains screenshots showing the inputs used for numerical modeling of chloride concentration. The inputs for the time of treatment, length of experiment (total duration of exposure), member thickness, depth of reinforcement, time of surface treatment application, time at which hydrodemolition (milling and filling) was performed, depth of concrete removal (milling), and thickness of new concrete (filling) were changed to reflect the parameters of each specific experiment. All other inputs were held constant, as depicted.

Prediction of a Chloride Ion Penetration Profile for a Concrete
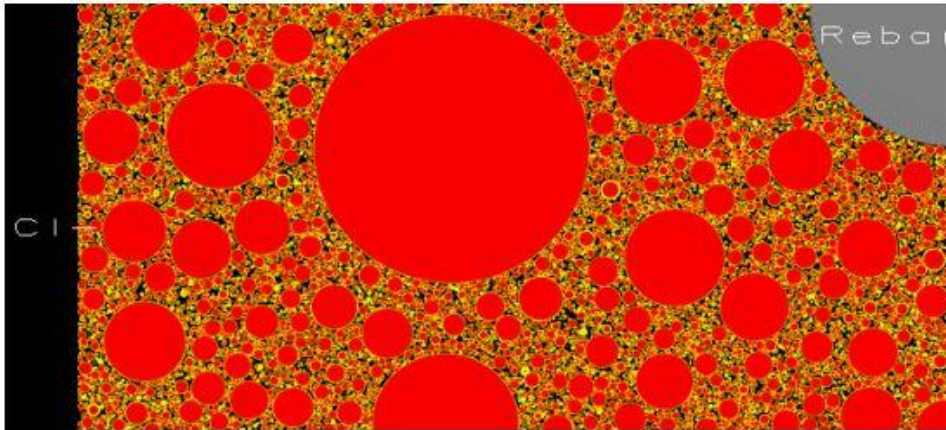
Prediction is based on a one-dimensional finite difference solution of Fick's second law of diffusion, with a variable external chloride concentration and a two-layer representation of the concrete. Surface treatment option has been added in 2006 and mill and fill option added in 2007 in collaboration with Prof. Guthrie of Brigham Young University.

Please supply the following parameters (defaults provided)

Environmental Parameters

Specify external chloride concentration and temperature as a function of month of the year:

Month	Ext. chloride conc. (moles/liter)	Temperature (°C)
January	4.273	-2.278
February	3.865	1.167
March	3.326	5.444
April	2.800	9.833
May	2.429	14.889

Figure A-1: Inputs used for numerical modeling program.

June	2.311	20.611
July	2.479	25.500
August	2.887	24.222
September	3.427	18.444
October	3.952	11.778
November	4.324	4.889
December	4.441	-1.278

Beginning month of exposure is: October ▾

Total duration of exposure 9125 days

Unexposed boundary condition is Constant at zero ▾

Structural Design Parameters

Member thickness 0.2032 m

Depth of Reinforcement 20.8 mm

Concrete Mixture Parameters

w/c ratio 0.44

Degree of hydration .8

Volume fraction of aggregate 65 %

Air content 6 %

Initial chloride concentration of concrete 0.0 g chloride/g cement Guidance

Diffusion Coefficients (D) of Original Concrete

Click here to view database of concrete diffusivities from literature.

Figure A-1: Continued.

Note that all diffusion coefficients are apparent diffusivity values, as we are modelling transport in the pore space of the concrete based on Fick's 2nd law.

Time dependent diffusion coefficient for bulk concrete takes the form of $D = D_{inf} + D_i * t^{-m}$

Be sure that you use values of m in the range (0,1).

Reference: Mangat and Molloy, Materials and Structures, Vol. **27**, 338-346, 1994. Note- Mangat and Molloy found m values ranging from 0.44 to 0.86 and also that approximately:

$m = 2.5(w/c) - 0.6$

To have a constant D value with time, simply set D_{inf} to this desired value and D_i to zero

D_{inf} [1.30E-11]   m*m/s at 25 C

D_i [0]   m*m/s

m [0.6]

Curing time before exposure of concrete to chlorides [28.0]   days (Recommended > 0)

The surface layer of the concrete may have a different (lower or higher) D value than the bulk concrete due to carbonation or poor curing practices. Input the surface layer D value relative to the bulk D value and the thickness of this layer. To bypass this feature, set the skin layer thickness to 0.0 or use D(surface concrete)/D(bulk concrete)=1.0.

Ratio D (surface concrete)/D (bulk concrete) [1.]

Thickness of surface layer [0]   mm

Activation Energy for diffusion [40.0]   kJ/mole

Chloride Binding Parameters Guidance

```
Based on a Langmuir isotherm of the form:
  C(bound)=(alpha*C(free))/(1.+beta*C(free))

where C(bound) is in (mole Cl-)/kg cement and
C(free) is in (mole Cl-)/L
```

Alpha [1.67]

Beta [4.08]

Rate constant for binding [1E-7]   s-1

Chloride Reaction Parameters Guidance

```
Assuming the formation of Freidel's salt from all of the
C₃A and C₄AF initially available in the cement powder.
```

Figure A-1: Continued.

65

C_3A content of cement [5.0]   % on a mass basis

C_4AF content of cement [5.0]   % on a mass basis

Rate constant for aluminate reactions with chloride [1.E-8]   s-1

New Feature (March 2006)

Allows application of a surface treatment at a specific time, beyond which further transfer of chlorides into/out of the top surface is prohibited.

Set this time to a time greater than the total exposure time to turn off this feature

Time at which surface treatment is applied [9125]   days

Mill and Fill Concrete Options (February 2007)

Time at which milling and filling is performed [9125]   days

Depth of milling [0.085725]   m

Thickness of new (filling) concrete [0.085725]   m

w/c ratio of new concrete [0.44]

Degree of hydration of new concrete [.8]

Volume fraction of aggregate for new concrete [65]   %

Air content of new concrete [6]   %

Initial chloride concentration of new concrete [0.0]   g chloride/g cement Guidance

Diffusion Coefficients (D) of New Concrete

Time dependent diffusion coefficient for bulk concrete takes the form of $D=D_{inf}+D_i*t^{-m}$

Be sure that you use values of m in the range (0,1).

To have a constant D value with time, simply set D_{inf} to this desired value and D_i to zero

D_{inf} [1.30E-11]   m*m/s at 25 C

D_i [0]   m*m/s

m [0.6]

Curing time before exposure of new concrete to external chlorides [28.0]   days (Recommended > 0)

Figure A-1: Continued.

66

The surface layer of the concrete may have a different (lower or higher) D value than the bulk concrete due to carbonation or poor curing practices. Input the surface layer D value relative to the bulk D value and the thickness of this layer. To bypass this feature, set the skin layer thickness to 0.0 or use D(surface concrete)/ D(bulk concrete)=1.0.

Ratio D (surface concrete)/D (bulk concrete) 1.

Thickness of surface layer 0   mm

Figure A-1: Continued.

APPENDIX B: BLOW-THROUGH ANALYSIS FOR CASE STUDY #1

Figures B-1 and B-2 show the sections of the bridge plans that were used to determine identifiers for the bar sizes used for the blow-through analyses for case study #1. Figures B-3 and B-4 show the bridge plans that were used to determine bar sizes for transverse reinforcement and longitudinal reinforcement, respectively. Figures B-5 through B-13 show the blow-through analysis outputs for each of the nine scenarios that were analyzed for case study #1.
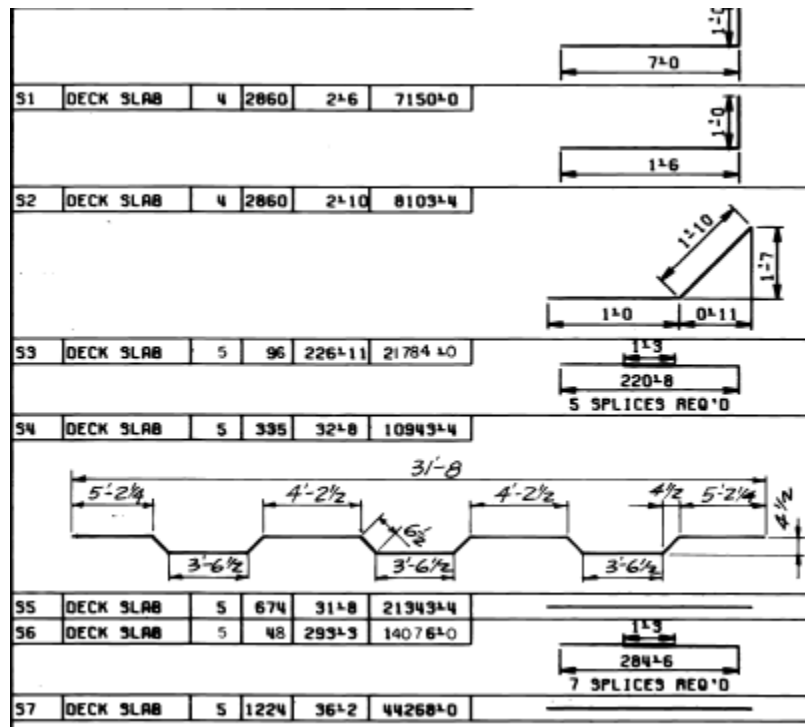
Figure B-1: First set of reinforcement plans for bridge deck in case study #1.

Mark	Description	Bar Size	Qty	Length	Total Length	Shape
S9	DECK SLAB	4	7	109'8	767'8	1'0 / 107'8 / 2 SPLICES REQ'D
S10	DECK SLAB	4	7	291'6	2040'6	1'0 / 284'6 / 7 SPLICES REQ'D
S11	DECK SLAB	4	36	5'7	201'0	3'0 / 0'5 / 0'8 / 0'6 / 1'0
S12	DECK SLAB	5	18	4'9	85'6	
S13	DECK SLAB	4	108	5'3	567'0	0'5 / 4'10
S14	DECK SLAB	5	288	6'0	1728'0	
S15	DECK SLAB	5	48	225'9	10836'0	1'3 / 219'6 / 5 SPLICES REQ'D
S16	DECK SLAB	10	48	80'5 ~~80'6~~	3860'0 ~~3864'0~~	3'5 / 77'0 / 1 SPLICES REQ'D
S17	DECK SLAB	4	7	222'6	1557'6	1'0 / 217'6 / 5 SPLICES REQ'D
S18	DECK SLAB	9	124	55'0	6820'0	
S19	DECK SLAB	10	48	52'0	2496'0	
S20	DECK SLAB	9	16	30'0	480'0	
S21	DECK SLAB	9	12	20'0	240'0	
S22	DECK SLAB	5	10	31'9	317'6	19'6 / 12'3 / CUT LINE / 19'6 / 12'3 / 10 BARS PER SET / 1 SETS REQ'D
S23	DECK SLAB	5	10	15'3	152'6	11'3 / 4'0 / CUT LINE / 11'3 / 4'0 / 10 BARS PER SET / 1 SETS REQ'D
S24	DECK SLAB	10	48	111'5	5348'0	3'5 / 108'0 / 1 SPLICES REQ'D

Figure B-2: Second set of reinforcement plans for bridge deck in case study #1.
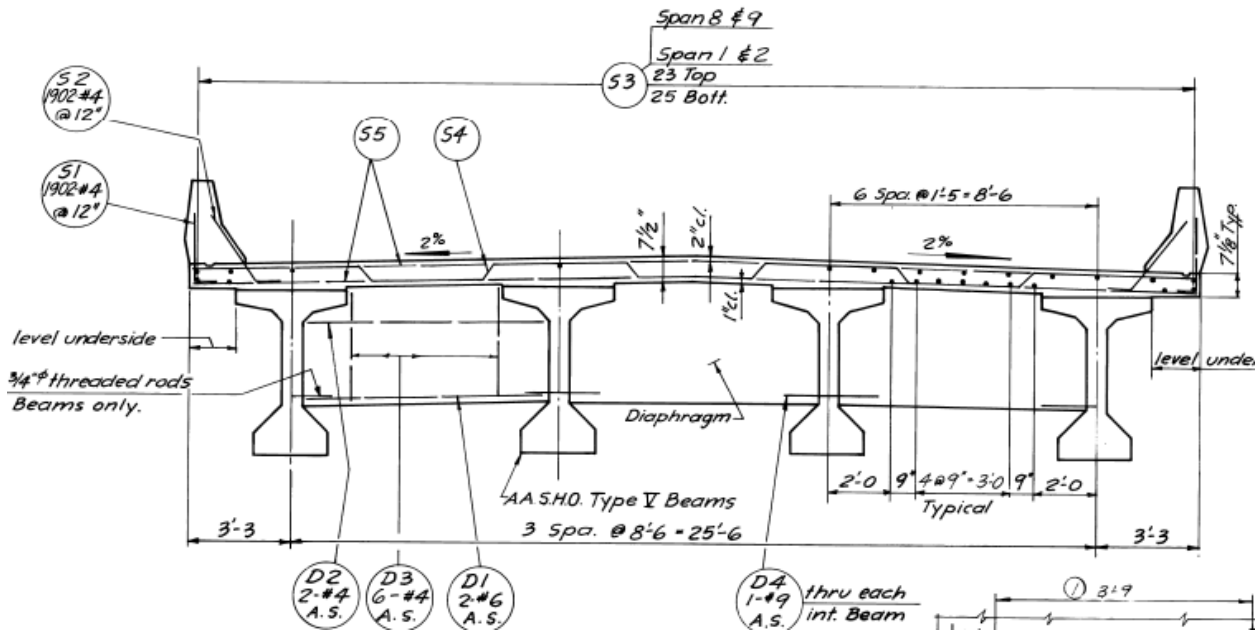
Figure B-3: Bridge schematic showing transverse reinforcing bar locations for bridge deck in case study #1.
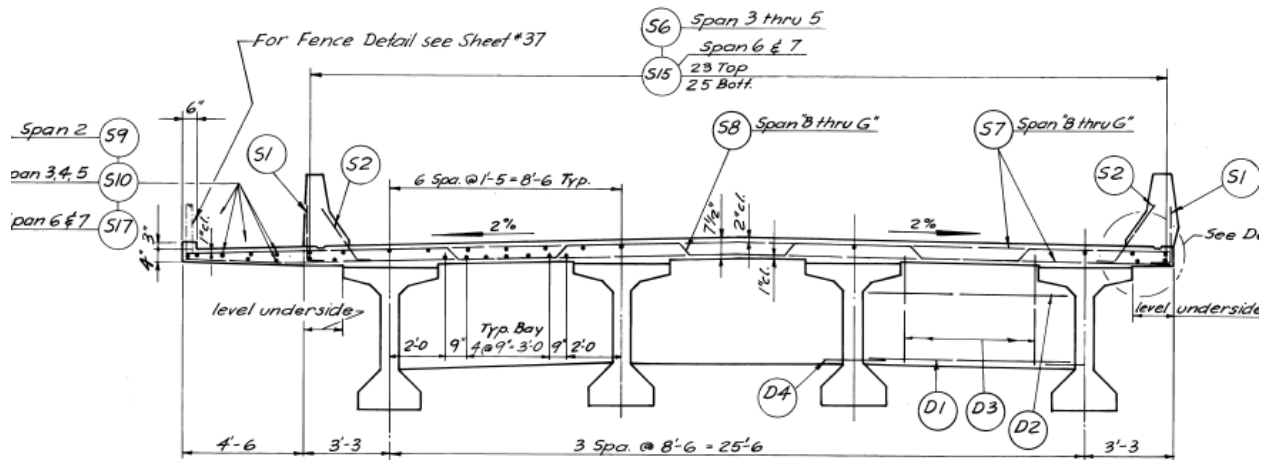
Figure B-4: Bridge schematic showing longitudinal reinforcing bar locations for bridge deck in case study #1.

70

The left side has vertical rotated text labels: "Analysis about y-axis, I>b | Analysis about x-axis, I>b"

Depth to Top Reinforcing Mat (OCD):	2.0	in.
Reinforcing Bar Size:	5	
Deck Thickness:	7.5	in.
Depth to Bottom Reinforcing Mat:	6	in.
Depth of Concrete Removal:	3.375	in.
Number of Jet Passes:	1	
Which Jet Pass:	1	
Nozzle Jet Pressure:	20000	psi
Nozzle Diameter:	0.100	in.
Angle of Load (θ):	10	deg
Point Load (P):	157.08	lb
Design Compressive Strength ($f'_{c(design)}$):	4000	psi
Schmidt Rebound Number Available:	No	
Average Schmidt Rebound Number:	25	
Compressive Strength Based on Schmidt Number ($f'_{c(measured)}$):	2325	psi
Length (l):	12	in
Base (b):	6	in
Height (h):	1.17	in
Concrete Type:	Normal	
Aggregate Replaced:	Not Applicable	
λ:	1	
Modulus of Rupture (f_r):	474.3	psi
Type of Span:	one-way	
Moment of Inertia (I_{xx}):	0.80	in^4
Moment of Inertia (I_{yy})	21.06	in^4
Distance to Neutral Axis (y):	0.59	in
Maximum Moment (M_{max}):	464.08	in-lb
Cracking Moment (M_{cr}):	649	in-lb
Cracking Due to Flexure:	NO	
Maximum Shear (V_{max}):	77.35	lb
One-Way Shear Strength of Concrete (V_{c1}):	888	lb
Failure in One-Way Shear:	NO	
Punching Shear Strength of Concrete (V_{c2}):	1775.9	
Failure in Punching Shear:	NO	
Maximum Moment (M_{max}):	232.04	in-lb
Cracking Moment (M_{cr}):	17076	in-lb
Cracking Due to Flexure:	NO	
Maximum Shear (V_{max}):	77.35	lb
One-Way Shear Strength of Concrete (V_{c1}):	1776	lb
Failure in One-Way Shear:	NO	
Punching Shear Strength of Concrete (V_{c2}):	3551.9	
Failure in Punching Shear:	NO	

Figure B-5: Blow-through analysis for scenario 1 of case study #1.

Depth to Top Reinforcing Mat (OCD):	2.0	in.
Reinforcing Bar Size:	5	
Deck Thickness:	7.5	in.
Depth to Bottom Reinforcing Mat:	6	in.
Depth of Concrete Removal:	3.375	in.
Number of Jet Passes:	1	
Which Jet Pass:	1	
Nozzle Jet Pressure:	20000	psi
Nozzle Diameter:	0.100	in.
Angle of Load (θ):	10	deg
Point Load (P):	157.08	lb
Design Compressive Strength ($f'_{c(design)}$):	4000	psi
Schmidt Rebound Number Available:	No	
Average Schmidt Rebound Number:	25	
Compressive Strength Based on Schmidt Number ($f'c(measured)$):	2325	psi
Length (l):	12	in
Base (b):	4	in
Height (h):	1.17	in
Concrete Type:	Normal	
Aggregate Replaced:	Not Applicable	
λ:	1	
Modulus of Rupture (f_r):	474.3	psi
Type of Span:	one-way	
Moment of Inertia (I_{xx}):	0.53	in^4
Moment of Inertia (I_{yy})	6.24	in^4
Distance to Neutral Axis (y):	0.59	in
Maximum Moment (M_{max}):	464.08	in-lb
Cracking Moment (M_{cr}):	433	in-lb
Cracking Due to Flexure:	YES	
Maximum Shear (V_{max}):	77.35	lb
One-Way Shear Strength of Concrete (V_{c1}):	592	lb
Failure in One-Way Shear:	NO	
Punching Shear Strength of Concrete (V_{c2}):	1184.0	
Failure in Punching Shear:	NO	
Maximum Moment (M_{max}):	154.69	in-lb
Cracking Moment (M_{cr}):	5060	in-lb
Cracking Due to Flexure:	NO	
Maximum Shear (V_{max}):	77.35	lb
One-Way Shear Strength of Concrete (V_{c1}):	1776	lb
Failure in One-Way Shear:	NO	
Punching Shear Strength of Concrete (V_{c2}):	3551.9	
Failure in Punching Shear:	NO	

Analysis about y-axis, Icb | Analysis about x-axis, Ixb

Figure B-6: Blow-through analysis for scenario 2 of case study #1.

Analysis about y-axis, l<b Analysis about x-axis, l>b

Depth to Top Reinforcing Mat (OCD):	2.0	in.
Reinforcing Bar Size:	5	
Deck Thickness:	7.5	in.
Depth to Bottom Reinforcing Mat:	6	in.
Depth of Concrete Removal:	3.375	in.
Number of Jet Passes:	1	
Which Jet Pass:	1	
Nozzle Jet Pressure:	20000	psi
Nozzle Diameter:	0.100	in.
Angle of Load (θ):	10	deg
Point Load (P):	157.08	lb
Design Compressive Strength (f'$_{c(design)}$):	3000	psi
Schmidt Rebound Number Available:	No	
Average Schmidt Rebound Number:	25	
Compressive Strength Based on Schmidt Number (f'c(measured)):	2325	psi
Length (l):	12	in
Base (b):	5	in
Height (h):	1.17	in
Concrete Type:	Normal	
Aggregate Replaced:	Not Applicable	
λ:	1	
Modulus of Rupture (f$_r$):	410.8	psi
Type of Span:	one-way	
Moment of Inertia (I$_{xx}$):	0.67	in^4
Moment of Inertia (I$_{yy}$)	12.19	in^4
Distance to Neutral Axis (y):	0.59	in
Maximum Moment (M$_{max}$):	464.08	in-lb
Cracking Moment (M$_{cr}$):	469	in-lb
Cracking Due to Flexure:	NO	
Maximum Shear (V$_{max}$):	77.35	lb
One-Way Shear Strength of Concrete (V$_{c1}$):	641	lb
Failure in One-Way Shear:	NO	
Punching Shear Strength of Concrete (V$_{c2}$):	1281.7	
Failure in Punching Shear:	NO	
Maximum Moment (M$_{max}$):	193.37	in-lb
Cracking Moment (M$_{cr}$):	8558	in-lb
Cracking Due to Flexure:	NO	
Maximum Shear (V$_{max}$):	77.35	lb
One-Way Shear Strength of Concrete (V$_{c1}$):	1538	lb
Failure in One-Way Shear:	NO	
Punching Shear Strength of Concrete (V$_{c2}$):	3076.0	
Failure in Punching Shear:	NO	

Figure B-7: Blow-through analysis for scenario 3 for case study #1.

73

Depth to Top Reinforcing Mat (OCD):	2.0	in.
Reinforcing Bar Size:	5	
Deck Thickness:	7.5	in.
Depth to Bottom Reinforcing Mat:	6	in.
Depth of Concrete Removal:	3.375	in.
Number of Jet Passes:	1	
Which Jet Pass:	1	
Nozzle Jet Pressure:	20000	psi
Nozzle Diameter:	0.100	in.
Angle of Load (θ):	10	deg
Point Load (P):	157.08	lb
Design Compressive Strength ($f'_{c(design)}$):	2000	psi
Schmidt Rebound Number Available:	No	
Average Schmidt Rebound Number:	25	
Compressive Strength Based on Schmidt Number ($f'c(measured)$):	2325	psi
Length (l):	12	in
Base (b):	4	in
Height (h):	1.42	in
Concrete Type:	Normal	
Aggregate Replaced:	Not Applicable	
λ:	1	
Modulus of Rupture (f_r):	335.4	psi
Type of Span:	one-way	
Moment of Inertia (I_{xx}):	0.95	in^4
Moment of Inertia (I_{yy})	7.57	in^4
Distance to Neutral Axis (y):	0.71	in
Maximum Moment (M_{max}):	464.08	in-lb
Cracking Moment (M_{cr}):	451	in-lb
Cracking Due to Flexure:	YES	
Maximum Shear (V_{max}):	77.35	lb
One-Way Shear Strength of Concrete (V_{c1}):	508	lb
Failure in One-Way Shear:	NO	
Punching Shear Strength of Concrete (V_{c2}):	1016.1	
Failure in Punching Shear:	NO	
Maximum Moment (M_{max}):	154.69	in-lb
Cracking Moment (M_{cr}):	3578	in-lb
Cracking Due to Flexure:	NO	
Maximum Shear (V_{max}):	77.35	lb
One-Way Shear Strength of Concrete (V_{c1}):	1524	lb
Failure in One-Way Shear:	NO	
Punching Shear Strength of Concrete (V_{c2}):	3048.2	
Failure in Punching Shear:	NO	

Analysis about y-axis, Icb   Analysis about x-axis, Isb

Figure B-8: Blow-through analysis for scenario 4 for case study #1.

74

Depth to Top Reinforcing Mat (OCD):	2.0	in.
Reinforcing Bar Size:	5	
Deck Thickness:	7.5	in.
Depth to Bottom Reinforcing Mat:	6	in.
Depth of Concrete Removal:	3.375	in.
Number of Jet Passes:	1	
Which Jet Pass:	1	
Nozzle Jet Pressure:	20000	psi
Nozzle Diameter:	0.100	in.
Angle of Load (θ):	10	deg
Point Load (P):	157.08	lb
Design Compressive Strength ($f'_{c(design)}$):	4000	psi
Schmidt Rebound Number Available:	No	
Average Schmidt Rebound Number:	25	
Compressive Strength Based on Schmidt Number ($f'c(measured)$):	2325	psi
Length (l):	12	in
Base (b):	6	in
Height (h):	0.92	in
Concrete Type:	Normal	
Aggregate Replaced:	Not Applicable	
λ:	1	
Modulus of Rupture (f_r):	474.3	psi
Type of Span:	one-way	
Moment of Inertia (I_{xx}):	0.39	in^4
Moment of Inertia (I_{yy}):	16.52	in^4
Distance to Neutral Axis (y):	0.46	in
Maximum Moment (M_{max}):	464.08	in-lb
Cracking Moment (M_{cr}):	400	in-lb
Cracking Due to Flexure:	YES	
Maximum Shear (V_{max}):	77.35	lb
One-Way Shear Strength of Concrete (V_{c1}):	697	lb
Failure in One-Way Shear:	NO	
Punching Shear Strength of Concrete (V_{c2}):	1393.4	
Failure in Punching Shear:	NO	
Maximum Moment (M_{max}):	232.04	in-lb
Cracking Moment (M_{cr}):	17076	in-lb
Cracking Due to Flexure:	NO	
Maximum Shear (V_{max}):	77.35	lb
One-Way Shear Strength of Concrete (V_{c1}):	1393	lb
Failure in One-Way Shear:	NO	
Punching Shear Strength of Concrete (V_{c2}):	2786.9	
Failure in Punching Shear:	NO	

Figure B-9: Blow-through analysis for scenario 5 for case study #1.

Depth to Top Reinforcing Mat (OCD):	2.0 in.
Reinforcing Bar Size:	5
Deck Thickness:	7.5 in.
Depth to Bottom Reinforcing Mat:	6 in.
Depth of Concrete Removal:	3.375 in.
Number of Jet Passes:	1
Which Jet Pass:	1
Nozzle Jet Pressure:	20000 psi
Nozzle Diameter:	0.100 in.
Angle of Load (θ):	10 deg
Point Load (P):	157.08 lb
Design Compressive Strength ($f'_{c(design)}$):	4000 psi
Schmidt Rebound Number Available:	No
Average Schmidt Rebound Number:	25
Compressive Strength Based on Schmidt Number ($f'c(measured)$):	2325 psi
Length (l):	12 in
Base (b):	7 in
Height (h):	0.92 in
Concrete Type:	Normal
Aggregate Replaced:	Not Applicable
λ:	1
Modulus of Rupture (f_r):	474.3 psi
Type of Span:	two-way
Moment of Inertia (I_{xx}):	0.45 in^4
Moment of Inertia (I_{yy})	26.23 in^4
Distance to Neutral Axis (y):	0.46 in
Maximum Moment (M_{max}):	464.08 in-lb
Cracking Moment (M_{cr}):	466 in-lb
Cracking Due to Flexure:	NO
Maximum Shear (V_{max}):	77.35 lb
One-Way Shear Strength of Concrete (V_{c1}):	812 lb
Failure in One-Way Shear:	NO
Punching Shear Strength of Concrete (V_{c2}):	1624.8
Failure in Punching Shear:	NO
Maximum Moment (M_{max}):	270.71 in-lb
Cracking Moment (M_{cr}):	27117 in-lb
Cracking Due to Flexure:	NO
Maximum Shear (V_{max}):	77.35 lb
One-Way Shear Strength of Concrete (V_{c1}):	1393 lb
Failure in One-Way Shear:	NO
Punching Shear Strength of Concrete (V_{c2}):	2785.3
Failure in Punching Shear:	NO

Analysis about y-axis, l>b   Analysis about x-axis, l>b

Figure B-10: Blow-through analysis for scenario 6 for case study #1.

Depth to Top Reinforcing Mat (OCD):	2.0	in.
Reinforcing Bar Size:	5	
Deck Thickness:	7.5	in.
Depth to Bottom Reinforcing Mat:	6	in.
Depth of Concrete Removal:	3.375	in.
Number of Jet Passes:	1	
Which Jet Pass:	1	
Nozzle Jet Pressure:	20000	psi
Nozzle Diameter:	0.100	in.
Angle of Load (θ):	10	deg
Point Load (P):	157.08	lb
Design Compressive Strength ($f'_{cf design}$):	4000	psi
Schmidt Rebound Number Available:	No	
Average Schmidt Rebound Number:	25	
Compressive Strength Based on Schmidt Number ($f'c$(measured)):	2325	psi
Length (l):	12	in
Base (b):	6	in
Height (h):	1.06	in
Concrete Type:	Normal	
Aggregate Replaced:	Not Applicable	
λ:	1	
Modulus of Rupture (f_r):	474.3	psi
Type of Span:	one-way	
Moment of Inertia (I_{xx}):	0.59	in^4
Moment of Inertia (I_{yy}):	19.07	in^4
Distance to Neutral Axis (y):	0.53	in
Maximum Moment (M_{max}):	464.08	in-lb
Cracking Moment (M_{cr}):	532	in-lb
Cracking Due to Flexure:	NO	
Maximum Shear (V_{max}):	77.35	lb
One-Way Shear Strength of Concrete (V_{c1}):	804	lb
Failure in One-Way Shear:	NO	
Punching Shear Strength of Concrete (V_{c2}):	1608.2	
Failure in Punching Shear:	NO	
Maximum Moment (M_{max}):	232.04	in-lb
Cracking Moment (M_{cr}):	17076	in-lb
Cracking Due to Flexure:	NO	
Maximum Shear (V_{max}):	77.35	lb
One-Way Shear Strength of Concrete (V_{c1}):	1608	lb
Failure in One-Way Shear:	NO	
Punching Shear Strength of Concrete (V_{c2}):	3216.4	
Failure in Punching Shear:	NO	

(left margin labels: Analysis about y-axis, I<b   I<b Analysis about x-axis, I>b)

Figure B-11: Blow-through analysis for scenario 7 for case study #1.

77

Analysis about y-axis, I<b | Analysis about x-axis, I>b

Depth to Top Reinforcing Mat (OCD):	2.0	in.
Reinforcing Bar Size:	5	
Deck Thickness:	7.5	in.
Depth to Bottom Reinforcing Mat:	6	in.
Depth of Concrete Removal:	3.375	in.
Number of Jet Passes:	1	
Which Jet Pass:	1	
Nozzle Jet Pressure:	20000	psi
Nozzle Diameter:	0.100	in.
Angle of Load (θ):	10	deg
Point Load (P):	157.08	lb
Design Compressive Strength (f'$_{c(design)}$):	3000	psi
Schmidt Rebound Number Available:	No	
Average Schmidt Rebound Number:	25	
Compressive Strength Based on Schmidt Number (f'c(measured)):	2325	psi
Length (l):	12	in
Base (b):	5	in
Height (h):	1.12	in
Concrete Type:	Normal	
Aggregate Replaced:	Not Applicable	
λ:	1	
Modulus of Rupture (f$_r$):	410.8	psi
Type of Span:	one-way	
Moment of Inertia (I$_{xx}$):	0.59	in^4
Moment of Inertia (I$_{yy}$)	11.69	in^4
Distance to Neutral Axis (y):	0.56	in
Maximum Moment (M$_{max}$):	464.08	in-lb
Cracking Moment (M$_{cr}$):	431	in-lb
Cracking Due to Flexure:	YES	
Maximum Shear (V$_{max}$):	77.35	lb
One-Way Shear Strength of Concrete (V$_{c1}$):	615	lb
Failure in One-Way Shear:	NO	
Punching Shear Strength of Concrete (V$_{c2}$):	1229.1	
Failure in Punching Shear:	NO	
Maximum Moment (M$_{max}$):	193.37	in-lb
Cracking Moment (M$_{cr}$):	8558	in-lb
Cracking Due to Flexure:	NO	
Maximum Shear (V$_{max}$):	77.35	lb
One-Way Shear Strength of Concrete (V$_{c1}$):	1475	lb
Failure in One-Way Shear:	NO	
Punching Shear Strength of Concrete (V$_{c2}$):	2949.8	
Failure in Punching Shear:	NO	

Figure B-12: Blow-through analysis for scenario 8 for case study #1.

Depth to Top Reinforcing Mat (OCD):	2.0	in.
Reinforcing Bar Size:	5	
Deck Thickness:	7.5	in.
Depth to Bottom Reinforcing Mat:	6	in.
Depth of Concrete Removal:	3.375	in.
Number of Jet Passes:	1	
Which Jet Pass:	1	
Nozzle Jet Pressure:	20000	psi
Nozzle Diameter:	0.100	in.
Angle of Load (θ):	10	deg
Point Load (P):	157.08	lb
Design Compressive Strength ($f'_{c(design)}$):	3000	psi
Schmidt Rebound Number Available:	No	
Average Schmidt Rebound Number:	25	
Compressive Strength Based on Schmidt Number ($f'c(measured)$):	2325	psi
Length (l):	12	in
Base (b):	6	in
Height (h):	1.06	in
Concrete Type:	Normal	
Aggregate Replaced:	Not Applicable	
λ:	1	
Modulus of Rupture (f_r):	410.8	psi
Type of Span:	one-way	
Moment of Inertia (I_{xx}):	0.59	in^4
Moment of Inertia (I_{yy}):	19.07	in^4
Distance to Neutral Axis (y):	0.53	in
Maximum Moment (M_{max}):	464.08	in-lb
Cracking Moment (M_{cr}):	461	in-lb
Cracking Due to Flexure:	YES	
Maximum Shear (V_{max}):	77.35	lb
One-Way Shear Strength of Concrete (V_{c1}):	696	lb
Failure in One-Way Shear:	NO	
Punching Shear Strength of Concrete (V_{c2}):	1392.7	
Failure in Punching Shear:	NO	
Maximum Moment (M_{max}):	232.04	in-lb
Cracking Moment (M_{cr}):	14789	in-lb
Cracking Due to Flexure:	NO	
Maximum Shear (V_{max}):	77.35	lb
One-Way Shear Strength of Concrete (V_{c1}):	1393	lb
Failure in One-Way Shear:	NO	
Punching Shear Strength of Concrete (V_{c2}):	2785.5	
Failure in Punching Shear:	NO	

Figure B-13: Blow-through analysis for scenario 9 for case study #1.

APPENDIX C: BLOW-THROUGH ANALYSIS FOR CASE STUDY #2

   Figure C-1 shows the sections of the bridge plans that were used to determine identifiers for the bar sizes used for the blow-through analyses for case study #2. Figures C-2 and C-3 show the bridge plans that were used to determine bar sizes for transverse reinforcement and longitudinal reinforcement, respectively. Figures C-4 through C-12 show the blow-through analysis outputs for each of the nine scenarios that were analyzed for case study #2.
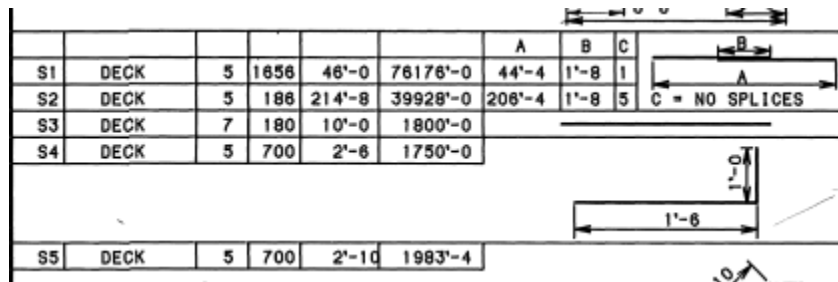

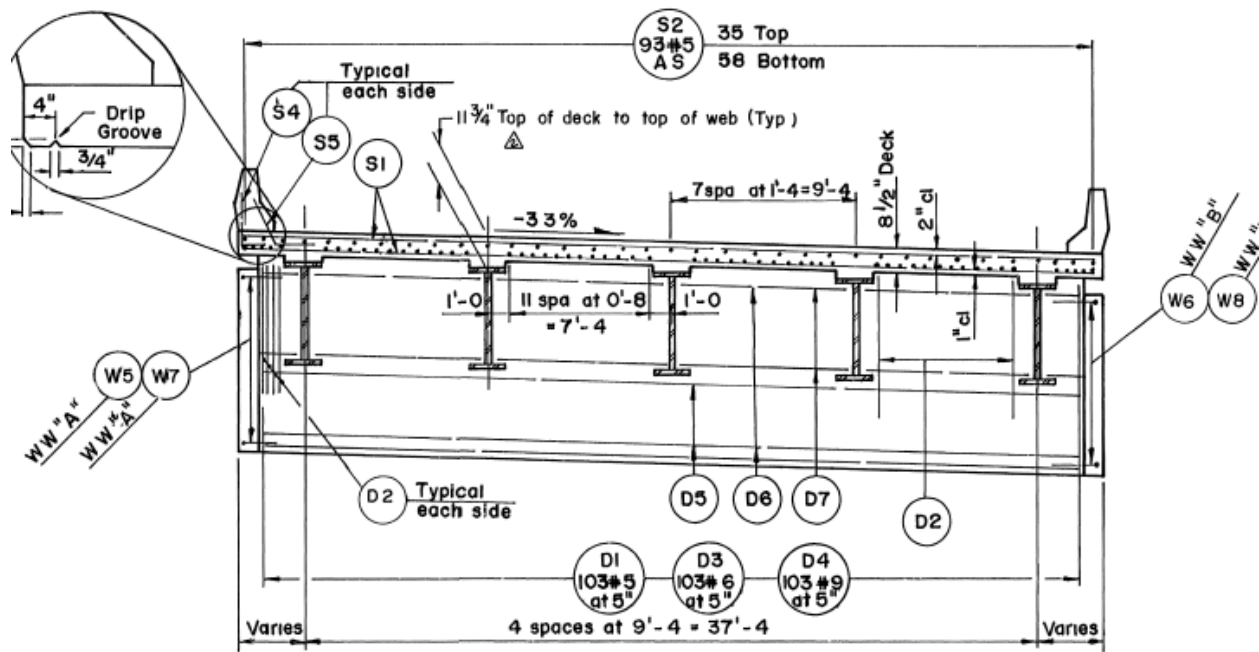**Figure C-1: Reinforcement plans for bridge deck in case study #2.**

Figure C-2: Bridge schematic showing transverse reinforcing bar locations, deck thickness, and cover depths for bridge deck in case study #2.
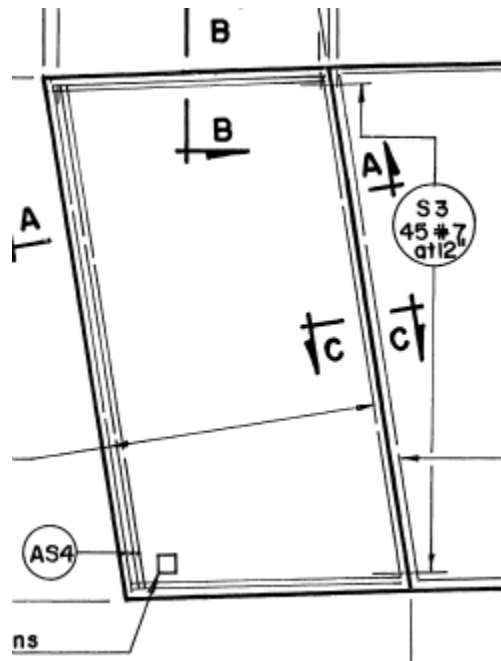

Figure C-3: Bridge schematic showing longitudinal reinforcing bar locations for bridge deck in case study #2.

Depth to Top Reinforcing Mat (OCD):	2.0	in.
Reinforcing Bar Size:	5	
Deck Thickness:	8.5	in.
Depth to Bottom Reinforcing Mat:	6	in.
Depth of Concrete Removal:	3.375	in.
Number of Jet Passes:	1	
Which Jet Pass:	1	
Nozzle Jet Pressure:	34000	psi
Nozzle Diameter:	0.100	in.
Angle of Load (θ):	10	deg
Point Load (P):	267.04	lb
Design Compressive Strength ($f'_{c(design)}$):	4000	psi
Schmidt Rebound Number Available:	No	
Average Schmidt Rebound Number:	25	
Compressive Strength Based on Schmidt Number ($f'c(measured)$):	2325	psi
Length (l):	12	in
Base (b):	6	in
Height (h):	2.56	in
Concrete Type:	Normal	
Aggregate Replaced:	Not Applicable	
λ:	1	
Modulus of Rupture (f_r):	474.3	psi
Type of Span:	one-way	
Moment of Inertia (I_{xx}):	8.41	in^4
Moment of Inertia (I_{yy})	46.13	in^4
Distance to Neutral Axis (y):	1.28	in
Maximum Moment (M_{max}):	788.94	in-lb
Cracking Moment (M_{cr}):	3115	in-lb
Cracking Due to Flexure:	NO	
Maximum Shear (V_{max}):	131.49	lb
One-Way Shear Strength of Concrete (V_{c1}):	1945	lb
Failure in One-Way Shear:	NO	
Punching Shear Strength of Concrete (V_{c2}):	3889.6	
Failure in Punching Shear:	NO	
Maximum Moment (M_{max}):	394.47	in-lb
Cracking Moment (M_{cr}):	17076	in-lb
Cracking Due to Flexure:	NO	
Maximum Shear (V_{max}):	131.49	lb
One-Way Shear Strength of Concrete (V_{c1}):	3890	lb
Failure in One-Way Shear:	NO	
Punching Shear Strength of Concrete (V_{c2}):	7779.2	
Failure in Punching Shear:	NO	

Analysis about y-axis, l<b   Analysis about x-axis, l>b

Figure C-4: Blow-through analysis for scenario 1 for case study #2.

Depth to Top Reinforcing Mat (OCD):	2.0	in.
Reinforcing Bar Size:	5	
Deck Thickness:	8.5	in.
Depth to Bottom Reinforcing Mat:	6	in.
Depth of Concrete Removal:	3.375	in.
Number of Jet Passes:	1	
Which Jet Pass:	1	
Nozzle Jet Pressure:	34000	psi
Nozzle Diameter:	0.100	in.
Angle of Load (θ):	10	deg
Point Load (P):	267.04	lb
Design Compressive Strength ($f'_{c(design)}$):	4000	psi
Schmidt Rebound Number Available:	No	
Average Schmidt Rebound Number:	25	
Compressive Strength Based on Schmidt Number (f'c(measured)):	2325	psi
Length (l):	12	in
Base (b):	6	in
Height (h):	2.19	in
Concrete Type:	Normal	
Aggregate Replaced:	Not Applicable	
λ:	1	
Modulus of Rupture (f_r):	474.3	psi
Type of Span:	one-way	
Moment of Inertia (I_{xx}):	5.25	in^4
Moment of Inertia (I_{yy})	39.42	in^4
Distance to Neutral Axis (y):	1.10	in
Maximum Moment (M_{max}):	788.94	in-lb
Cracking Moment (M_{cr}):	2275	in-lb
Cracking Due to Flexure:	NO	
Maximum Shear (V_{max}):	131.49	lb
One-Way Shear Strength of Concrete (V_{c1}):	1662	lb
Failure in One-Way Shear:	NO	
Punching Shear Strength of Concrete (V_{c2}):	3324.2	
Failure in Punching Shear:	NO	
Maximum Moment (M_{max}):	394.47	in-lb
Cracking Moment (M_{cr}):	17076	in-lb
Cracking Due to Flexure:	NO	
Maximum Shear (V_{max}):	131.49	lb
One-Way Shear Strength of Concrete (V_{c1}):	3324	lb
Failure in One-Way Shear:	NO	
Punching Shear Strength of Concrete (V_{c2}):	6648.4	
Failure in Punching Shear:	NO	

Analysis about y-axis, l>b   Analysis about x-axis, l>b

Figure C-5: Blow-through analysis for scenario 2 for case study #2.

Depth to Top Reinforcing Mat (OCD):	2.0	in.
Reinforcing Bar Size:	5	
Deck Thickness:	8.5	in.
Depth to Bottom Reinforcing Mat:	6	in.
Depth of Concrete Removal:	3.375	in.
Number of Jet Passes:	1	
Which Jet Pass:	1	
Nozzle Jet Pressure:	34000	psi
Nozzle Diameter:	0.100	in.
Angle of Load (θ):	10	deg
Point Load (P):	267.04	lb
Design Compressive Strength ($f'_{c(design)}$):	2000	psi
Schmidt Rebound Number Available:	No	
Average Schmidt Rebound Number:	25	
Compressive Strength Based on Schmidt Number ($f'c(measured)$):	2325	psi
Length (l):	12	in
Base (b):	4	in
Height (h):	2.19	in
Concrete Type:	Normal	
Aggregate Replaced:	Not Applicable	
λ:	1	
Modulus of Rupture (f_r):	335.4	psi
Type of Span:	one-way	
Moment of Inertia (I_{xx}):	3.50	in^4
Moment of Inertia (I_{yy}):	11.68	in^4
Distance to Neutral Axis (y):	1.10	in
Maximum Moment (M_{max}):	788.94	in-lb
Cracking Moment (M_{cr}):	1072	in-lb
Cracking Due to Flexure:	NO	
Maximum Shear (V_{max}):	131.49	lb
One-Way Shear Strength of Concrete (V_{c1}):	784	lb
Failure in One-Way Shear:	NO	
Punching Shear Strength of Concrete (V_{c2}):	1567.0	
Failure in Punching Shear:	NO	
Maximum Moment (M_{max}):	262.98	in-lb
Cracking Moment (M_{cr}):	3578	in-lb
Cracking Due to Flexure:	NO	
Maximum Shear (V_{max}):	131.49	lb
One-Way Shear Strength of Concrete (V_{c1}):	2351	lb
Failure in One-Way Shear:	NO	
Punching Shear Strength of Concrete (V_{c2}):	4701.1	
Failure in Punching Shear:	NO	

Analysis about y-axis, I<b   Analysis about x-axis, I>b

Figure C-6: Blow-through analysis for scenario 3 for case study #2.

Depth to Top Reinforcing Mat (OCD):	2.0	in.
Reinforcing Bar Size:	5	
Deck Thickness:	8.5	in.
Depth to Bottom Reinforcing Mat:	6	in.
Depth of Concrete Removal:	3.375	in.
Number of Jet Passes:	1	
Which Jet Pass:	1	
Nozzle Jet Pressure:	34000	psi
Nozzle Diameter:	0.100	in.
Angle of Load (θ):	10	deg
Point Load (P):	267.04	lb
Design Compressive Strength ($f'_{c(design)}$):	2000	psi
Schmidt Rebound Number Available:	No	
Average Schmidt Rebound Number:	25	
Compressive Strength Based on Schmidt Number ($f'c(measured)$):	2325	psi
Length (l):	12	in
Base (b):	4	in
Height (h):	1.94	in
Concrete Type:	Normal	
Aggregate Replaced:	Not Applicable	
λ:	1	
Modulus of Rupture (f_r):	335.4	psi
Type of Span:	one-way	
Moment of Inertia (I_{xx}):	2.43	in^4
Moment of Inertia (I_{yy})	10.35	in^4
Distance to Neutral Axis (y):	0.97	in
Maximum Moment (M_{max}):	788.94	in-lb
Cracking Moment (M_{cr}):	842	in-lb
Cracking Due to Flexure:	NO	
Maximum Shear (V_{max}):	131.49	lb
One-Way Shear Strength of Concrete (V_{c1}):	694	lb
Failure in One-Way Shear:	NO	
Punching Shear Strength of Concrete (V_{c2}):	1388.2	
Failure in Punching Shear:	NO	
Maximum Moment (M_{max}):	262.98	in-lb
Cracking Moment (M_{cr}):	3578	in-lb
Cracking Due to Flexure:	NO	
Maximum Shear (V_{max}):	131.49	lb
One-Way Shear Strength of Concrete (V_{c1}):	2082	lb
Failure in One-Way Shear:	NO	
Punching Shear Strength of Concrete (V_{c2}):	4164.5	
Failure in Punching Shear:	NO	

Analysis about y-axis, I<b Analysis about x-axis, I>b

Figure C-7: Blow-through analysis for scenario 4 for case study #2.

Depth to Top Reinforcing Mat (OCD):	2.0	in.
Reinforcing Bar Size:	5	
Deck Thickness:	8.5	in.
Depth to Bottom Reinforcing Mat:	6	in.
Depth of Concrete Removal:	3.375	in.
Number of Jet Passes:	1	
Which Jet Pass:	1	
Nozzle Jet Pressure:	34000	psi
Nozzle Diameter:	0.100	in.
Angle of Load (θ):	10	deg
Point Load (P):	267.04	lb
Design Compressive Strength ($f'_{c(design)}$):	2000	psi
Schmidt Rebound Number Available:	No	
Average Schmidt Rebound Number:	25	
Compressive Strength Based on Schmidt Number ($f'c(measured)$):	2325	psi
Length (l):	12	in
Base (b):	5	in
Height (h):	2.19	in
Concrete Type:	Normal	
Aggregate Replaced:	Not Applicable	
λ:	1	
Modulus of Rupture (f_r):	335.4	psi
Type of Span:	one-way	
Moment of Inertia (I_{xx}):	4.38	in^4
Moment of Inertia (I_{yy})	22.81	in^4
Distance to Neutral Axis (y):	1.10	in
Maximum Moment (M_{max}):	788.94	in-lb
Cracking Moment (M_{cr}):	1341	in-lb
Cracking Due to Flexure:	NO	
Maximum Shear (V_{max}):	131.49	lb
One-Way Shear Strength of Concrete (V_{c1}):	979	lb
Failure in One-Way Shear:	NO	
Punching Shear Strength of Concrete (V_{c2}):	1958.8	
Failure in Punching Shear:	NO	
Maximum Moment (M_{max}):	328.72	in-lb
Cracking Moment (M_{cr}):	6988	in-lb
Cracking Due to Flexure:	NO	
Maximum Shear (V_{max}):	131.49	lb
One-Way Shear Strength of Concrete (V_{c1}):	2351	lb
Failure in One-Way Shear:	NO	
Punching Shear Strength of Concrete (V_{c2})	4701.1	
Failure in Punching Shear:	NO	

Analysis about y-axis, I_{yb} / Analysis about x-axis, I_{xb}

Figure C-8: Blow-through analysis for scenario 5 for case study #2.

Depth to Top Reinforcing Mat (OCD):	2.0	in.
Reinforcing Bar Size:	5	
Deck Thickness:	8.5	in.
Depth to Bottom Reinforcing Mat:	6	in.
Depth of Concrete Removal:	3.375	in.
Number of Jet Passes:	1	
Which Jet Pass:	1	
Nozzle Jet Pressure:	34000	psi
Nozzle Diameter:	0.100	in.
Angle of Load (θ):	10	deg
Point Load (P):	267.04	lb
Design Compressive Strength ($f'_{c(design)}$):	2000	psi
Schmidt Rebound Number Available:	No	
Average Schmidt Rebound Number:	25	
Compressive Strength Based on Schmidt Number ($f'c(measured)$):	2325	psi
Length (l):	12	in
Base (b):	5	in
Height (h):	1.94	in
Concrete Type:	Normal	
Aggregate Replaced:	Not Applicable	
λ:	1	
Modulus of Rupture (f_r):	335.4	psi
Type of Span:	one-way	
Moment of Inertia (I_{xx}):	3.04	in^4
Moment of Inertia (I_{yy})	20.21	in^4
Distance to Neutral Axis (y):	0.97	in
Maximum Moment (M_{max}):	788.94	in-lb
Cracking Moment (M_{cr}):	1052	in-lb
Cracking Due to Flexure:	NO	
Maximum Shear (V_{max}):	131.49	lb
One-Way Shear Strength of Concrete (V_{c1}):	868	lb
Failure in One-Way Shear:	NO	
Punching Shear Strength of Concrete (V_{c2}):	1735.2	
Failure in Punching Shear:	NO	
Maximum Moment (M_{max}):	328.72	in-lb
Cracking Moment (M_{cr}):	6988	in-lb
Cracking Due to Flexure:	NO	
Maximum Shear (V_{max}):	131.49	lb
One-Way Shear Strength of Concrete (V_{c1}):	2082	lb
Failure in One-Way Shear:	NO	
Punching Shear Strength of Concrete (V_{c2}):	4164.5	
Failure in Punching Shear:	NO	

Analysis about y-axis, I>b   Analysis about x-axis, I>b

Figure C-9: Blow-through analysis for scenario 6 for case study #2.

87

Depth to Top Reinforcing Mat (OCD):	2.0	in.
Reinforcing Bar Size:	5	
Deck Thickness:	8.5	in.
Depth to Bottom Reinforcing Mat:	6	in.
Depth of Concrete Removal:	3.375	in.
Number of Jet Passes:	1	
Which Jet Pass:	1	
Nozzle Jet Pressure:	34000	psi
Nozzle Diameter:	0.100	in.
Angle of Load (θ):	10	deg
Point Load (P):	267.04	lb
Design Compressive Strength ($f'_{c(design)}$):	3000	psi
Schmidt Rebound Number Available:	No	
Average Schmidt Rebound Number:	25	
Compressive Strength Based on Schmidt Number (f'c(measured)):	2325	psi
Length (l):	12	in
Base (b):	5	in
Height (h):	2.19	in
Concrete Type:	Normal	
Aggregate Replaced:	Not Applicable	
λ:	1	
Modulus of Rupture (f_r):	410.8	psi
Type of Span:	one-way	
Moment of Inertia (I_{xx}):	4.38	in^4
Moment of Inertia (I_{yy})	22.81	in^4
Distance to Neutral Axis (y):	1.10	in
Maximum Moment (M_{max}):	788.94	in-lb
Cracking Moment (M_{cr}):	1642	in-lb
Cracking Due to Flexure:	NO	
Maximum Shear (V_{max}):	131.49	lb
One-Way Shear Strength of Concrete (V_{c1}):	1200	lb
Failure in One-Way Shear:	NO	
Punching Shear Strength of Concrete (V_{c2}):	2399.0	
Failure in Punching Shear:	NO	
Maximum Moment (M_{max}):	328.72	in-lb
Cracking Moment (M_{cr}):	8558	in-lb
Cracking Due to Flexure:	NO	
Maximum Shear (V_{max}):	131.49	lb
One-Way Shear Strength of Concrete (V_{c1}):	2879	lb
Failure in One-Way Shear:	NO	
Punching Shear Strength of Concrete (V_{c2}):	5757.7	
Failure in Punching Shear:	NO	

(left margin, vertical text) Analysis about y-axis, I<b | Icb Analysis about x-axis, I>b

Figure C-10: Blow-through analysis for scenario 7 for case study #2.

88

Depth to Top Reinforcing Mat (OCD):	2.0	in.
Reinforcing Bar Size:	5	
Deck Thickness:	8.5	in.
Depth to Bottom Reinforcing Mat:	6	in.
Depth of Concrete Removal:	3.375	in.
Number of Jet Passes:	1	
Which Jet Pass:	1	
Nozzle Jet Pressure:	34000	psi
Nozzle Diameter:	0.100	in.
Angle of Load (θ):	10	deg
Point Load (P):	267.04	lb
Design Compressive Strength ($f'_{c(design)}$):	3000	psi
Schmidt Rebound Number Available:	No	
Average Schmidt Rebound Number:	25	
Compressive Strength Based on Schmidt Number ($f'c(measured)$):	2325	psi
Length (l):	12	in
Base (b):	4	in
Height (h):	1.94	in
Concrete Type:	Normal	
Aggregate Replaced:	Not Applicable	
λ:	1	
Modulus of Rupture (f_r):	410.8	psi
Type of Span:	one-way	
Moment of Inertia (I_{xx}):	2.43	in^4
Moment of Inertia (I_{yy}):	10.35	in^4
Distance to Neutral Axis (y):	0.97	in
Maximum Moment (M_{max}):	788.94	in-lb
Cracking Moment (M_{cr}):	1031	in-lb
Cracking Due to Flexure:	NO	
Maximum Shear (V_{max}):	131.49	lb
One-Way Shear Strength of Concrete (V_{c1}):	850	lb
Failure in One-Way Shear:	NO	
Punching Shear Strength of Concrete (V_{c2}):	1700.1	
Failure in Punching Shear:	NO	
Maximum Moment (M_{max}):	262.98	in-lb
Cracking Moment (M_{cr}):	4382	in-lb
Cracking Due to Flexure:	NO	
Maximum Shear (V_{max}):	131.49	lb
One-Way Shear Strength of Concrete (V_{c1}):	2550	lb
Failure in One-Way Shear:	NO	
Punching Shear Strength of Concrete (V_{c2}):	5100.4	
Failure in Punching Shear:	NO	

Figure C-11: Blow-through analysis for scenario 8 for case study #2.

89

Analysis about y-axis, I>b   Analysis about x-axis, I<b

Depth to Top Reinforcing Mat (OCD):	2.0	in.
Reinforcing Bar Size:	5	
Deck Thickness:	8.5	in.
Depth to Bottom Reinforcing Mat:	6	in.
Depth of Concrete Removal:	3.375	in.
Number of Jet Passes:	1	
Which Jet Pass:	1	
Nozzle Jet Pressure:	34000	psi
Nozzle Diameter:	0.100	in.
Angle of Load (θ):	10	deg
Point Load (P):	267.04	lb
Design Compressive Strength ($f'_{c(design)}$):	3000	psi
Schmidt Rebound Number Available:	No	
Average Schmidt Rebound Number:	25	
Compressive Strength Based on Schmidt Number ($f'c(measured)$):	2325	psi
Length (l):	12	in
Base (b):	6	in
Height (h):	1.94	in
Concrete Type:	Normal	
Aggregate Replaced:	Not Applicable	
λ:	1	
Modulus of Rupture (f_r):	410.8	psi
Type of Span:	one-way	
Moment of Inertia (I_{xx}):	3.65	in^4
Moment of Inertia (I_{yy})	34.92	in^4
Distance to Neutral Axis (y):	0.97	in
Maximum Moment (M_{max}):	788.94	in-lb
Cracking Moment (M_{cr}):	1546	in-lb
Cracking Due to Flexure:	NO	
Maximum Shear (V_{max}):	131.49	lb
One-Way Shear Strength of Concrete (V_{c1}):	1275	lb
Failure in One-Way Shear:	NO	
Punching Shear Strength of Concrete (V_{c2}):	2550.2	
Failure in Punching Shear:	NO	
Maximum Moment (M_{max}):	394.47	in-lb
Cracking Moment (M_{cr}):	14789	in-lb
Cracking Due to Flexure:	NO	
Maximum Shear (V_{max}):	131.49	lb
One-Way Shear Strength of Concrete (V_{c1}):	2550	lb
Failure in One-Way Shear:	NO	
Punching Shear Strength of Concrete (V_{c2}):	5100.4	
Failure in Punching Shear:	NO	

Figure C-12: Blow-through analysis for scenario 9 for case study #2.

90

APPENDIX D: CHLORIDE CONCENTRATION AT TOP MAT OF REINFORCING STEEL WITH AN APPLIED SURFACE TREATMENT

Figures D-1, D-2, and D-3 show the numerical modeling results for the top mat of reinforcing steel in a concrete bridge deck with a 2.0-, 2.5-, or 3.0-in. OCD, respectively, with an applied surface treatment.
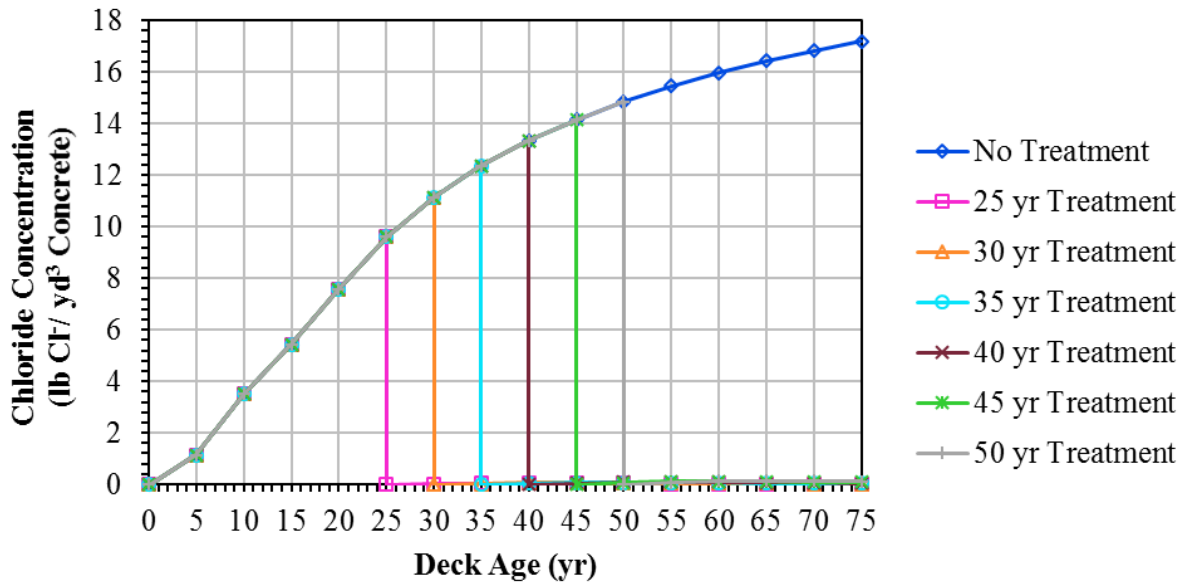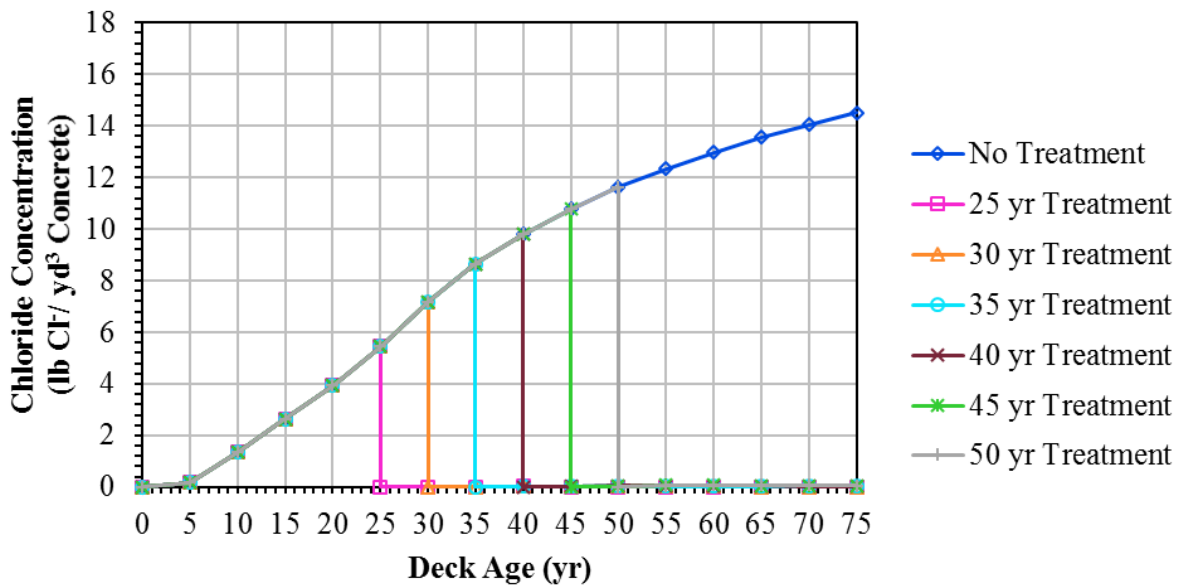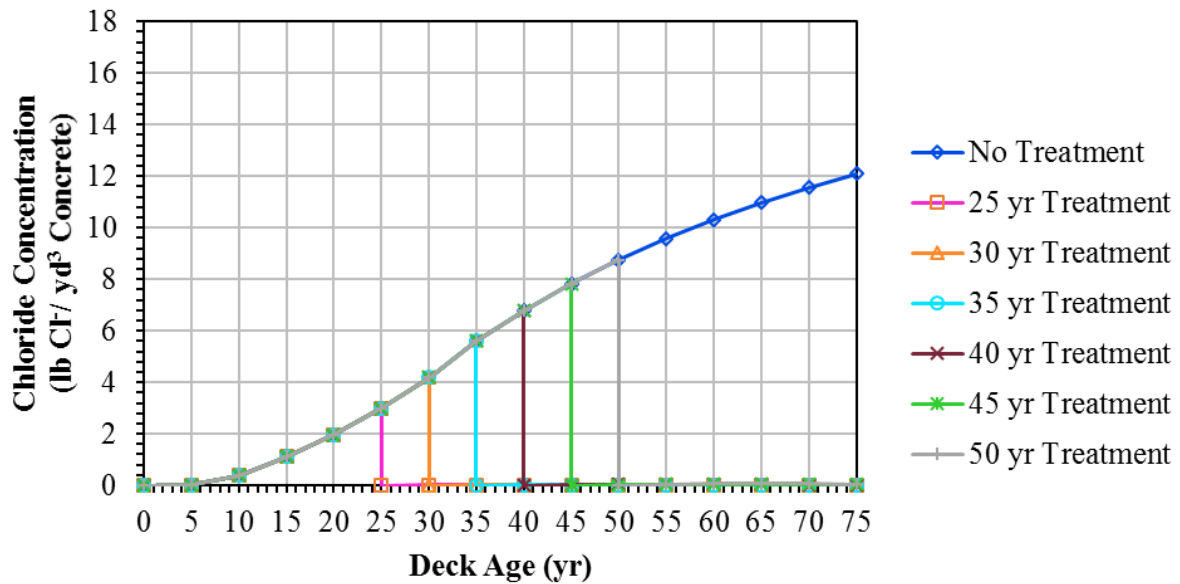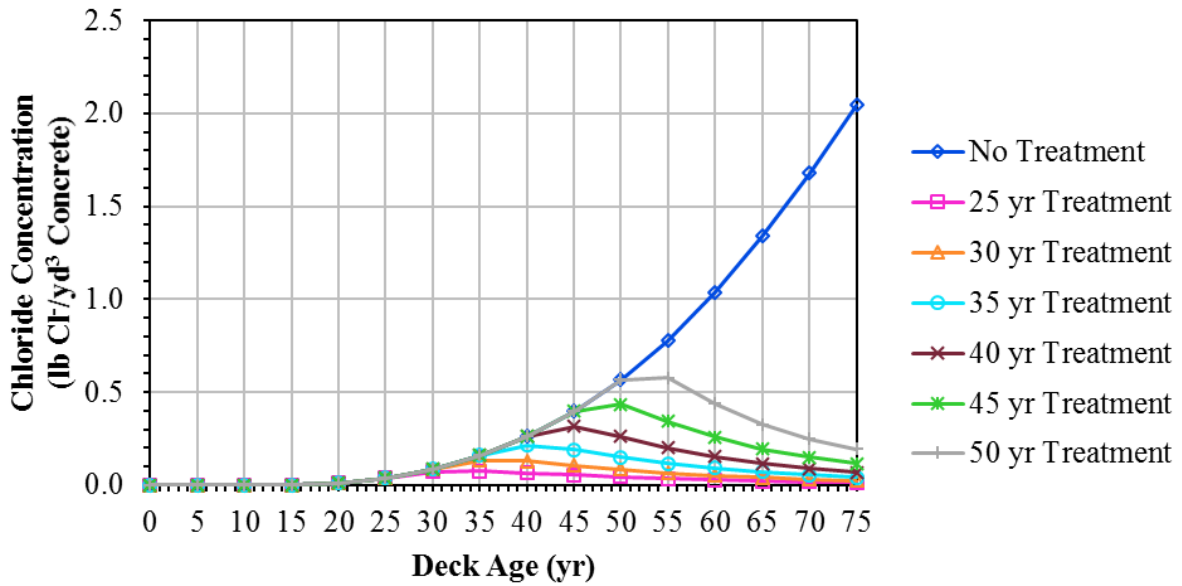

Figure D-1: Simulated chloride concentrations at the top mat of reinforcement for a deck with 2.0-in. OCD and a 3.375-in. removal depth with an applied surface treatment.
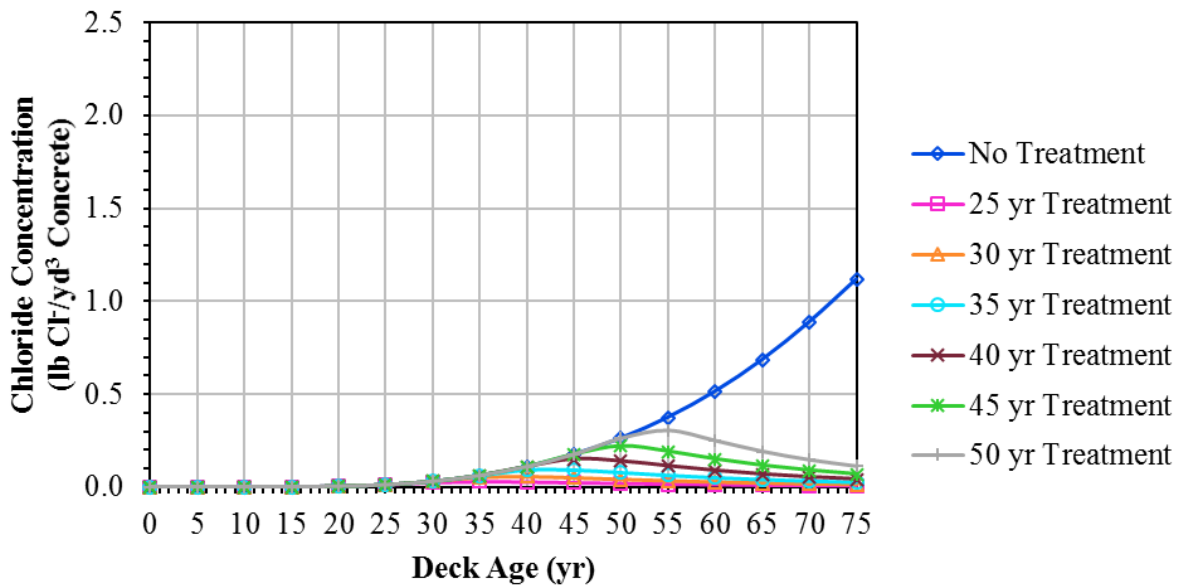
Figure D-2: Simulated chloride concentrations at the top mat of reinforcement for a deck with 2.5-in. OCD and a 3.875-in. removal depth with an applied surface treatment.
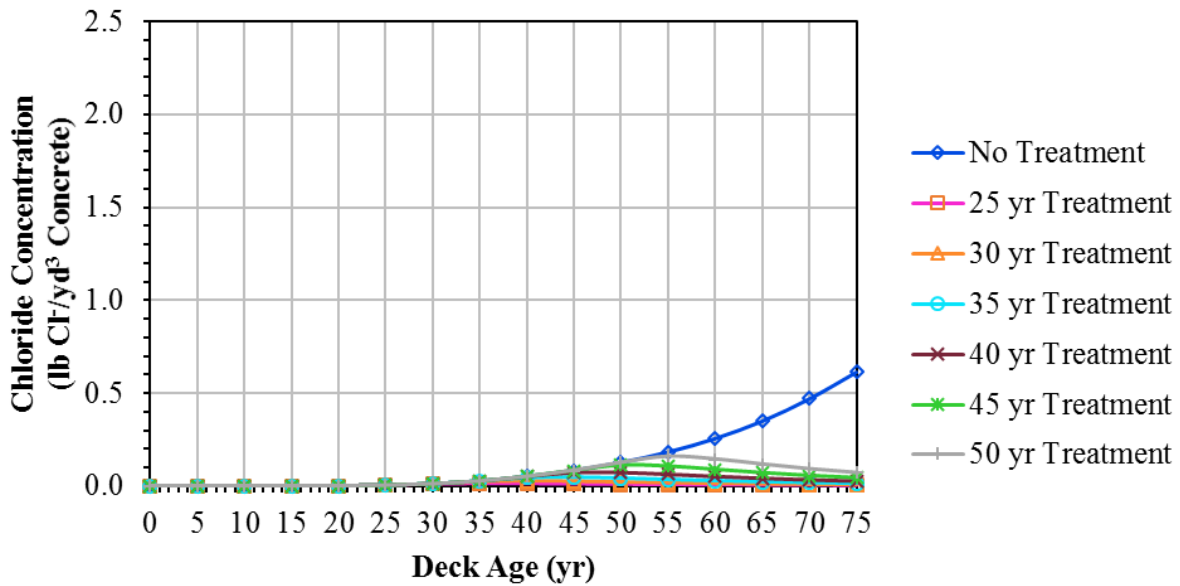

Figure D-3: Simulated chloride concentrations at the top mat of reinforcement for a deck with 3.0-in. OCD and a 4.375-in. removal depth with an applied surface treatment.

APPENDIX E: CHLORIDE CONCENTRATION AT BOTTOM MAT OF REINFORCING STEEL WITH AN APPLIED SURFACE TREATMENT

Figures E-1, E-2, and E-3 show the numerical modeling results for the bottom mat of reinforcing steel in a concrete bridge deck with a 2.0-, 2.5-, or 3.0-in. OCD, respectively, with an applied surface treatment.
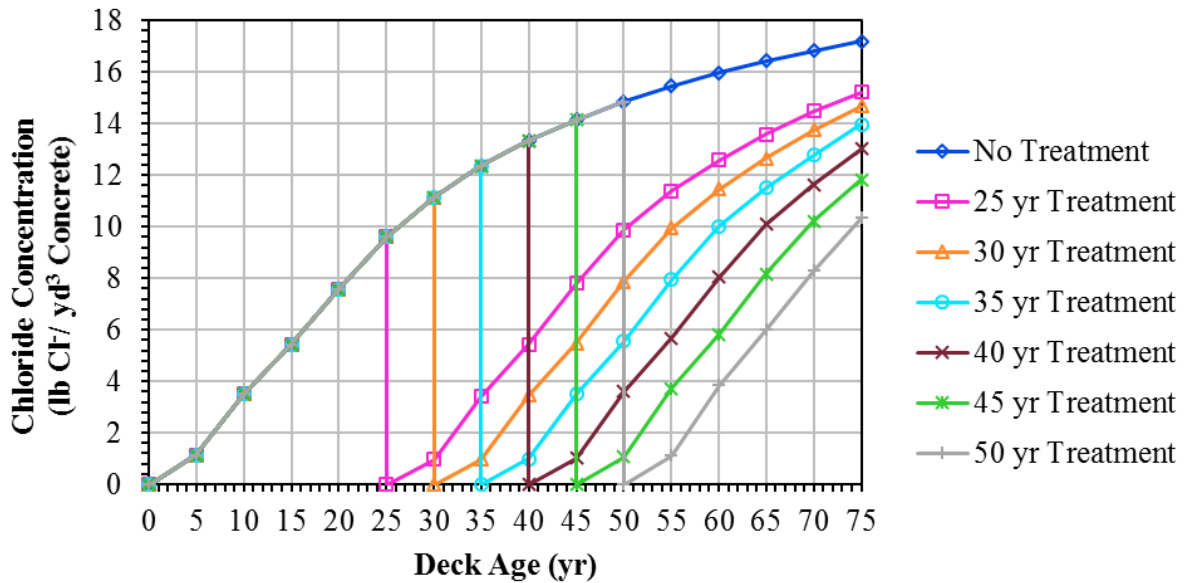

Figure E-1: Simulated chloride concentrations at the bottom mat of reinforcement for a deck with 2.0-in. OCD and a 3.375-in. removal depth with an applied surface treatment.
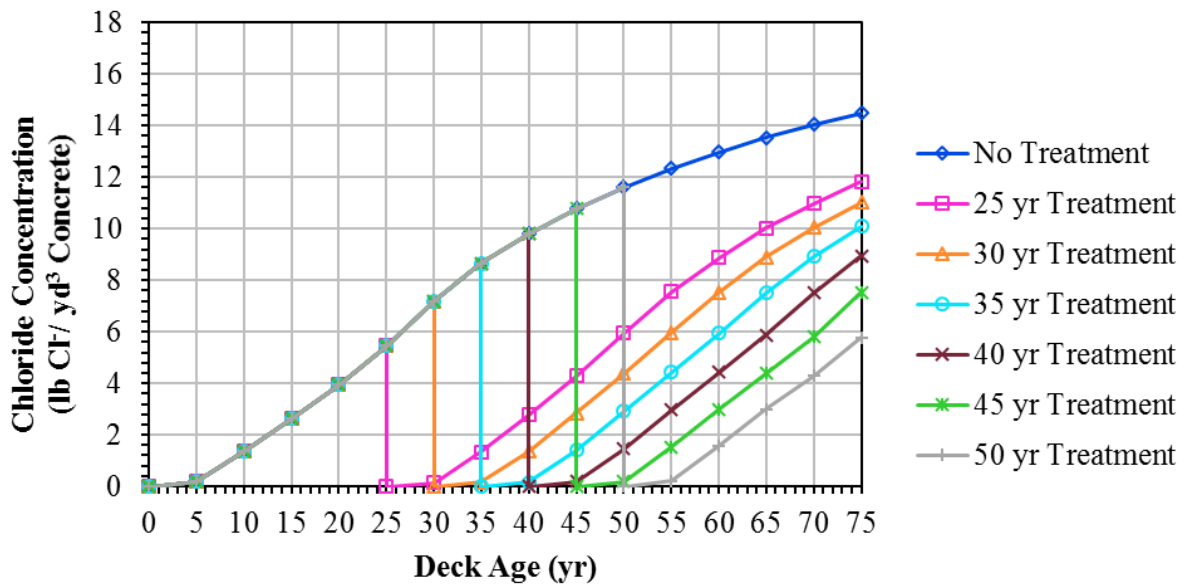
Figure E-2: Simulated chloride concentrations at the bottom mat of reinforcement for a deck with 2.5-in. OCD and a 3.875-in. removal depth with an applied surface treatment.
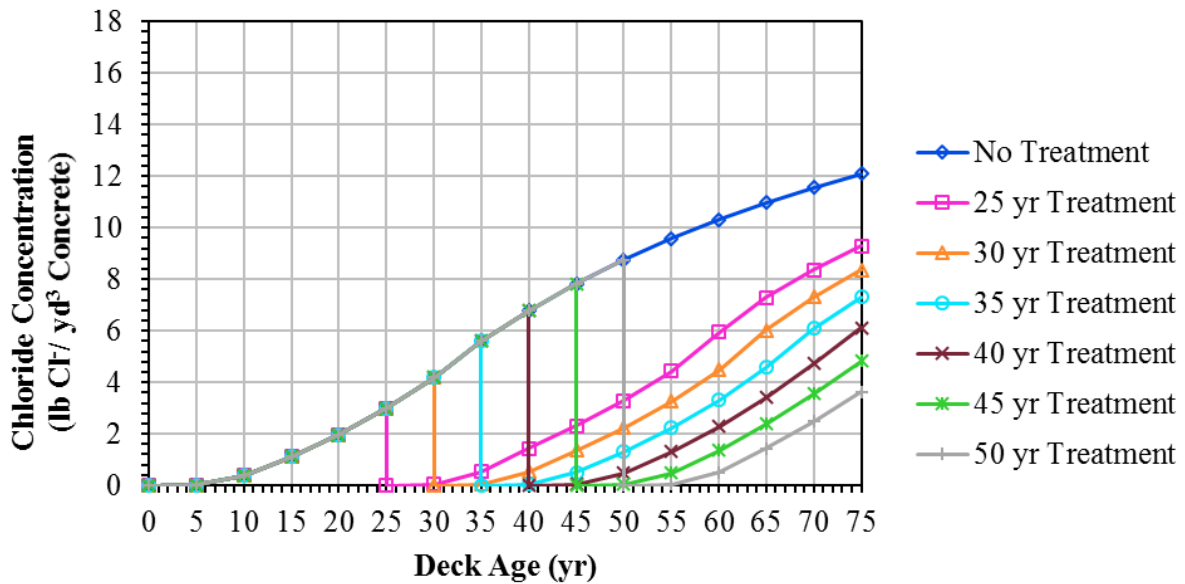

Figure E-3: Simulated chloride concentrations at the bottom mat of reinforcement for a deck with 3.0-in. OCD and a 4.375-in. removal depth with an applied surface treatment.

APPENDIX F: CHLORIDE CONCENTRATION AT TOP MAT OF REINFORCING STEEL WITHOUT AN APPLIED SURFACE TREATMENT

Figures F-1, F-2, and F-3 show the numerical modeling results for the top mat of reinforcing steel in a concrete bridge deck with a 2.0-, 2.5-, or 3.0-in. OCD, respectively, without an applied surface treatment.

Figure F-1: Simulated chloride concentrations at the top mat of reinforcement for a deck with 2.0-in. OCD and a 3.375-in. removal depth without an applied surface treatment.

Figure F-2: Simulated chloride concentrations at the top mat of reinforcement for a deck with 2.5-in. OCD and a 3.875-in. removal depth without an applied surface treatment.

Figure F-3: Simulated chloride concentrations at the top mat of reinforcement for a deck with 3.0-in. OCD and a 4.375-in. removal depth without an applied surface treatment.

APPENDIX G: CHLORIDE CONCENTRATION AT BOTTOM MAT OF REINFORCING STEEL WITHOUT AN APPLIED SURFACE TREATMENT

Figures G-1, G-2, and G-3 show the numerical modeling results for the bottom mat of reinforcing steel in a concrete bridge deck with a 2.0-, 2.5-, or 3.0-in. OCD, respectively, without an applied surface treatment.
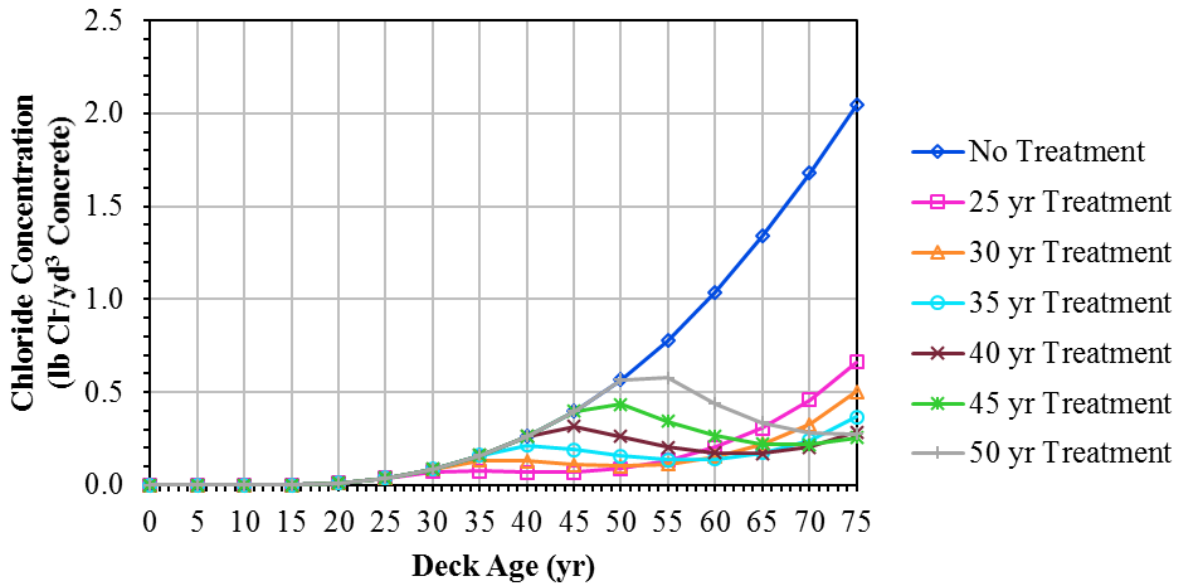

Figure G-1: Simulated chloride concentrations at the bottom mat of reinforcement for a deck with 2.0-in. OCD and a 3.375-in. removal depth without an applied surface treatment.
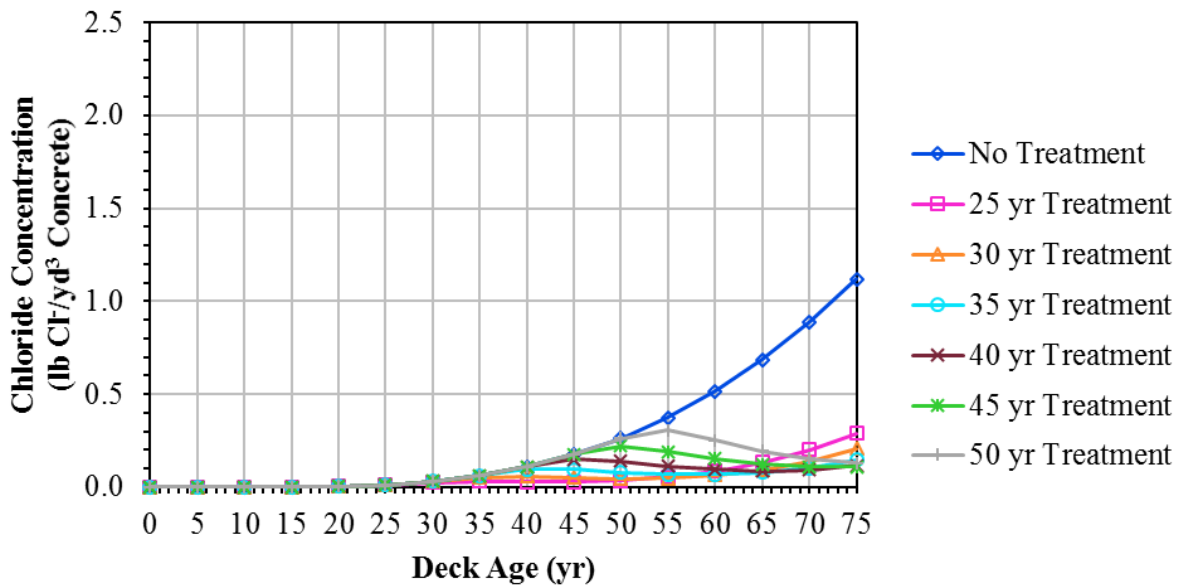
Figure G-2: Simulated chloride concentrations at the bottom mat of reinforcement for a deck with 2.5-in. OCD and a 3.875-in. removal depth without an applied surface treatment.
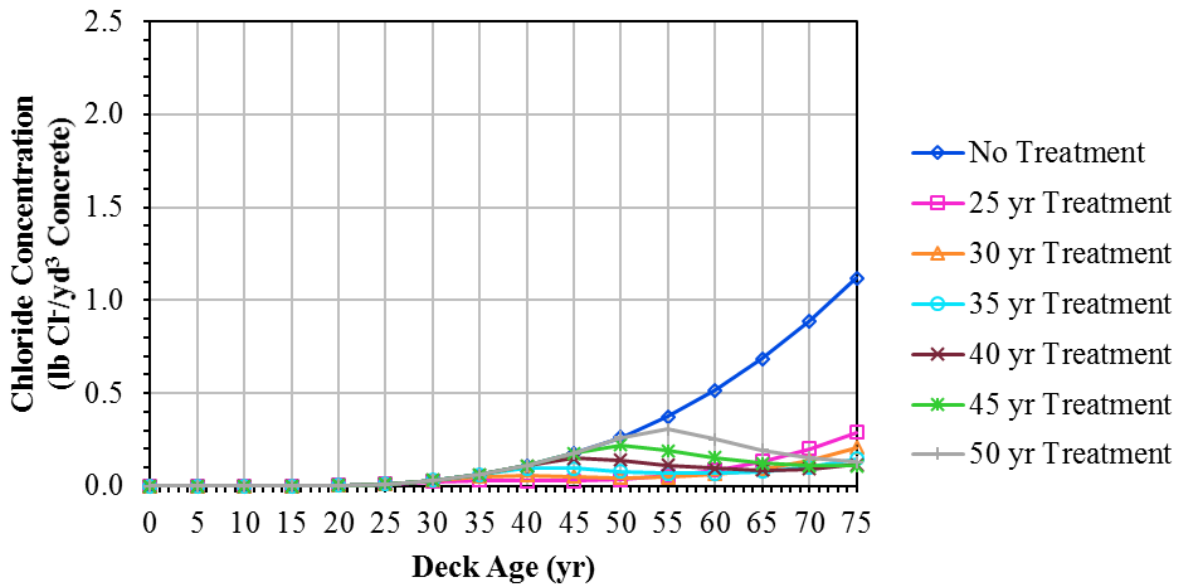

Figure G-3: Simulated chloride concentrations at the bottom mat of reinforcement for a deck with 3.0-in. OCD and a 4.375-in. removal depth without an applied surface treatment.